Contents lists available at ScienceDirect

Physics Letters B

www.elsevier.com/locate/physletb

Measurements of Higgs boson production and couplings in diboson final states with the ATLAS detector at the LHC ☆

ATLAS Collaboration ⋆

A B S T R A C T

Measurements are presented of production properties and couplings of the recently discovered Higgs boson using the decays into boson pairs, $H \to \gamma\gamma$, $H \to ZZ^* \to 4\ell$ and $H \to WW^* \to \ell\nu\ell\nu$. The results are based on the complete pp collision data sample recorded by the ATLAS experiment at the CERN Large Hadron Collider at centre-of-mass energies of $\sqrt{s} = 7$ TeV and $\sqrt{s} = 8$ TeV, corresponding to an integrated luminosity of about 25 fb^{-1}. Evidence for Higgs boson production through vector-boson fusion is reported. Results of combined fits probing Higgs boson couplings to fermions and bosons, as well as anomalous contributions to loop-induced production and decay modes, are presented. All measurements are consistent with expectations for the Standard Model Higgs boson.

1. Introduction

The discovery of a new particle of mass about 125 GeV in the search for the Standard Model (SM) Higgs boson at the CERN Large Hadron Collider (LHC) [1], reported in July 2012 by the ATLAS [2] and CMS [3] Collaborations, is a milestone in the quest to understand the origin of electroweak symmetry breaking [4–9].

This Letter presents measurements of several properties of the newly observed particle, including its mass, production strengths and couplings to fermions and bosons, using diboson final states[1]: $H \to \gamma\gamma$, $H \to ZZ^* \to 4\ell$, and $H \to WW^* \to \ell\nu\ell\nu$. Spin studies are reported elsewhere [10]. Due to the outstanding performance of the LHC accelerator throughout 2012, the present data sample is a factor of ~ 2.5 larger than that used in Ref. [2]. With these additional data, many aspects of the ATLAS studies have been improved: several experimental uncertainties have been reduced and new exclusive analyses have been included. In particular, event categories targeting specific production modes have been introduced, providing enhanced sensitivity to different Higgs boson couplings.

The results reported here are based on the data samples recorded with the ATLAS detector [11] in 2011 (at $\sqrt{s} = 7$ TeV) and 2012 (at $\sqrt{s} = 8$ TeV), corresponding to integrated luminosities of about 4.7 fb^{-1} and 20.7 fb^{-1}, respectively. Similar studies, including also fermionic decays, have been reported recently by the CMS Collaboration using a smaller dataset [12].

This Letter is organised as follows. Section 2 describes the data sample and the event reconstruction. Section 3 summarises the

Monte Carlo (MC) samples used to model signal and background processes. The analyses of the three decay channels are presented in Sections 4–6. Measurements of the Higgs boson mass, production properties and couplings are discussed in Section 7. Section 8 is devoted to the conclusions.

2. Data sample and event reconstruction

After data quality requirements, the integrated luminosities of the samples used for the studies reported here are about 4.7 fb^{-1} in 2011 and 20.7 fb^{-1} in 2012, with uncertainties given in Table 1 (determined as described in Ref. [13]). Because of the high LHC peak luminosity (up to 7.7×10^{33} cm^{-2} s^{-1} in 2012) and the 50 ns bunch spacing, the number of proton–proton interactions occurring in the same bunch crossing is large (on average 20.7, up to about 40). This "pile-up" of events requires the use of dedicated algorithms and corrections to mitigate its impact on the reconstruction of e.g. leptons, photons and jets.

For the $H \to ZZ^* \to 4\ell$ and $H \to WW^* \to \ell\nu\ell\nu$ channels, the primary vertex of the event is defined as the reconstructed vertex with the highest $\sum p_T^2$, where p_T is the magnitude of the transverse momentum[2] of each associated track; it is required to have at least three associated tracks with $p_T > 0.4$ GeV. For the

---

☆ © CERN for the benefit of the ATLAS Collaboration.

⋆ *E-mail address:* atlas.publications@cern.ch.

[1] Throughout this Letter, the symbol ℓ stands for electron or muon.

[2] ATLAS uses a right-handed coordinate system with its origin at the nominal interaction point (IP) in the centre of the detector, and the z-axis along the beam line. The x-axis points from the IP to the centre of the LHC ring, and the y-axis points upwards. Cylindrical coordinates (r, ϕ) are used in the transverse plane, ϕ being the azimuthal angle around the beam line. Observables labelled "transverse" are projected into the x–y plane. The pseudorapidity is defined in terms of the polar angle θ as $\eta = -\ln \tan(\theta/2)$.

Table 1

Main sources of experimental uncertainty, and of theoretical uncertainty on the signal yield, common to the three channels considered in this study. Theoretical uncertainties are given for a SM Higgs boson of mass $m_H = 125$ GeV and are taken from Refs. [14–16]. "QCD scale" indicates (here and throughout this Letter) QCD renormalisation and factorisation scales and "PDFs" indicates parton distribution functions. The ranges for the experimental uncertainties cover the variations with p_T and η.

Source (experimental)	Uncertainty (%)
Luminosity	± 1.8 (2011), ± 3.6 (2012)
Electron efficiency	± 2–5
Jet energy scale	± 1–5
Jet energy resolution	± 2–40
Source (theory)	Uncertainty (%)
QCD scale	± 8 (ggF), ± 1 (VBF, VH), $^{+4}_{-9}$ (ttH)
PDFs $+ \alpha_s$	± 8 (ggF, ttH), ± 4 (VBF, VH)

Table 2

Event generators used to model the signal and the main background processes. "PYTHIA" indicates that PYTHIA6 [31] and PYTHIA8 [32] are used for the simulations of 7 TeV and 8 TeV data, respectively.

Process	Generator
ggF, VBF	POWHEG [33,34] + PYTHIA
WH, ZH, $t\bar{t}H$	PYTHIA
$H \rightarrow ZZ^* \rightarrow 4\ell$ decay	PROPHECY4f [35,36]
$W +$ jets, $Z/\gamma^* +$ jets	ALPGEN [37] + HERWIG [38], POWHEG + PYTHIA, SHERPA [39]
$t\bar{t}$, tW, tb	MC@NLO [40] + HERWIG
tqb	AcerMC [41] + PYTHIA6
$q\bar{q} \rightarrow WW$	POWHEG + PYTHIA6
$gg \rightarrow WW$	gg2WW [42,43] + HERWIG
$q\bar{q} \rightarrow ZZ^*$	POWHEG [44] + PYTHIA
$gg \rightarrow ZZ^*$	gg2ZZ [43,45] + HERWIG
$W\gamma +$ jets	ALPGEN + HERWIG
$W\gamma^*$, $m_\gamma < 7$ GeV	MadGraph [46–48] + PYTHIA6
$WZ/W\gamma^*$, $m_{Z/\gamma^*} > 7$ GeV	POWHEG + PYTHIA
$q\bar{q}/gg \rightarrow \gamma\gamma$	SHERPA

$H \rightarrow \gamma\gamma$ analysis a different primary vertex definition is used, as described in Section 4.

Muon candidates [17] are formed by matching reconstructed tracks in the inner detector (ID) with either complete tracks or track segments reconstructed in the muon spectrometer (MS). The muon acceptance is extended to the region $2.5 < |\eta| < 2.7$, which is outside the ID coverage, using tracks reconstructed in the forward part of the MS.

Electron candidates [18] must have a well-reconstructed ID track pointing to a cluster of cells with energy depositions in the electromagnetic calorimeter. The cluster should satisfy a set of identification criteria requiring the longitudinal and transverse shower profiles to be consistent with those expected for electromagnetic showers. Tracks associated with electromagnetic clusters are fitted using a Gaussian Sum Filter [19], which allows bremsstrahlung energy losses to be taken into account. The identification criteria described in Ref. [18] have been modified with time to maintain optimal performance as a function of pile-up, in particular for low-p_T electrons.

The reconstruction, identification and trigger efficiencies for electrons and muons, as well as their energy and momentum scales and resolutions, are determined using large samples of $Z \rightarrow \ell\ell$, $W \rightarrow \ell\nu$ and $J/\psi \rightarrow \ell\ell$ events [18,20]. The resulting uncertainties are smaller than $\pm 1\%$ in most cases, one exception being the uncertainty on the electron selection efficiency which varies between $\pm 2\%$ and $\pm 5\%$ as a function of p_T and η.

Photon candidates [21] are reconstructed and identified using shower shapes in the electromagnetic calorimeter, with or without associated conversion tracks, as described in Section 4.

Jets [22,23] are built from topological clusters [24] using the anti-k_t algorithm [25] with a distance parameter $R = 0.4$. They are typically required to have transverse energies greater than 25 GeV (30 GeV) for $|\eta| < 2.4$ ($2.4 \leqslant |\eta| < 4.5$), where the higher threshold in the forward region reduces the contribution from jet candidates produced by pile-up. To reduce this contribution further, jets within the ID acceptance ($|\eta| < 2.47$) are required to have more than 25–75% (depending on the pile-up conditions and Higgs boson decay mode) of the summed scalar p_T of their associated tracks coming from tracks originating from the event primary vertex. Pile-up corrections based on the average event transverse energy density in the jet area [26] and the number of reconstructed vertices in the data are also applied.

Jets originating from b-quarks [27–29] are identified ("b-tagged") by combining information from algorithms exploiting the impact parameter of tracks (defined as the distance of closest approach to the primary vertex in the transverse plane), the presence of a displaced vertex, and the reconstruction of D- and B-hadron decays.

The missing transverse momentum, E_T^{miss} [30], is the magnitude of the negative vector sum of the p_T of muons, electrons, photons, jets and clusters of calorimeter cells with $|\eta| < 4.9$ not associated with these objects. The uncertainty on the E_T^{miss} energy scale is obtained from the propagation of the uncertainties on the contributing components and thus depends on the considered final state. A track-based missing transverse momentum, $\mathbf{p}_T^{\text{miss}}$, is calculated as the negative vector sum of the transverse momenta of tracks associated with the primary vertex.

The main sources of experimental uncertainty common to all the channels considered in this study are summarised in the top part of Table 1.

3. Signal and background simulation

The SM Higgs boson production processes considered in these studies are gluon fusion ($gg \rightarrow H$, denoted ggF), vector-boson fusion ($qq' \rightarrow qq'H$, denoted VBF), and Higgs-strahlung ($q\bar{q}' \rightarrow WH, ZH$, denoted WH/ZH or jointly VH). The small contribution from the associated production with a $t\bar{t}$ pair ($gg/q\bar{q} \rightarrow t\bar{t}H$, denoted ttH) is taken into account in the $H \rightarrow \gamma\gamma$ and $H \rightarrow ZZ^*$ analyses. Samples of MC-simulated events are employed to model Higgs boson production and compute signal selection efficiencies. The event generators are listed in Table 2. Cross-section normalisations and other corrections (*e.g.* Higgs boson p_T spectrum) are obtained from up-to-date calculations as described in Refs. [2, 14–16,49–77]. Table 3 shows the production cross sections and the branching ratios for the final states considered in this study for a Higgs boson with mass $m_H = 125$ GeV, while Table 1 summarises the theoretical uncertainties on the expected signal common to all channels.

Backgrounds are determined using data alone or a combination of data and MC simulation, as discussed in Sections 4–6. The generators employed in most cases are also listed in Table 2. To generate parton showers and their hadronisation, and to simulate the underlying event [78–80], PYTHIA6 (for 7 TeV samples as well as for 8 TeV samples produced with MadGraph or AcerMC) or PYTHIA8 (for other 8 TeV samples) is used. Alternatively, HERWIG is employed, combined with the underlying event simulation provided by JIMMY [81]. When PYTHIA6 or HERWIG is used, PHOTOS [82,83] is employed to describe additional photon radiation from charged leptons. The small contributions from $Z^{(*)}$ and $W^{(*)}$ decays to electrons and muons through intermediate τ-leptons are included in the signal and background generation.

The following parton distribution function (PDF) sets are used in most cases: CT10 [84] for the POWHEG, MC@NLO, gg2WW and

Table 3

SM Higgs boson cross sections (in pb) at $\sqrt{s} = 8$ (7) TeV for $m_H = 125$ GeV. The total values as well as the contributions from the individual production modes are listed. The branching ratios to the final-state channels considered in this Letter are also given (where ℓ stands for electron or muon), together with their relative uncertainty. Up-to-date theoretical calculations are used [14–16,89,35,36].

Cross section (pb) at $\sqrt{s} = 8$ (7) TeV		Branching ratio (relative uncertainty)	
ggF	19.52 (15.32)	$H \to WW^* \to \ell\nu\ell\nu$	0.010 ($\pm 5\%$)
VBF	1.58 (1.22)	$H \to \gamma\gamma$	2.28×10^{-3} ($\pm 5\%$)
WH	0.70 (0.57)	$H \to ZZ^* \to 4\ell$	1.25×10^{-4} ($\pm 5\%$)
ZH	0.39 (0.31)		
$t\bar{t}H$	0.13 (0.09)		
Total	22.32 (17.51)		

gg2ZZ samples; CTEQ6L1 [85] for the PYTHIA8, ALPGEN, AcerMC, MadGraph, HERWIG and SHERPA samples; and MRSTMCal [86] for the PYTHIA6 samples. In most cases, the generated MC samples are processed through a full simulation [87] of the ATLAS detector based on GEANT4 [88]. Corrections obtained from measurements in the data are applied to the simulation to account for small differences between data and simulation in *e.g.* the reconstruction of leptons, photons and jets. The simulation also includes realistic modelling (tuned to the data) of the event pile-up from the same and nearby bunch crossings.

4. The $H \to \gamma\gamma$ channel

This channel is particularly sensitive to physics beyond the Standard Model since the decay proceeds via loops (which in the SM are dominated by W boson exchange).

Events are required to have two high-p_T photons with invariant mass in the range 100–160 GeV. The main background is continuum $\gamma\gamma$ production, with smaller contributions from $\gamma + $ jet and dijet processes. Compared to the previously published results [2], additional categories of events are introduced in the analysis of the 8 TeV data to increase the sensitivity to production through VBF or in association with a W or Z boson.

4.1. Event selection

The data used in this channel are selected using a diphoton trigger [90] requiring two clusters formed from energy depositions in the electromagnetic calorimeter, with shapes compatible with electromagnetic showers. An E_T threshold of 20 GeV is applied to each cluster for the 7 TeV data, while at 8 TeV the thresholds are increased to 35 GeV on the leading (highest E_T) and 25 GeV on the sub-leading (next-highest E_T) cluster. The trigger efficiency is larger than 99% for events passing the final event selection.

In the offline analysis, photon candidates are required to have $E_T > 40$ GeV and 30 GeV for the leading and sub-leading photon, respectively. Both photons must be reconstructed in the fiducial region $|\eta| < 2.37$, excluding the calorimeter barrel/end-cap transition region $1.37 \leqslant |\eta| < 1.56$.

Photon candidates are required to pass tight identification criteria based mainly on shower shapes in the electromagnetic calorimeter [2]. They are classified as converted if they are associated with two tracks consistent with a $\gamma \to e^+e^-$ conversion process or a single track leaving no hit in the innermost layer of the inner detector, and as unconverted otherwise [91]. Identification efficiencies, averaged over η, range from 85% to above 95% for the E_T range under consideration. Jets misidentified as photons are further rejected by applying calorimeter and track isolation requirements to the photon candidates. The calorimeter isolation is defined as the sum of the transverse energies of positive-energy topological clusters within a cone of size $\Delta R = \sqrt{\Delta\phi^2 + \Delta\eta^2} = 0.4$

around the photon candidates, excluding the core of the showers. It is required to be smaller than 4 GeV and 6 GeV for the 7 TeV and 8 TeV data, respectively. The pile-up contribution is corrected on an event-by-event basis [92]. The track isolation, applied to the 8 TeV data only, is defined as the scalar sum of the transverse momenta of all tracks with $p_T > 1$ GeV associated with the diphoton production vertex (defined below) and lying within a cone of size $\Delta R = 0.2$ around the photon candidate; it is required to be smaller than 2.6 GeV. Conversion tracks associated with either photon candidate are excluded.

For the precise measurement of the diphoton invariant mass ($m_{\gamma\gamma}$), as well as for the computation of track-based quantities (*e.g.* track isolation, selection of jets associated with the hard interaction), the diphoton production vertex should be known precisely. The determination of the vertex position along the beam axis is based on so-called "photon pointing", where the directions of the two photons, measured using the longitudinal and lateral segmentation of the electromagnetic calorimeter, are combined with a constraint from the average beam-spot position. For converted photons the position of the conversion vertex is also used. This technique alone is sufficient to ensure that the contribution of angular measurement uncertainties to the diphoton invariant mass resolution is negligible. For a more precise identification of the primary vertex, needed for the computation of track-based quantities, this pointing information is combined with tracking information from each reconstructed vertex: the Σp_T^2 for the tracks associated with a given vertex and, for the 8 TeV data, the Σp_T of the tracks and the azimuthal angle between the transverse momentum of the diphoton system and that of the vector sum of the track $\mathbf{p}_T$. A Neural Network (likelihood) discriminant is used for the 8 TeV (7 TeV) data. The performance of this algorithm is studied using $Z \to ee$ decays, ignoring the tracks associated with the electrons and weighting the events so that the p_T and rapidity distributions of the Z boson match those expected from the Higgs boson signal. The probability of finding a vertex within 0.3 mm of the one computed from the electron tracks is larger than 75%.

The photon energy calibration is obtained from a detailed simulation of the detector geometry and response, independently for converted and unconverted photons. The calibration is refined by applying η-dependent correction factors determined from studies of $Z \to ee$ events in data [18]: they range from $\pm 0.5\%$ to $\pm 1.5\%$ depending on the pseudorapidity of the photon. Samples of radiative $Z \to \ell\ell\gamma$ decays are used to verify the photon energy scale. The energy response of the calorimeter shows a stability of better than $\pm 0.1\%$ with time and various pile-up conditions.

The signal efficiency of the above selections at 8 TeV is estimated to be 37.5% for a Higgs boson with $m_H = 125$ GeV.

The number of events in the diphoton mass region 100–160 GeV passing this inclusive selection is 23 788 in the 7 TeV data and 118 893 in the 8 TeV data. The fraction of genuine $\gamma\gamma$ events, as estimated from data [93], is $(75^{+3}_{-4})\%$.

4.2. Event categorisation

To increase the sensitivity to the overall Higgs boson signal, as well as to the specific VBF and VH production modes, the selected events are separated into 14 mutually exclusive categories for further analysis, following the order of preference listed below.

Lepton category (8 TeV data only): This category targets mainly VH events where the W or Z bosons decay to charged leptons. An isolated electron ($E_T > 15$ GeV) or muon ($p_T > 10$ GeV) candidate is required. To remove contamination from $Z\gamma$ production with $Z \to ee$, electrons forming an invariant mass with either photon in the range 84 GeV $< m_{e\gamma} < 94$ GeV are not considered.
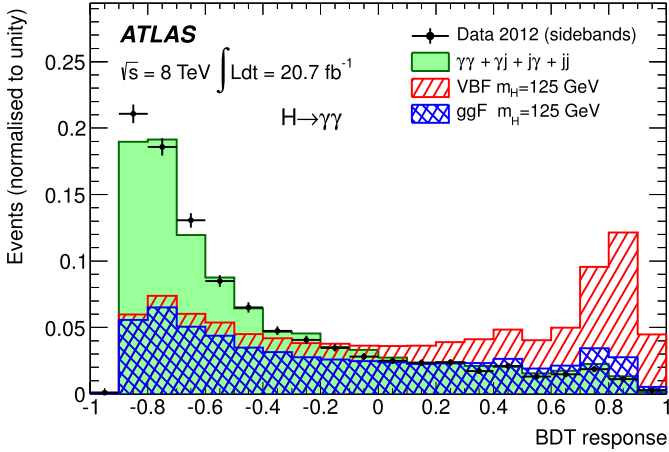
Fig. 1. Distribution of the VBF BDT response after applying the selection of the inclusive analysis and requiring in addition the presence of two jets with $|\Delta\eta_{jj}| > 2$ and $|\eta^*| < 5$. The data in the signal sidebands (*i.e.* excluding the $m_{\gamma\gamma}$ region 120–130 GeV), the expected background, and the expected signal from VBF and ggF production are shown. They are all normalised to unity except ggF, which is normalised to the ratio between the numbers of ggF and VBF events passing the selection described above.

E_T^{miss} *category* (8 TeV data only): This category targets mainly *VH* events with $W \to \ell\nu$ or $Z \to \nu\nu$. An E_T^{miss} significance (defined as $E_T^{\text{miss}}/\sigma_{E_T^{\text{miss}}}$, where in this case $\sigma_{E_T^{\text{miss}}} = 0.67 \text{ GeV}^{1/2}\sqrt{\Sigma E_T}$ with ΣE_T being the event total transverse energy) greater than five is required, corresponding to $E_T^{\text{miss}} > 70$–100 GeV depending on ΣE_T.

Low-mass two-jet category (8 TeV data only): To select *VH* events where the *W* or *Z* boson decays hadronically, a pair of jets with invariant mass in the range 60 GeV $< m_{jj} <$ 110 GeV is required. To reduce the ggF contamination, the pseudorapidity difference between the dijet and diphoton systems is required to be $|\Delta\eta_{\gamma\gamma,jj}| < 1$, and the component of the diphoton transverse momentum orthogonal to the diphoton thrust axis in the transverse plane[3] [94,95] is required to satisfy $p_{\text{Tt}} > 70$ GeV.

High-mass two-jet categories: These categories are designed to select events produced through the VBF process, which is characterised by the presence of two forward jets with little hadronic activity in the central part of the detector. Jets are reconstructed as described in Section 2. The selection for the 8 TeV data is based on a multivariate technique using a Boosted Decision Tree (BDT), whose input quantities are: the pseudorapidities of the two jets (η_{j1}, η_{j2}) and their separation in η; the invariant mass of the dijet system; the difference $\eta^* = \eta_{\gamma\gamma} - (\eta_{j1} + \eta_{j2})/2$, where $\eta_{\gamma\gamma}$ is the pseudorapidity of the diphoton system; the minimal radial distance ($\Delta R = \sqrt{\Delta\phi^2 + \Delta\eta^2}$) of any jet–photon pair; and the difference $\Delta\phi_{\gamma\gamma,jj}$ between the azimuthal angles of the diphoton and dijet momenta. The BDT training is performed using a signal sample, as well as a background sample composed of simulated $\gamma\gamma$ events combined with γj and jj components obtained from data. The BDT response distributions for data and simulation are shown in Fig. 1. The BDT output is used to define two high-mass two-jet categories: a "tight" category corresponding to BDT $\geqslant 0.74$, and a "loose" category for $0.44 \leqslant$ BDT < 0.74. For the 7 TeV data, the same cut-based selection as described in Ref. [2] is applied, namely $m_{jj} > 400$ GeV, $|\Delta\eta_{jj}| > 2.8$ and $|\Delta\phi_{\gamma\gamma,jj}| > 2.8$.

Untagged categories: Events not selected in any of the above categories (corresponding to more than 90% of the expected signal, dominated by ggF production) are classified in nine additional categories according to the properties of their diphoton system. Events with both photons unconverted are classified into *unconverted central* if $|\eta| < 0.75$ for both photons, and *unconverted rest* otherwise. Events with at least one converted photon are similarly separated into *converted central* if $|\eta| < 0.75$ for both photons, *converted transition* if $1.3 < |\eta| < 1.75$ for either photon, and *converted rest* otherwise. Finally, all untagged categories except *converted transition* are split into *low* p_{Tt} and *high* p_{Tt} sub-categories by a cut at $p_{\text{Tt}} = 60$ GeV. This classification is motivated by differences in mass resolution and signal-to-background ratio for the various categories.

The use of the 14 categories improves the sensitivity of the analysis by about 40% compared to the inclusive analysis.

4.3. Background estimation

The background is obtained from fits to the diphoton mass spectrum in the data over the range 100–160 GeV after the full selection. The procedure, the choice of the analytical forms for the background and the determination of the corresponding uncertainties follow the method described in Ref. [2]. Depending on the category, the analytical form is either a fourth-order Bernstein polynomial [96] (used also for the inclusive sample), an exponential of a second-order polynomial, or a single exponential. In these fits, the Higgs boson signal is described by the sum of a Crystal Ball function [97] for the core of the distribution and a Gaussian function for the tails.

4.4. Systematic uncertainties

Systematic uncertainties can affect the signal yield, the signal fractions in the various categories (with possible migrations between them), the signal mass resolution and the mass measurement. The main sources specific to the $H \to \gamma\gamma$ channel are listed in Table 4, while sources in common with other decay channels are summarised in Section 2 and Table 1. The uncertainties described below are those affecting the 8 TeV analysis (see Ref. [2] for the 7 TeV analysis).

Signal yield: Relevant experimental uncertainties on the signal yield come from the knowledge of the luminosity (Table 1) and the photon identification efficiency. The latter is estimated by comparing the efficiencies obtained using MC simulations and several data-driven methods: $Z \to ee$ events with a simulation-based extrapolation from electrons to photons, an isolation sideband technique using an inclusive photon sample, and photons from $Z \to \ell\ell\gamma$ radiative decays. Owing to several analysis improvements and the large size of the 8 TeV data sample, the resulting uncertainty is significantly reduced compared to that reported in Ref. [2] and amounts to $\pm2.4\%$. Smaller experimental uncertainties come from the knowledge of the trigger efficiency, the impact of the photon isolation requirement and the photon energy scale. In addition to the theoretical uncertainties on inclusive Higgs boson production listed in Table 1, the ggF contribution to the two-jet categories is subject to large uncertainties (Table 4) due to missing higher-order corrections; they are estimated using the method described in Ref. [98] and the MCFM [99] generator calculations. Finally, the background modelling contributes an uncertainty between $\pm2\%$ and $\pm14\%$ depending on the category.

Event migration: Mis-modelling of the detector material could cause event migration between the unconverted and converted photon categories in the simulation. The uncertainty is obtained from MC samples produced with variations of the material de-

---

[3] $p_{\text{Tt}} = |(\mathbf{p}_T^{\gamma_1} + \mathbf{p}_T^{\gamma_2}) \times \hat{\mathbf{t}}|$, where $\hat{\mathbf{t}} = \frac{\mathbf{p}_T^{\gamma_1} - \mathbf{p}_T^{\gamma_2}}{|\mathbf{p}_T^{\gamma_1} - \mathbf{p}_T^{\gamma_2}|}$ denotes the thrust axis in the transverse plane, and $\mathbf{p}_T^{\gamma_1}$, $\mathbf{p}_T^{\gamma_2}$ are the transverse momenta of the two photons.

Table 4

For $m_H = 125$ GeV and the 8 TeV data analysis, the impact of the main sources of systematic uncertainty specific to the $H \to \gamma\gamma$ channel on the signal yield, event migration between categories and mass measurement and resolution. Uncertainties common to all channels are listed in Table 1. The $\pm$ ($\mp$) sign indicates correlations (anticorrelations) between categories.

Source	Uncertainty (%)
On signal yield	
Photon identification	± 2.4
Trigger	± 0.5
Isolation	± 1.0
Photon energy scale	± 0.25
ggF (theory), tight high-mass two-jet cat.	± 48
ggF (theory), loose high-mass two-jet cat.	± 28
ggF (theory), low-mass two-jet cat.	± 30
Impact of background modelling	$\pm (2$–$14)$, cat.-dependent
On category population (migration)	
Material modelling	-4 (unconv), $+3.5$ (conv)
p_T modelling	± 1 (low-p_{Tt}),
	$\mp (9$–$12)$ (high-p_{Tt}, jets),
	$\pm (2$–$4)$ (lepton, E_T^{miss})
$\Delta\phi_{\gamma\gamma,jj}$, η^* modelling in ggF	$\pm (9$–$12)$, $\pm (6$–$8)$
Jet energy scale and resolution	$\pm (7$–$12)$ (jets),
	$\mp (0$–$1)$ (others)
Underlying event two-jet cat.	± 4 (high-mass tight),
	± 8 (high-mass loose),
	± 12 (low-mass)
E_T^{miss}	± 4 (E_T^{miss} category)
On mass scale and resolution	
Mass measurement	± 0.6, cat.-dependent
Signal mass resolution	$\pm (14$–$23)$, cat.-dependent

scription. The uncertainty in the population of the p_{Tt} categories due to the description of the Higgs boson p_T spectrum is determined by varying the QCD scales and PDFs used in the HqT program [62]. Uncertainties on the modelling of two-jet variables for the ggF process, in particular $\Delta\phi_{\gamma\gamma,jj}$ and η^*, affect the contribution of ggF events to the high-mass two-jet categories. They are estimated by comparing the baseline POWHEG generator with SHERPA and MCFM. Uncertainties on the jet energy scale and resolution affect the selection of jets used in some category definitions, thereby causing migration between jet-based and other categories. The uncertainty due to the modelling of the underlying event is estimated by comparing simulations with and without multi-parton interactions. Uncertainties on the E_T^{miss} reconstruction are assessed by varying the transverse energies of its components (photons, electrons, jets, soft energy deposits) within their respective uncertainties.

Mass measurement and mass resolution: The measurement of the Higgs boson mass in the $H \to \gamma\gamma$ channel is discussed in Section 7.2. Uncertainties on the diphoton mass scale come from the following sources: the calibration of the electron energy scale (obtained from $Z \to ee$ events); the uncertainty on its extrapolation to the energy scale of photons, dominated by the description of the detector material; and the knowledge of the energy scale of the presampler detector located in front of the electromagnetic calorimeter. The total uncertainty amounts to $\pm 0.55\%$ (corresponding to ± 0.7 GeV). The mass resolution, obtained from the Crystal Ball function used in the fits described in Section 4.3, ranges from 1.4 GeV to 2.5 GeV depending on the category. The main uncertainties come from the calorimeter energy scale and the extrapolation from the electron to the photon response. Smaller contributions arise from pile-up and the primary vertex selection.

4.5. Results

The diphoton invariant mass distribution after selections for the full data sample is shown in Fig. 2. The data are fitted by
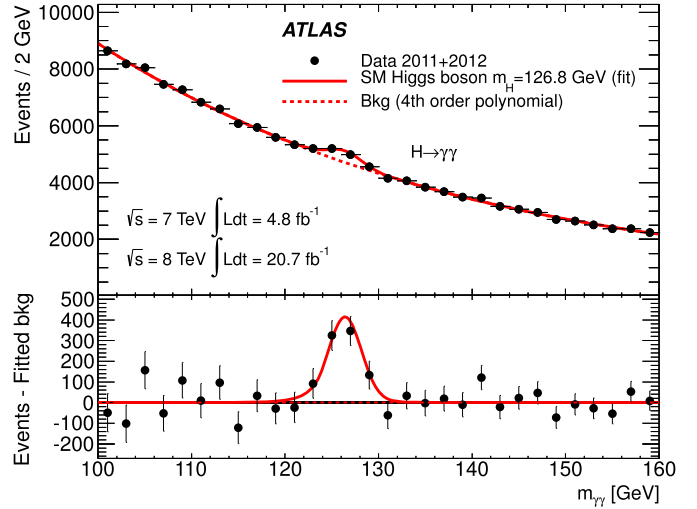
Fig. 2. Invariant mass distribution of diphoton candidates after all selections of the inclusive analysis for the combined 7 TeV and 8 TeV data. The result of a fit to the data with the sum of a SM Higgs boson signal (with $m_H = 126.8$ GeV and free signal strength) and background is superimposed. The residuals of the data with respect to the fitted background are displayed in the lower panel.

categories, using background shapes (see Section 4.3), as well as parameters for the Crystal Ball and Gaussian functions describing the signal, specific to each category. At the maximum deviation from the background-only expectation, which occurs for $m_H \sim 126.5$ GeV, the significance of the observed peak is 7.4σ for the combined 7 TeV and 8 TeV data (compared with 4.3σ expected from SM Higgs boson production at this mass), which establishes a discovery-level signal in the $\gamma\gamma$ channel alone. Table 5 lists the observed number of events in the main categories, the estimated background from fits to the data (described in Section 4.3), and the predicted signal contributions from the various production processes.

Additional interpretation of these results is presented in Section 7.

5. The $H \to ZZ^* \to 4\ell$ channel

Despite the small branching ratio, this channel provides good sensitivity to Higgs boson studies, *e.g.* to the coupling to Z bosons, mainly because of the large signal-to-background ratio.

Events are required to have two pairs of same-flavour, opposite-charge, isolated leptons: $4e$, $2e2\mu$, $2\mu2e$, 4μ (where final states with two electrons and two muons are ordered by the flavour of the dilepton pair with mass closest to the Z boson mass). The largest background comes from continuum $(Z^{(*)}/\gamma^*)(Z^{(*)}/\gamma^*)$ production, referred to hereafter as ZZ^*. Important contributions arise also from $Z + $ jets and $t\bar{t}$ production, where two of the charged lepton candidates can come from decays of hadrons with b- or c-quark content, misidentification of light-quark jets, and photon conversions.

The analysis presented here is largely the same as that described in Ref. [100] with only minor changes. The electron identification is tightened in the 8 TeV data to improve the background rejection for final states with a pair of electrons forming the lower-mass Z^* boson. The mass measurement uses a constrained fit to the Z mass to improve the resolution. The lepton pairing is modified to reduce the mis-pairing in the 4μ and $4e$ final states, and the minimum requirement on the mass of the second Z^* boson is relaxed. Final-state radiation (FSR) is included in the reconstruction of the first $Z^{(*)}$ in events containing muons. Finally, a classification

Table 5
For the $H \to \gamma\gamma$ analysis of the $\sqrt{s} = 8$ TeV data, the numbers of events observed in the data (N_D), the numbers of background events (N_B) estimated from fits to the data, and the expected SM Higgs boson signal (N_S) for $m_H = 126.8$ GeV, split by category. All numbers are given in a mass window centred at $m_H = 126.8$ GeV and containing 90% of the expected signal (the size of this window changes from category to category and for the inclusive sample). The predicted numbers of signal events in each of the ggF, VBF, WH, ZH and $t\bar{t}H$ processes are also given.

Category	N_D	N_B	N_S	ggF	VBF	WH	ZH	$t\bar{t}H$
Untagged	14 248	13 582	350	320	19	7.0	4.2	1.0
Loose high-mass two-jet	41	28	5.0	2.3	2.7	< 0.1	< 0.1	< 0.1
Tight high-mass two-jet	23	13	7.7	1.8	5.9	< 0.1	< 0.1	< 0.1
Low-mass two-jet	19	21	3.1	1.5	< 0.1	0.92	0.54	< 0.1
E_T^{miss} significance	8	4	1.2	< 0.1	< 0.1	0.43	0.57	0.14
Lepton	20	12	2.7	< 0.1	< 0.1	1.7	0.41	0.50
All categories (inclusive)	13 931	13 205	370	330	27	10	5.8	1.7

which separates Higgs boson candidate events into ggF-like, VBF-like and VH-like categories is introduced.

5.1. Event selection

The data are selected using single-lepton or dilepton triggers. The p_T threshold of the single-muon trigger is 24 GeV (18 GeV) in 2012 (2011) and the E_T threshold of the single-electron trigger is 24 GeV (20–22 GeV). The dielectron trigger threshold is $E_T = 12$ GeV and the dimuon trigger threshold is $p_T = 13$ GeV (10 GeV in 2011) for both leptons. In addition, an asymmetric dimuon trigger and electron–muon triggers are used as described in Ref. [100]. The efficiency for events passing the offline analysis cuts to be selected by at least one of the above triggers is between 97% and 100%.

Muon and electron candidates are reconstructed as described in Section 2. In the region $|\eta| < 0.1$, which has limited MS coverage, ID tracks with $p_T > 15$ GeV are identified as muons if their calorimetric energy deposits are consistent with a minimum ionising particle. Only one muon per event is allowed to be reconstructed either in the MS alone or without MS information. For the 2012 data, the electron requirements are tightened in the transition region between the barrel and end-cap calorimeters ($1.37 < |\eta| < 1.52$), and the pixel-hit requirements are stricter to improve the rejection of photon conversions.

Each electron (muon) must satisfy $E_T > 7$ GeV ($p_T > 6$ GeV) and be measured in the pseudorapidity range $|\eta| < 2.47$ ($|\eta| < 2.7$). The highest-p_T lepton in the quadruplet must satisfy $p_T > 20$ GeV, and the second (third) lepton must satisfy $p_T > 15$ GeV ($p_T > 10$ GeV). To reject cosmic rays, muon tracks are required to have a transverse impact parameter of less than 1 mm.

Multiple quadruplets within a single event are possible. For each quadruplet, the same-flavour, opposite-charge lepton pair with invariant mass closest to the Z boson mass (m_Z) is referred to as the leading lepton pair. Its invariant mass, denoted by m_{12}, is required to be between 50 GeV and 106 GeV. The invariant mass of the other (sub-leading) lepton pair, m_{34}, is required to be in the range $m_{min} < m_{34} < 115$ GeV. The value of m_{min} is 12 GeV for a reconstructed four-lepton mass $m_{4\ell} < 140$ GeV, rises linearly to 50 GeV at $m_{4\ell} = 190$ GeV, and remains constant for higher masses. If two or more quadruplets satisfy the above requirements, the one with m_{34} closest to the Z boson mass is selected. For further analysis, events are classified in four sub-channels, $4e$, $2e2\mu$, $2\mu2e$, 4μ.

The $Z + $jets and $t\bar{t}$ background contributions are reduced by applying requirements on the lepton transverse impact parameter divided by its uncertainty, $|d_0|/\sigma_{d_0}$. This ratio must be smaller than 3.5 for muons and smaller than 6.5 for electrons (the electron impact parameter is affected by bremsstrahlung and thus its distribution has longer tails). In addition, leptons must satisfy isolation requirements based on tracking and calorimetric information, similar to those described in Section 4.1, as discussed in Ref. [2].

The impact of FSR photon emission on the reconstructed invariant mass is modelled using the MC simulation (PHOTOS), which reproduces the rate of collinear photons with $E_T > 1.3$ GeV in $Z \to \mu\mu$ decays in data to $\pm 5\%$ [101]. Leading muon pairs with 66 GeV $< m_{12} < 89$ GeV are corrected for FSR by including any reconstructed photon with E_T above 1 GeV lying close (typically within $\Delta R < 0.15$) to the muon tracks, provided that the corrected m_{12} satisfies $m_{12} < 100$ GeV. The MC simulation predicts that about 4% of all $H \to ZZ^* \to 4\mu$ candidate events should have this correction.

For the 8 TeV data, the signal reconstruction and selection efficiency for a SM Higgs boson with $m_H = 125$ GeV is 39% for the 4μ sub-channel, 26% for the $2e2\mu/2\mu2e$ sub-channels and 19% for the $4e$ sub-channel.

The final discriminating variable in this analysis is the 4ℓ invariant mass. Its resolution, which is improved by typically 15% by applying a Z-mass constrained kinematic fit to the leading lepton pair, is about 1.6 GeV, 1.9 GeV and 2.4 GeV for the 4μ, $2e2\mu/2\mu2e$ and $4e$ sub-channels, respectively, and for $m_H = 125$ GeV.

5.2. Event categorisation

To enhance the sensitivity to the individual production modes, events passing the above selection are assigned to one of three categories, named VBF-like, VH-like, and ggF-like. Events are VBF-like if the two highest p_T jets are separated by more than three units in pseudorapidity and have an invariant mass greater than 350 GeV. Events that do not qualify as VBF-like are considered for the VH-like category. They are accepted in this category if they contain an additional lepton (e or μ) with $p_T > 8$ GeV, satisfying the same requirements as the four leading leptons. The remaining events are assigned to the ggF-like category. No classification based on the 4ℓ flavour is made in the VBF-like and VH-like categories. Higgs boson production through VBF and VH is expected to account for about 60% and 70% of the total signal events in the VBF-like and VH-like categories, respectively. The signal-to-background ratio in the signal peak region is about five for the VBF-like category, about three for the VH-like category, and about 1.5 for the inclusive analysis.

5.3. Background estimation

The expected background yield and composition are estimated using the MC simulation for ZZ^* production, and methods based on control regions (CRs) from data for the $Z + $jets and $t\bar{t}$ processes [2]. The transfer factors used to extrapolate the background yields from the CRs to the signal region are obtained from MC simulation and cross-checked with data. Since the background composition depends on the flavour of the sub-leading lepton pair, different approaches are followed for the $\ell\ell + \mu\mu$ and the $\ell\ell + ee$ final states.

Table 6

For $m_H = 125$ GeV and the 8 TeV data analysis, the impact of the main sources of systematic uncertainty specific to the $H \rightarrow ZZ^*$ channel on the signal yield, estimated reducible background, event migration between categories and mass measurement. Uncertainties common to all channels are listed in Table 1.

Source	Uncertainty (%)			
Signal yield	4μ	$2\mu 2e$	$2e2\mu$	$4e$
Muon reconstruction and identification	±0.8	±0.4	±0.4	–
Electron reconstruction and identification	–	±8.7	±2.4	±9.4
Reducible background (inclusive analysis)	±24	±10	±23	±13
Migration between categories				
ggF/VBF/VH contributions to VBF-like cat.		±32/11/11		
ZZ^* contribution to VBF-like cat.		±36		
ggF/VBF/VH contributions to VH-like cat.		±15/5/6		
ZZ^* contribution to VH-like cat.		±30		
Mass measurement	4μ	$2\mu 2e$	$2e2\mu$	$4e$
Lepton energy and momentum scale	±0.2	±0.2	±0.3	±0.4

The reducible $\ell\ell + \mu\mu$ background is dominated by $t\bar{t}$ and $Z + $ jets (mostly $Zb\bar{b}$) events. A CR is defined by removing the isolation requirement for the muons of the sub-leading pair, and by requiring that at least one of them fails the transverse impact parameter selection. This procedure allows the $t\bar{t}$ and $Z +$ jets backgrounds to be estimated simultaneously from a fit to the m_{12} distribution.

To determine the reducible $\ell\ell + ee$ background, a CR is formed by relaxing the selection criteria for the electrons of the sub-leading pair: each of these electrons is then classified as "electron-like" or "fake-like" based on requirements on appropriate discriminating variables [102]. The numbers of events with different combinations of "electron-like" or "fake-like" objects are then used to estimate the true composition of the CR (in terms of isolated electrons, non-prompt electrons from heavy-flavour decays, electrons from photon conversions and jets misidentified as electrons), from which the expected yields in the signal region can be obtained using transfer factors from the MC simulation.

Similar techniques are used to determine the backgrounds for the VBF-like and VH-like categories.

5.4. Systematic uncertainties

The dominant sources of systematic uncertainty affecting the $H \rightarrow ZZ^*$ 8 TeV analysis are listed in Table 6 (see Ref. [2] for the 7 TeV analysis). Lepton reconstruction, identification and selection efficiencies, as well as energy and momentum resolutions and scales, are determined using large control samples from the data, as described in Section 2. Only the electron uncertainty contributes significantly to the uncertainty on the signal yield.

The background uncertainty is dominated by the uncertainty on the transfer factors from the CRs to the signal region and the available number of events in the control regions.

The uncertainty on the population of the various categories (migration) comes mainly from the knowledge of the theoretical cross sections for the various production processes, the modelling of the underlying event and the knowledge of the jet energy scale.

The $H \rightarrow ZZ^* \rightarrow 4\ell$ mass measurement is discussed in Section 7.2. The main sources contributing to the electron energy scale uncertainty are described in Section 4.4; the largest impact (±0.4%) is on the $4e$ final state. Systematic uncertainties from the knowledge of the muon momentum scale (discussed in detail in Ref. [100]) are smaller. Mass scale uncertainties related to FSR and background contamination are below ±0.1%.
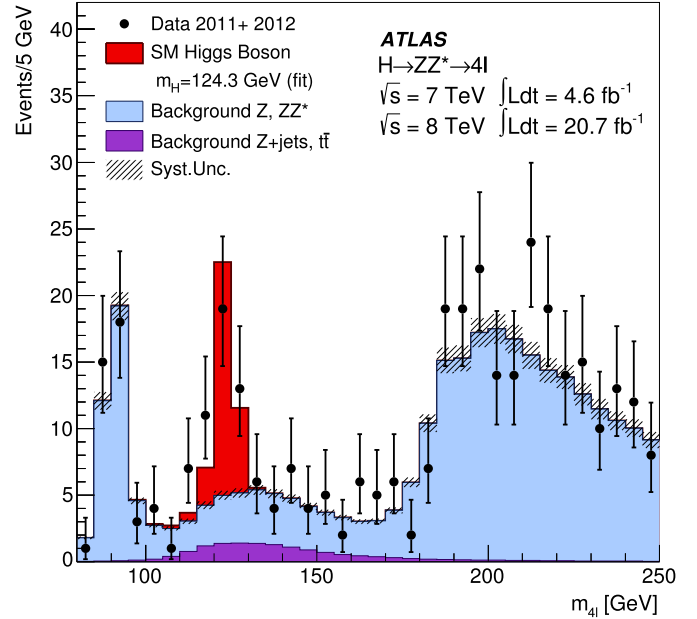
Fig. 3. The distribution of the four-lepton invariant mass, $m_{4\ell}$, for the selected candidates in the data. The estimated background, as well as the expected SM Higgs boson signal for $m_H = 124.3$ GeV (scaled by the signal strength obtained from fits to the data), are also shown. The single-resonant peak at $m_{4\ell} \sim 90$ GeV includes contributions from s-channel Z/γ^* and t-channel $(Z^*/\gamma^*)(Z^*/\gamma^*)$ production.

Table 7

For the $H \rightarrow ZZ^* \rightarrow 4\ell$ inclusive analysis, the number of expected signal ($m_H = 125$ GeV) and background events, together with the number of events observed in the data, in a window of size ±5 GeV around $m_{4\ell} = 125$ GeV, for the combined $\sqrt{s} = 7$ TeV and $\sqrt{s} = 8$ TeV data.

	Signal	ZZ^*	$Z +$ jets, $t\bar{t}$	Observed
4μ	6.3 ± 0.8	2.8 ± 0.1	0.55 ± 0.15	13
$2e2\mu/2\mu2e$	7.0 ± 0.6	3.5 ± 0.1	2.11 ± 0.37	13
$4e$	2.6 ± 0.4	1.2 ± 0.1	1.11 ± 0.28	6

5.5. Results

The reconstructed four-lepton mass spectrum after all selections of the inclusive analysis is shown in Fig. 3. The data are compared to the (scaled) expected Higgs boson signal for $m_H = 124.3$ GeV and to the estimated backgrounds. At the maximum deviation from the background-only expectation (occurring at $m_H = 124.3$ GeV), the significance of the observed peak is 6.6σ for the combined 7 TeV and 8 TeV data, to be compared with 4.4σ expected from SM Higgs boson production at this mass. This result establishes a discovery-level signal in the 4ℓ channel alone.

Table 7 presents the numbers of observed and expected events in the peak region. Out of a total of 32 events selected in the data, one and zero candidates are found in the VBF-like and VH-like categories, respectively, compared with an expectation of 0.7 and 0.1 events from the signal and 0.14 and 0.04 events from the background.

Additional interpretation of these results is presented in Section 7.

6. The $H \rightarrow WW^* \rightarrow \ell\nu\ell\nu$ channel

This decay mode provides direct access to the Higgs boson couplings to W bosons. Its rate is large, but a narrow mass peak cannot be reconstructed due to the presence of two neutrinos in the

final state. The reconstructed topology consists of two opposite-charge leptons and a large momentum imbalance from the neutrinos. The dominant SM backgrounds are WW (which includes WW^*), $t\bar{t}$ and Wt, all of which produce two W bosons. The classification of events by jet multiplicity (N_{jet}) allows the control of the background from top quarks, which contains b-quark jets, as well as the extraction of the signal strengths for the ggF and VBF production processes. For the hypothesis of a SM Higgs boson, the spin-zero initial state and the $V{-}A$ structure of the W boson decays imply a correlation between the directions of the charged leptons, which can be exploited to reject the WW background. These correlations lead to the use of quantities such as the dilepton invariant mass $m_{\ell\ell}$ and angular separation $\Delta\phi_{\ell\ell}$ in the selection criteria described below. Drell–Yan (DY) events ($pp \rightarrow Z/\gamma^* \rightarrow \ell\ell$) may be reconstructed with significant missing transverse momentum because of leptonic τ decays or the degradation of the $E_{\text{T}}^{\text{miss}}$ measurement in the high pile-up environment of the 2012 run. Finally, $W +$ jets production in which a jet is reconstructed as a lepton, and the diboson processes $W\gamma^{(*)}$, WZ, and ZZ^*, are also significant backgrounds after all event selection.

The studies presented here are a significant update of those reported in Ref. [2]. The signal regions considered include ee, $e\mu$, and $\mu\mu$ final states with zero, one, or at least two reconstructed jets. The $N_{\text{jet}} \geqslant 2$ analysis has been re-optimised to increase the sensitivity to Higgs boson production through VBF for $m_H = 125$ GeV. Improved DY rejection and estimation techniques have allowed the inclusion of ee and $\mu\mu$ events from the 8 TeV data. The analysis of the 7 TeV data, most recently documented in Ref. [103], has been updated to apply improvements from the 8 TeV analysis, including more stringent lepton isolation requirements, which reduce the $W +$ jets background by 40%.

6.1. Event selection

Events are required to have two opposite-charge leptons (e or μ) and to pass the same single-lepton triggers as described in Section 5 for the $H \rightarrow ZZ^*$ channel. The leading lepton must satisfy $p_{\text{T}} > 25$ GeV and the sub-leading lepton $p_{\text{T}} > 15$ GeV. Electron and muon identification and isolation requirements (see Ref. [2]) are more restrictive than those used in the $H \rightarrow ZZ^*$ analysis in order to suppress the $W +$ jets background.

In the $ee/\mu\mu$ channels, $Z \rightarrow \ell\ell$ and low-mass $\gamma^* \rightarrow \ell\ell$ events, including J/ψ and Υ production, are rejected by requiring $|m_{\ell\ell} - m_Z| > 15$ GeV and $m_{\ell\ell} > 12$ GeV, respectively. In the $e\mu$ channels, low-mass $\gamma^* \rightarrow \tau\tau \rightarrow e\nu\nu\mu\nu\nu$ production is rejected by imposing $m_{\ell\ell} > 10$ GeV.

Drell–Yan and multi-jet backgrounds are suppressed by requiring large missing transverse momentum. For $N_{\text{jet}} \leqslant 1$, a requirement is made on $E_{\text{T,rel}}^{\text{miss}} = E_{\text{T}}^{\text{miss}} \cdot \sin|\Delta\phi_{\text{closest}}|$, where $\Delta\phi_{\text{closest}}$ is the smallest azimuthal angle between the $\mathbf{E}_{\text{T}}^{\text{miss}}$ vector and any jet or high-p_{T} charged lepton in the event; if $|\Delta\phi_{\text{closest}}| > \pi/2$, then $E_{\text{T,rel}}^{\text{miss}} = E_{\text{T}}^{\text{miss}}$ is taken. For additional rejection of the DY background in the $ee/\mu\mu$ channels with $N_{\text{jet}} \leqslant 1$, the track-based $\mathbf{p}_{\text{T}}^{\text{miss}}$ described in Section 2 is used, modified to $p_{\text{T,rel}}^{\text{miss}}$ in a similar way as $E_{\text{T,rel}}^{\text{miss}}$. For these channels, requirements are also made on f_{recoil}, an estimate of the magnitude of the soft hadronic recoil opposite to the system consisting of the leptons and any accompanying jet, normalised to the momentum of the system itself. The f_{recoil} value in DY events is on average larger than that of non-DY events, where the high-p_{T} system is balanced at least in part by recoiling neutrinos.

The $N_{\text{jet}} \geqslant 2$ analysis uses $E_{\text{T}}^{\text{miss}}$ instead of $E_{\text{T,rel}}^{\text{miss}}$ because the larger number of jets in the final states reduces the signal efficiency of the $E_{\text{T,rel}}^{\text{miss}}$ criterion. For the $ee/\mu\mu$ channels with $N_{\text{jet}} \geqslant 2$, an $E_{\text{T}}^{\text{miss}}$ variant called "$E_{\text{T,STVF}}^{\text{miss}}$" is also employed. In the calculation of $E_{\text{T,STVF}}^{\text{miss}}$, the energies of (soft) calorimeter deposits unassociated with high-p_{T} leptons, photons, or jets are scaled by the ratio of the summed scalar p_{T} of tracks from the primary vertex unmatched with such objects to the summed scalar p_{T} of all tracks from any vertex in the event which are also unmatched with objects [104].

For all jet multiplicities, selections exploiting the kinematic features of $H \rightarrow WW^* \rightarrow \ell\nu\ell\nu$ events are applied. The dilepton invariant mass is required to be small, $m_{\ell\ell} < 50$ GeV for $N_{\text{jet}} \leqslant 1$ and $m_{\ell\ell} < 60$ GeV for $N_{\text{jet}} \geqslant 2$; the azimuthal separation of the leptons is also required to be small, $\Delta\phi_{\ell\ell} < 1.8$.

6.2. Event categorisation

The analysis is divided into categories with $N_{\text{jet}} = 0$, $N_{\text{jet}} = 1$, and $N_{\text{jet}} \geqslant 2$. In the $N_{\text{jet}} = 0$ analysis, $E_{\text{T,rel}}^{\text{miss}} > 25$ GeV ($E_{\text{T,rel}}^{\text{miss}} > 45$ GeV and $p_{\text{T,rel}}^{\text{miss}} > 45$ GeV) is required for $e\mu$ ($ee/\mu\mu$) final states. The transverse momentum of the dilepton system is required to be large, $p_{\text{T}}^{\ell\ell} > 30$ GeV. For $ee/\mu\mu$ events, the hadronic recoil is required to be typical of events with neutrinos in the final state, $f_{\text{recoil}} < 0.05$. Finally, the azimuthal separation between the $\mathbf{p}_{\text{T}}^{\ell\ell}$ and $\mathbf{E}_{\text{T}}^{\text{miss}}$ vectors must satisfy $|\Delta\phi_{\ell\ell, E_{\text{T}}^{\text{miss}}}| > \pi/2$, in order to remove potentially poorly reconstructed events.

In the $N_{\text{jet}} = 1$ analysis, the $E_{\text{T,rel}}^{\text{miss}}$ and $p_{\text{T,rel}}^{\text{miss}}$ requirements are the same as for $N_{\text{jet}} = 0$, but the hadronic recoil threshold is looser, $f_{\text{recoil}} < 0.2$. The top-quark background is suppressed by rejecting events with a b-tagged jet. The b-tagging algorithm described in Section 2 is used, at an operating point with 85% efficiency for b-quark jets and a mis-tag rate of 11% for light-quark and gluon jets, as measured in a sample of simulated $t\bar{t}$ events. The $Z \rightarrow \tau\tau$ background in $e\mu$ final states is suppressed using an invariant mass $m_{\tau\tau}$ computed assuming that the neutrinos from τ decays are collinear with the charged leptons [105] and that they are the only source of $E_{\text{T}}^{\text{miss}}$. The requirement $|m_{\tau\tau} - m_Z| \geqslant 25$ GeV is applied.

The $N_{\text{jet}} \geqslant 2$ analysis is optimised for the selection of the VBF production process. The two leading jets, referred to as "tagging jets", are required to have a large rapidity separation, $|\Delta y_{jj}| > 2.8$, and a high invariant mass, $m_{jj} > 500$ GeV. To reduce the contribution from ggF, events containing any jet with $p_{\text{T}} > 20$ GeV in the rapidity gap between the two tagging jets are rejected. Both leptons are required to be in the rapidity gap. The DY background is suppressed by imposing $E_{\text{T}}^{\text{miss}} > 20$ GeV for $e\mu$, and $E_{\text{T}}^{\text{miss}} > 45$ GeV and $E_{\text{T,STVF}}^{\text{miss}} > 35$ GeV for $ee/\mu\mu$. The same $Z \rightarrow \tau\tau$ veto and b-jet veto are applied as in the $N_{\text{jet}} = 1$ analysis. The $t\bar{t}$ background is further reduced by requiring a small total transverse momentum, $|\mathbf{p}_{\text{T}}^{\text{tot}}| < 45$ GeV, where $\mathbf{p}_{\text{T}}^{\text{tot}} = \mathbf{p}_{\text{T}}^{\ell\ell} + \mathbf{p}_{\text{T}}^{\text{jets}} + \mathbf{E}_{\text{T}}^{\text{miss}}$, and $\mathbf{p}_{\text{T}}^{\text{jets}}$ is the vectorial sum of all jets in the event with $p_{\text{T}} > 25$ GeV.

The total signal selection efficiency for $H \rightarrow WW^* \rightarrow \ell\nu\ell\nu$ events produced with $\ell = e, \mu$, including all the final state topologies considered, is about 5.3% at 8 TeV for a Higgs boson mass of 125 GeV.

The dilepton transverse mass m_{T} is the discriminating variable used in the fit to the data to extract the signal strength. It is defined as $m_{\text{T}} = ((E_{\text{T}}^{\ell\ell} + E_{\text{T}}^{\text{miss}})^2 - |\mathbf{p}_{\text{T}}^{\ell\ell} + \mathbf{E}_{\text{T}}^{\text{miss}}|^2)^{1/2}$ with $E_{\text{T}}^{\ell\ell} = (|\mathbf{p}_{\text{T}}^{\ell\ell}|^2 + m_{\ell\ell}^2)^{1/2}$. For the $e\mu$ channels with $N_{\text{jet}} \leqslant 1$, the fit is performed separately for events with 10 GeV $< m_{\ell\ell} < 30$ GeV and events with 30 GeV $< m_{\ell\ell} < 50$ GeV, since the signal-to-background ratio varies across the $m_{\ell\ell}$ distribution, as shown in Fig. 4.
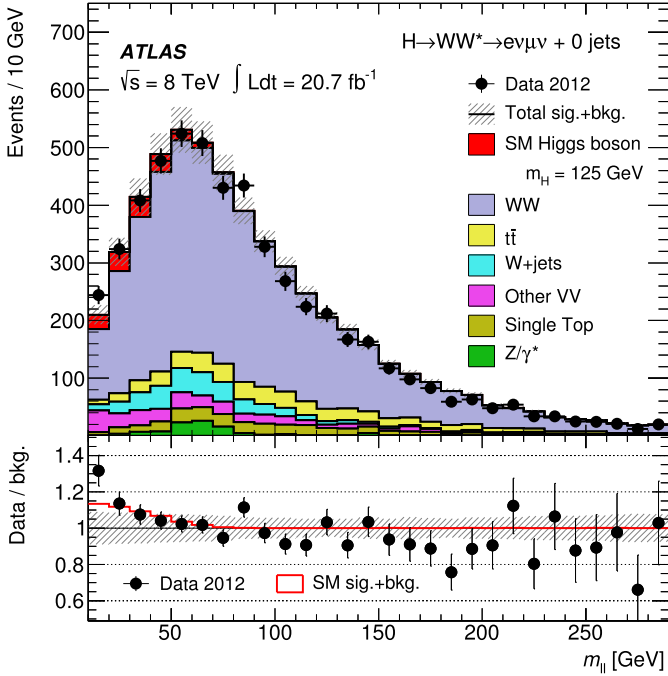
Fig. 4. The $m_{\ell\ell}$ distribution of $e\mu$ events with $N_{jet} = 0$ for the 8 TeV $H \to WW^* \to \ell\nu\ell\nu$ analysis. The events with $m_{\ell\ell} < 50$ GeV correspond to the signal region except that the $\Delta\phi_{\ell\ell} < 1.8$ requirement is not applied here, and the events with 50 GeV $< m_{\ell\ell} < 100$ GeV correspond to the $N_{jet} = 0$ WW control region. The signal is stacked on top of the background. The hatched area represents the total uncertainty on the sum of the signal and background yields from statistical, experimental, and theoretical sources. The lower part of the figure shows the ratio of the data to the predicted background. For comparison, the expected ratio of the signal plus background to the background alone is also shown.

6.3. Background estimation

The leading SM processes producing two isolated high-p_T leptons and large values of E_T^{miss} are WW and top-quark production, where the latter includes (here and in the following) both $t\bar{t}$ and single top-quark processes (tW, tb and tqb). These backgrounds, as well as $Z \to \tau\tau$, are normalised to the data in control regions defined by selections similar to those used for the signal region, but with some criteria reversed or modified to obtain signal-depleted samples enriched in particular backgrounds. The event yield in the CR (after subtracting contributions from processes other than the targeted one) is extrapolated to the signal region using transfer factors obtained from MC simulation.

Additional significant backgrounds arise from W + jets and Z/γ^*, which are dissimilar to the signal but have large cross sections. A small fraction of these pass the event selection through rare final-state configurations and/or mis-measurements. This type of background is difficult to model reliably with the simulation and is therefore estimated mainly from data.

A third category of background consists of diboson processes with smaller cross sections, including $W\gamma^{(*)}$, WZ, and ZZ^* (inclusively indicated in the following as *Other VV*), and the WW background in the $N_{jet} \geq 2$ analysis. These processes are estimated using the MC simulation normalised to the NLO cross sections from MCFM [106], except for the $N_{jet} \geq 2$ WW background, for which the cross section from the relevant MC generators (see Table 2) is used. The *Other VV* processes all produce same-charge and opposite-charge lepton pairs, as does W + jets. The number and kinematic features of same-charge events which would otherwise pass the full event selection are compared to the above-

mentioned predictions for these backgrounds, and good agreement is observed.

6.3.1. W + jets

The W + jets background is estimated using a CR in the data in which one of the two leptons satisfies the identification and isolation criteria, and the other lepton (denoted here as "anti-identified") fails these criteria but satisfies looser requirements. All other analysis selections are applied. The contribution to the signal region is then obtained by scaling the number of events in the CR by transfer factors, defined as the ratio of the number of fully identified lepton candidates passing all selections to the number of anti-identified leptons. The transfer factors are obtained from a dijet sample as a function of the p_T and η of the anti-identified lepton.

6.3.2. Z/γ*

The Z/γ^* yield in the $ee/\mu\mu$ channels for $N_{jet} \leq 1$ is estimated using the f_{recoil} requirement efficiency in data for DY and non-DY processes. The former is measured in $ee/\mu\mu$ events in the Z boson peak region. The latter is measured in the $e\mu$ signal region, taking advantage of the fact that the f_{recoil} distribution is nearly identical for all non-DY processes including the signal, as well as for $e\mu$ and $ee/\mu\mu$ final states. The DY normalisation in the $ee/\mu\mu$ signal region can then be extracted, given the two measured efficiencies and the total number of events in the $ee/\mu\mu$ signal region before and after the f_{recoil} requirement. For the $ee/\mu\mu$ channels with $N_{jet} \geq 2$, the two-dimensional distribution (E_T^{miss}, $m_{\ell\ell}$) in the data is used to estimate the total Z/γ^* yield, as in Ref. [103].

The $Z \to \tau\tau$ background is normalised to the data using an $e\mu$ CR defined by the back-to-back configuration of the leptons, $\Delta\phi_{\ell\ell} > 2.8$. For the corresponding CR with $N_{jet} \geq 2$, no b-tagged jets are allowed, and $|\mathbf{p}_T^{tot}| < 45$ GeV is required in addition, in order to reduce the contamination from top-quark production. A separate CR in the $Z \to \ell\ell$ peak region is used to correct the modelling of the VBF-related event selection.

6.3.3. $t\bar{t}$ and single top-quark

The top-quark background for the $N_{jet} = 0$ category is estimated using the procedure described in Ref. [2], namely from the number of events in data with any number of reconstructed jets passing the $E_{T,rel}^{miss}$ requirement (a sample dominated by top-quark production), multiplied by the fraction of top-quark events with no reconstructed jets obtained from simulation. This estimate is corrected using a CR containing b-tagged jets. The top-quark background in the $N_{jet} \geq 1$ channels is normalised to the data in a CR defined by requiring exactly one b-tagged jet and all other signal selections except for the requirements on $\Delta\phi_{\ell\ell}$ and $m_{\ell\ell}$.

6.3.4. WW

The WW background for $N_{jet} \leq 1$ is normalised using CRs in data defined with the same selection as the signal region except that the $\Delta\phi_{\ell\ell}$ requirement is removed and the $m_{\ell\ell}$ bound is modified: for $N_{jet} = 0$ 50 GeV $\leq m_{\ell\ell} < 100$ GeV is required, while for $N_{jet} = 1$ $m_{\ell\ell} > 80$ GeV is used to define the CR. Fig. 4 shows the $m_{\ell\ell}$ distribution of $e\mu$ events with $N_{jet} = 0$ in the 8 TeV data. The level of agreement between the predicted background and the data for $m_{\ell\ell} > 100$ GeV, a region with negligible signal contribution, validates the WW background normalisation and the extrapolation procedure based on the simulation. The $N_{jet} \geq 2$ prediction is taken from simulation because of the difficulty of isolating a kinematic region with enough events and small contamination from the top-quark background.

Table 8

For $m_H = 125$ GeV, the leading systematic uncertainties on the total signal and background yields for the 8 TeV $H \to WW^* \to \ell\nu\ell\nu$ analysis. All numbers are summed over lepton flavours. Sources contributing less than 4% are omitted, and individual entries below 1% are indicated with a '−'. Relative signs indicate correlation and anticorrelation (migration) between the N_{jet} categories represented by adjacent columns, and a $\pm$ indicates an uncorrelated uncertainty. The exception is the jet energy scale and resolution, which includes multiple sources of uncertainty treated as correlated across categories but uncorrelated with each other. All rows are uncorrelated.

Source	$N_{\mathrm{jet}} = 0$	$N_{\mathrm{jet}} = 1$	$N_{\mathrm{jet}} \geqslant 2$
Theoretical uncertainties on total signal yield (%)			
QCD scale for ggF, $N_{\mathrm{jet}} \geqslant 0$	+13	−	−
QCD scale for ggF, $N_{\mathrm{jet}} \geqslant 1$	+10	−27	−
QCD scale for ggF, $N_{\mathrm{jet}} \geqslant 2$	−	−15	+4
QCD scale for ggF, $N_{\mathrm{jet}} \geqslant 3$	−	−	+4
Parton shower and underlying event	+3	−10	±5
QCD scale (acceptance)	+4	+4	±3
Experimental uncertainties on total signal yield (%)			
Jet energy scale and resolution	5	2	6
Uncertainties on total background yield (%)			
Jet energy scale and resolution	2	3	7
WW transfer factors (theory)	±1	±2	±4
b-tagging efficiency	−	+7	+2
f_{recoil} efficiency	±4	±2	−

6.4. Systematic uncertainties

The systematic uncertainties affecting this analysis are summarized here and described in detail in Ref. [107]. The leading sources, i.e., those resulting in at least 4% uncertainty on the total signal or background yield in at least one N_{jet} category, are reported in Table 8.

Theoretical uncertainties on the inclusive signal production cross sections are given in Section 2. Additional, larger uncertainties from the QCD renormalisation and factorisation scales affect the predicted distribution of the ggF signal among the exclusive jet bins and can produce migration between categories. These uncertainties are estimated using the HNNLO program [108, 109] and the method reported in Ref. [110]. Their impact on the signal yield is summarised in Table 8, in addition to other non-negligible contributions (parton shower and underlying event modelling, as well as acceptance uncertainties due to QCD scale variations).

The experimental uncertainties affecting the expected signal and background yields are associated primarily with the reconstruction and identification efficiency, and with the energy and momentum scale and resolution, of the final-state objects (leptons, jets, and $E_{\mathrm{T}}^{\mathrm{miss}}$), as described in Section 2. The largest impact on the signal expectation comes from the knowledge of the jet energy scale and resolution (up to 6% in the $N_{\mathrm{jet}} \geqslant 2$ channel).

For the backgrounds normalised using control regions, uncertainties come from the numbers of events in the CR and the contributions of other processes, as well as the transfer factors to the signal region.

For the WW background in the $N_{\mathrm{jet}} \leqslant 1$ final states, the theoretical uncertainties on the transfer factors (evaluated according to the prescription of Ref. [15]) include the impact of missing higher-order QCD corrections, PDF variations, and MC modelling choices. They amount to $\pm 2\%$ and ± 4–6% relative to the predicted WW background in the $N_{\mathrm{jet}} = 0$ and $N_{\mathrm{jet}} = 1$ final states, respectively. For the WW yield in the $N_{\mathrm{jet}} \geqslant 2$ channel, which is obtained from simulation, the total uncertainty is 42% for QCD production with gluon emission, and 11% for the smaller but non-negligible contribution from purely electroweak processes; the latter includes the size of possible interference with Higgs boson production through

VBF. The resulting uncertainties on the total background yield for all N_{jet} are quoted in Table 8.

The leading uncertainties on the top-quark background are experimental. The b-tagging efficiency is the most important of these, and it appears in Table 8 primarily through its effect on this background. Theoretical uncertainties on the top-quark background have the greatest relative importance, $\pm 2\%$ on the total background yield, for $N_{\mathrm{jet}} \geqslant 2$, and therefore do not appear in Table 8.

The $W +$ jets transfer factor uncertainty ($\pm(40$–45)%) is dominated by differences in the jet composition between dijet and $W +$ jets samples as observed in the MC simulation. The uncertainties on the muon and electron transfer factors are treated as correlated among the N_{jet} categories but uncorrelated with each other. The impact on the total background uncertainty is at most $\pm 2.5\%$. The main uncertainty on the DY contribution in the $N_{\mathrm{jet}} \leqslant 1$ channels comes from the use of the f_{recoil} efficiency evaluated at the peak of the Z boson mass distribution for the estimation of the DY contamination in the low-$m_{\ell\ell}$ region.

The uncertainty on the m_{T} shape for the total background, which is used in the fit to extract the signal yield, is dominated by the uncertainties on the normalisations of the individual components. The only explicit m_{T} shape uncertainty is applied to the WW background, and is determined by comparing several generators and showering algorithms.

The estimated background contributions with their uncertainties are listed in Table 9.

6.5. Results

Fig. 5 shows the transverse mass distributions after the full selection for $N_{\mathrm{jet}} \leqslant 1$ and $N_{\mathrm{jet}} \geqslant 2$ final states. The regions with $m_{\mathrm{T}} > 150$ GeV are depleted of signal contribution; the level of agreement of the data with the expectation in these regions, which are different from those used to normalise the backgrounds, illustrates the quality of the background estimates. The expected numbers of signal and background events at 8 TeV are presented in Table 9. The VBF process contributes 2%, 12% and 81% of the predicted signal in the $N_{\mathrm{jet}} = 0, = 1$, and $\geqslant 2$ final states, respectively. The total number of observed events in the same m_{T} windows as in Table 9 is 218 in the 7 TeV data and 1195 in the 8 TeV data.

An excess of events relative to the background-only expectation is observed in the data, with the maximum deviation (4.1σ) occurring at $m_H = 140$ GeV. For $m_H = 125.5$ GeV, a significance of 3.8σ is observed, compared with an expected value of 3.8σ for a SM Higgs boson.

Additional interpretation of these results is presented in Section 7.

7. Higgs boson property measurements

The results from the individual channels described in the previous sections are combined here to extract information about the Higgs boson mass, production properties and couplings.

7.1. Statistical method

The statistical treatment of the data is described in Refs. [111–115]. Hypothesis testing and confidence intervals are based on the profile likelihood ratio [116] $\Lambda(\boldsymbol{\alpha})$. The latter depends on one or more parameters of interest $\boldsymbol{\alpha}$, such as the Higgs boson production strength μ normalised to the SM expectation (so that $\mu = 1$ corresponds to the SM Higgs boson hypothesis and $\mu = 0$ to the background-only hypothesis), mass m_H, coupling strengths $\boldsymbol{\kappa}$, ratios of coupling strengths $\boldsymbol{\lambda}$, as well as on nuisance parameters $\boldsymbol{\theta}$:
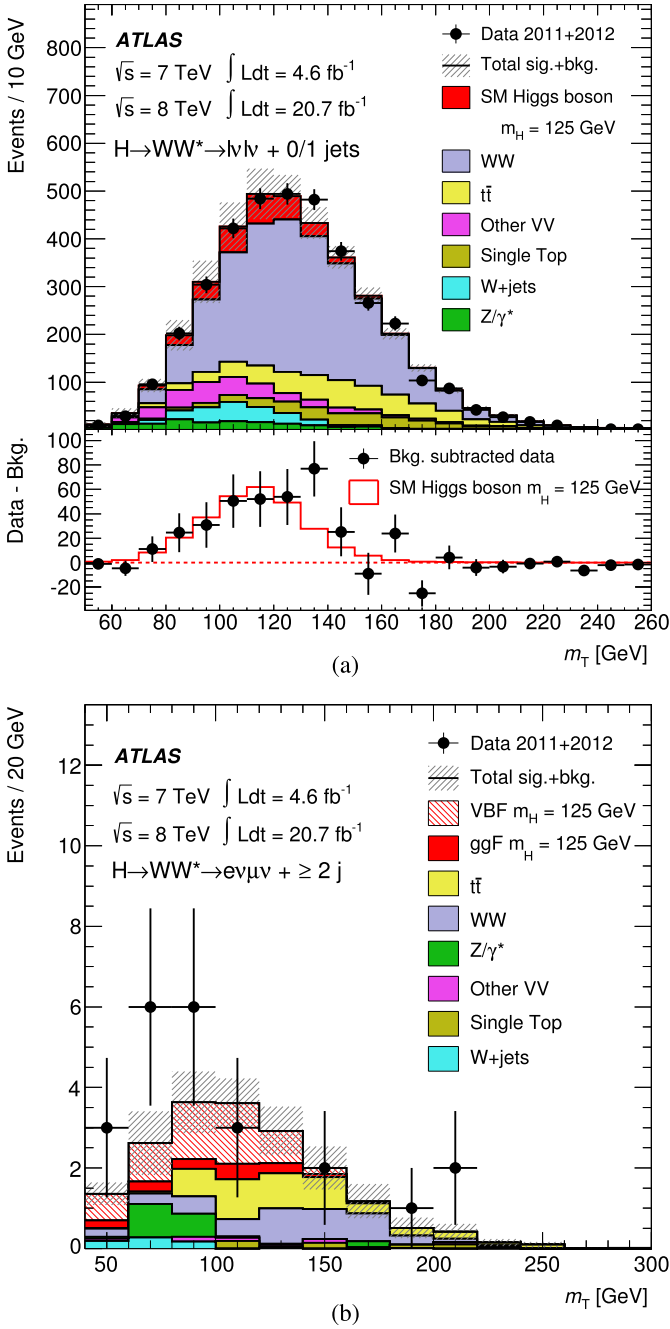
Fig. 5. The transverse mass distributions for events passing the full selection of the $H \to WW^* \to \ell\nu\ell\nu$ analysis: (a) summed over all lepton flavours for final states with $N_{jet} \leqslant 1$; (b) different-flavour final states with $N_{jet} \geqslant 2$. The signal is stacked on top of the background, and in (b) is shown separately for the ggF and VBF production processes. The hatched area represents the total uncertainty on the sum of the signal and background yields from statistical, experimental, and theoretical sources. In the lower part of (a), the residuals of the data with respect to the estimated background are shown, compared to the expected m_T distribution of a SM Higgs boson.

$$\Lambda(\boldsymbol{\alpha}) = \frac{L(\boldsymbol{\alpha}, \hat{\hat{\boldsymbol{\theta}}}(\boldsymbol{\alpha}))}{L(\hat{\boldsymbol{\alpha}}, \hat{\boldsymbol{\theta}})}. \qquad (1)$$

The likelihood functions in the numerator and denominator of the above equation are built using sums of signal and background probability density functions (pdfs) in the discriminating variables (chosen to be the $\gamma\gamma$ and 4ℓ mass spectra for $H \to \gamma\gamma$ and $H \to ZZ^* \to 4\ell$, respectively, and the m_T distribution for the

Table 9

For the $H \to WW^* \to \ell\nu\ell\nu$ analysis of the 8 TeV data, the numbers of events observed in the data and expected from signal ($m_H = 125.5$ GeV) and backgrounds inside the transverse mass regions $0.75m_H < m_T < m_H$ for $N_{jet} \leqslant 1$ and $m_T < 1.2m_H$ for $N_{jet} \geqslant 2$. All lepton flavours are combined. The total background as well as its main components are shown. The quoted uncertainties include the statistical and systematic contributions, and account for anticorrelations between the background predictions.

	$N_{jet} = 0$	$N_{jet} = 1$	$N_{jet} \geqslant 2$
Observed	831	309	55
Signal	100 ± 21	41 ± 14	10.9 ± 1.4
Total background	739 ± 39	261 ± 28	36 ± 4
WW	551 ± 41	108 ± 40	4.1 ± 1.5
Other VV	58 ± 8	27 ± 6	1.9 ± 0.4
Top-quark	39 ± 5	95 ± 28	5.4 ± 2.1
Z+jets	30 ± 10	12 ± 6	22 ± 3
W +jets	61 ± 21	20 ± 5	0.7 ± 0.2

$H \to WW^* \to \ell\nu\ell\nu$ channel). The pdfs are derived from MC simulation for the signal and from both data and simulation for the background, as described in Sections 4–6. Likelihood fits to the observed data are done for the parameters of interest. The single circumflex in Eq. (1) denotes the unconditional maximum likelihood estimate of a parameter and the double circumflex denotes the conditional maximum likelihood estimate for given fixed values of the parameters of interest $\boldsymbol{\alpha}$. Systematic uncertainties and their correlations [111] are modelled by introducing nuisance parameters $\boldsymbol{\theta}$ described by likelihood functions associated with the estimate of the corresponding effect. The choice of the parameters of interest depends on the test under consideration, with the remaining parameters being "profiled", *i.e.*, similarly to nuisance parameters they are set to the values that maximise the likelihood function for the given fixed values of the parameters of interest.

7.2. Mass and production strength

The mass of the new particle is measured from the data using the two channels with the best mass resolution, $H \to \gamma\gamma$ and $H \to ZZ^* \to 4\ell$. In the two cases, $m_H = 126.8 \pm 0.2(\text{stat}) \pm 0.7(\text{sys})$ GeV and $m_H = 124.3^{+0.6}_{-0.5}(\text{stat})^{+0.5}_{-0.3}(\text{sys})$ GeV are obtained from fits to the mass spectra.

To derive a combined mass measurement, the profile likelihood ratio $\Lambda(m_H)$ is used; the signal production strengths $\mu^{\gamma\gamma}$ and $\mu^{4\ell}$, giving the signal yields measured in the two individual channels normalised to the SM expectation, are treated as independent nuisance parameters in order to allow for the possibility of different deviations from the SM prediction in the two decay modes. The ratios of the cross sections for the various production modes for each channel are fixed to the SM values. It was verified that this restriction does not cause any bias in the results. The combined mass is measured to be:

$$m_H = 125.5 \pm 0.2(\text{stat})^{+0.5}_{-0.6}(\text{sys}) \text{ GeV}. \qquad (2)$$

As discussed in Sections 4.4 and 5.4, the main sources of systematic uncertainty are the photon and lepton energy and momentum scales. In the combination, the consistency between the muon and electron final states in the $H \to ZZ^* \to 4\ell$ channel causes a $\sim 0.8\sigma$ adjustment of the overall e/γ energy scale, which translates into a ~ 350 MeV downward shift of the fitted $m_H^{\gamma\gamma}$ value with respect to the value measured from the $H \to \gamma\gamma$ channel alone.

To quantify the consistency between the fitted $m_H^{\gamma\gamma}$ and $m_H^{4\ell}$ masses, the data are fitted with the profile likelihood ratio $\Lambda(\Delta m_H)$, where the parameter of interest is the mass difference $\Delta m_H = m_H^{\gamma\gamma} - m_H^{4\ell}$. The average mass m_H and the signal strengths

ATLAS
m_H = 125.5 GeV

σ(stat) — Total uncertainty
σ(sys)   ± 1σ on μ
σ(theo)

Channel	μ	σ(stat)	σ(sys)	σ(theo)
H → γγ	$\mu = 1.55^{+0.33}_{-0.28}$	±0.23	±0.21	±0.15
Low p_{Tt}	$\mu = 1.6^{+0.5}_{-0.4}$	±0.3		
High p_{Tt}	$\mu = 1.7^{+0.7}_{-0.6}$	±0.5		
2 jet high mass (VBF)	$\mu = 1.9^{+0.8}_{-0.6}$	±0.6		
VH categories	$\mu = 1.3^{+1.2}_{-1.1}$	±0.9		
H → ZZ* → 4l	$\mu = 1.43^{+0.40}_{-0.35}$	±0.33	±0.17	±0.14
VBF+VH-like categories	$\mu = 1.2^{+1.6}_{-0.9}$	+1.6 −0.9		
Other categories	$\mu = 1.45^{+0.43}_{-0.36}$	±0.35		
H → WW* → lνlν	$\mu = 0.99^{+0.31}_{-0.28}$	±0.21	±0.21	±0.12
0+1 jet	$\mu = 0.82^{+0.33}_{-0.32}$	±0.22		
2 jet VBF	$\mu = 1.4^{+0.7}_{-0.6}$	±0.5		
Comb. H→γγ, ZZ*, WW*	$\mu = 1.33^{+0.21}_{-0.18}$	±0.14	±0.15	±0.11

0   1   2   3
Signal strength (μ)

$\sqrt{s}$ = 7 TeV ∫Ldt = 4.6-4.8 fb⁻¹
$\sqrt{s}$ = 8 TeV ∫Ldt = 20.7 fb⁻¹

Fig. 6. The measured production strengths for a Higgs boson of mass m_H = 125.5 GeV, normalised to the SM expectations, for the individual diboson final states and their combination. Results are also given for the main categories of each analysis (described in Sections 4.2, 5.2 and 6.2). The best-fit values are shown by the solid vertical lines, with the total ±1σ uncertainty indicated by the shaded band, and the statistical uncertainty by the superimposed horizontal error bars. The numbers in the second column specify the contributions of the (symmetrised) statistical uncertainty (top), the total (experimental and theoretical) systematic uncertainty (middle), and the theory uncertainty (bottom) on the signal cross section (from QCD scale, PDF, and branching ratios) alone; for the individual categories only the statistical uncertainty is given.

$\mu^{\gamma\gamma}$ and $\mu^{4\ell}$ are treated as independent nuisance parameters. The result is:

$$\Delta m_H = 2.3^{+0.6}_{-0.7}\text{(stat)} \pm 0.6\text{(sys) GeV} \qquad (3)$$

where the uncertainties are 68% confidence intervals computed with the asymptotic approximation [116]. From the value of the likelihood at $\Delta m_H = 0$, the probability for a single Higgs boson to give a value of $\Lambda(\Delta m_H)$ disfavouring the $\Delta m_H = 0$ hypothesis more strongly than observed in the data is found to be at the level of 1.2% (2.5σ) using the asymptotic approximation, and 1.5% (2.4σ) using Monte Carlo ensemble tests. In order to test the effect of a possible non-Gaussian behaviour of the three principal sources contributing to the electron and photon energy scale systematic uncertainty (the $Z \to ee$ calibration procedure, the knowledge of the material upstream of the electromagnetic calorimeter and the energy scale of the presampler detector) the consistency between the two mass measurements is also evaluated by considering ±1σ values for these uncertainties. With this treatment, the consistency increases to up to 8%.

To measure the Higgs boson production strength, the parameter μ is determined from a fit to the data using the profile likelihood ratio $\Lambda(\mu)$ for a fixed mass hypothesis corresponding to the measured value m_H = 125.5 GeV. The results are shown in Fig. 6,

where the production strengths measured in the three channels and in their main analysis categories are presented. The signal production strength normalised to the SM expectation, obtained by combining the three channels, is:

$$\mu = 1.33 \pm 0.14\text{(stat)} \pm 0.15\text{(sys)} \qquad (4)$$

where the systematic uncertainty receives similar contributions from the theoretical uncertainty on the signal cross section (ggF QCD scale and PDF, see Table 1) and all other, mainly experimental, sources. The uncertainty on the mass measurement reported in Eq. (2) produces a ±3% variation of μ. The consistency between this measurement and the SM Higgs boson expectation ($\mu = 1$) is about 7%; the use of a flat likelihood for the ggF QCD scale systematic uncertainty in the quoted ±1σ interval yields a similar level of consistency with the $\mu = 1$ hypothesis. The overall compatibility between the signal strengths measured in the three final states and the SM predictions is about 14%, with the largest deviation ($\sim 1.9\sigma$) observed in the $H \to \gamma\gamma$ channel. Good consistency between the measured and expected signal strengths is also found for the various categories of the $H \to \gamma\gamma$, $H \to ZZ^* \to 4\ell$ and $H \to WW^* \to \ell\nu\ell\nu$ analyses, which are the primary experimental inputs to the fit discussed in this section. If the preliminary $H \to \tau\tau$ [117] and $H \to b\bar{b}$ [118] results, for which only part of the 8 TeV dataset is used (13 fb⁻¹), were included, the combined signal strength would be $\mu = 1.23 \pm 0.18$.

7.3. Evidence for production via vector-boson fusion

The measurements of the signal strengths described in the previous section do not give direct information on the relative contributions of the different production mechanisms. Furthermore, fixing the ratios of the production cross sections for the various processes to the values predicted by the Standard Model may conceal tensions between the data and the theory. Therefore, in addition to the signal strengths for different decay modes, the signal strengths of different production processes contributing to the same decay mode[4] are determined, exploiting the sensitivity offered by the use of event categories in the analyses of the three channels.

The data are fitted separating vector-boson-mediated processes, VBF and *VH*, from gluon-mediated processes, ggF and *ttH*, involving fermion (mainly top-quark) loops or legs.[5] Two signal strength parameters, $\mu^f_{\text{ggF}+ttH} = \mu^f_{\text{ggF}} = \mu^f_{ttH}$ and $\mu^f_{\text{VBF}+VH} = \mu^f_{\text{VBF}} = \mu^f_{VH}$, which scale the SM-predicted rates to those observed, are introduced for each of the considered final states ($f = H \to \gamma\gamma$, $H \to ZZ^* \to 4\ell$, $H \to WW^* \to \ell\nu\ell\nu$). The results are shown in Fig. 7. The 95% CL contours of the measurements are consistent with the SM expectation. A combination of all channels would provide a higher-sensitivity test of the theory. This can be done in a model-independent way (*i.e.* without assumptions on the Higgs boson branching ratios) by measuring the ratios $\mu_{\text{VBF}+VH}/\mu_{\text{ggF}+ttH}$ for the individual final states and their combination. The results of the fit to the data with the likelihood $\Lambda(\mu_{\text{VBF}+VH}/\mu_{\text{ggF}+ttH})$ are shown in Fig. 8. Good agreement with the SM expectation is observed for the individual final states and their combination.

To test the sensitivity to VBF production alone, the data are also fitted with the ratio $\mu_{\text{VBF}}/\mu_{\text{ggF}+ttH}$. A value

$$\mu_{\text{VBF}}/\mu_{\text{ggF}+ttH} = 1.4^{+0.4}_{-0.3}\,\text{(stat)}^{+0.6}_{-0.4}\text{(sys)} \qquad (5)$$

---

[4] Such an approach avoids model assumptions needed for a consistent parameterisation of production and decay modes in terms of Higgs boson couplings.

[5] Such a separation is possible under the assumption that the kinematic properties of these production modes agree with the SM predictions within uncertainties.
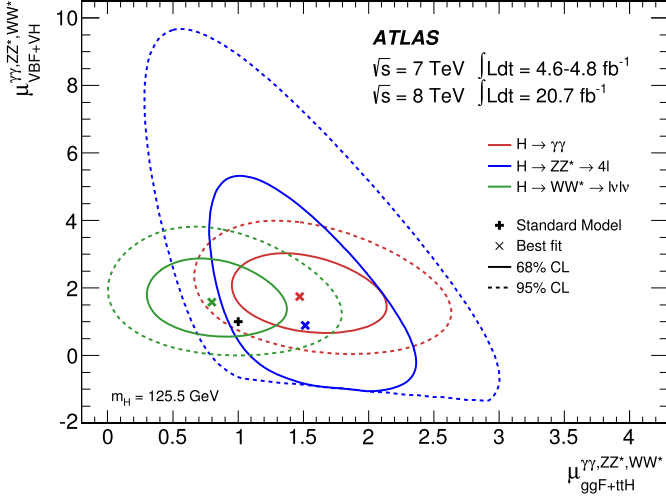
Fig. 7. Likelihood contours in the $(\mu^f_{ggF+ttH}, \mu^f_{VBF+VH})$ plane for the final states $f = H \to \gamma\gamma, H \to ZZ^* \to 4\ell, H \to WW^* \to \ell\nu\ell\nu$ and a Higgs boson mass $m_H = 125.5$ GeV. The sharp lower edge of the $H \to ZZ^* \to 4\ell$ contours is due to the small number of events in this channel and the requirement of a positive pdf. The best fits to the data ($\times$) and the 68% (full) and 95% (dashed) CL contours are indicated, as well as the SM expectation ($+$).
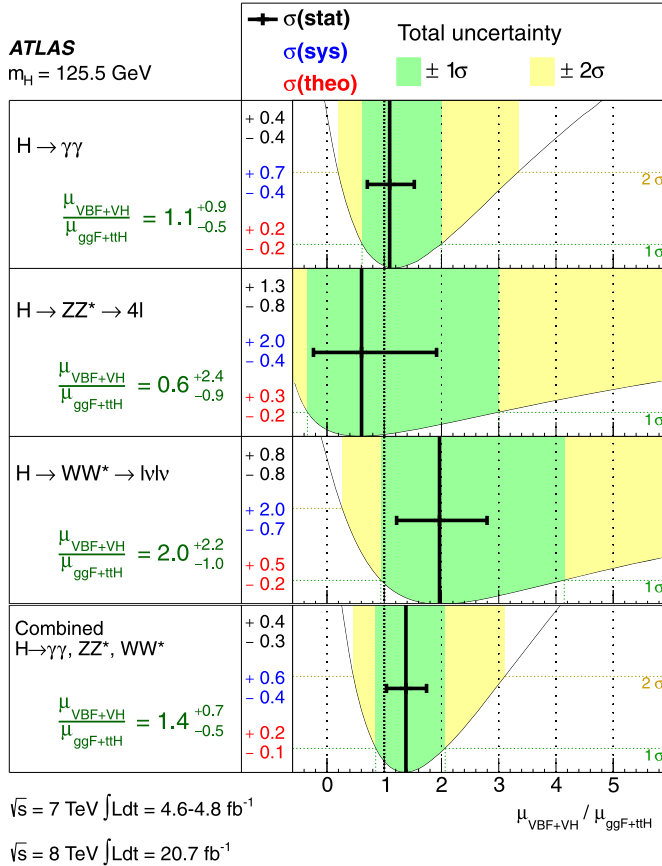
Fig. 8. Measurements of the $\mu_{VBF+VH}/\mu_{ggF+ttH}$ ratios for the individual diboson final states and their combination, for a Higgs boson mass $m_H = 125.5$ GeV. The best-fit values are represented by the solid vertical lines, with the total $\pm 1\sigma$ and $\pm 2\sigma$ uncertainties indicated by the dark- and light-shaded band, respectively, and the statistical uncertainties by the superimposed horizontal error bars. The numbers in the second column specify the contributions of the statistical uncertainty (top), the total (experimental and theoretical) systematic uncertainty (middle), and the theoretical uncertainty (bottom) on the signal cross section (from QCD scale, PDF, and branching ratios) alone. For a more complete illustration, the distributions of the likelihood ratios from which the total uncertainties are extracted are overlaid.
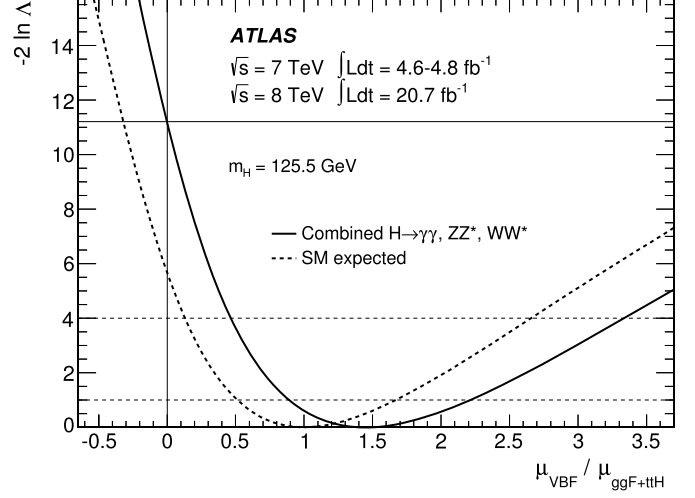
Fig. 9. Likelihood curve for the ratio $\mu_{VBF}/\mu_{ggF+ttH}$ for the combination of the $H \to \gamma\gamma, H \to ZZ^* \to 4\ell$ and $H \to WW^* \to \ell\nu\ell\nu$ channels and a Higgs boson mass $m_H = 125.5$ GeV. The parameter $\mu_{VH}/\mu_{ggF+ttH}$ is profiled in the fit. The dashed curve shows the SM expectation. The horizontal dashed lines indicate the 68% and 95% CL.

is obtained from the combination of the three channels (Fig. 9), where the main components of the systematic uncertainty come from the theoretical predictions for the ggF contributions to the various categories and jet multiplicities and the knowledge of the jet energy scale and resolution. This result provides evidence at the 3.3σ level that a fraction of Higgs boson production occurs through VBF (as Fig. 9 shows, the probability for a vanishing value of $\mu_{VBF}/\mu_{ggF+ttH}$, given the observation in the data, is 0.04%). The inclusion of preliminary $H \to \tau\tau$ results [117], which also provide some sensitivity to this ratio, would give a significance of 3.1σ.

7.4. Couplings measurements

Following the approach and benchmarks recommended in Ref. [119], measurements of couplings are implemented using a leading-order tree-level motivated framework. This framework is based on the following assumptions:

– The signals observed in the different search channels originate from a single resonance. A mass of 125.5 GeV is assumed here; the impact of the uncertainty reported in Eq. (2) on the results discussed in this section is negligible.
– The width of the Higgs boson is narrow, justifying the use of the zero-width approximation. Hence the predicted rate for a given channel can be decomposed in the following way:

$$\sigma \cdot B (i \to H \to f) = \frac{\sigma_i \cdot \Gamma_f}{\Gamma_H} \qquad (6)$$

where σ_i is the production cross section through the initial state i, B and Γ_f are the branching ratio and partial decay width into the final state f, respectively, and Γ_H the total width of the Higgs boson.
– Only modifications of coupling strengths are considered, while the tensor structure of the Lagrangian is assumed to be the same as in the Standard Model. This implies in particular that the observed state is a CP-even scalar.[6]

The coupling scale factors κ_j are defined in such a way that the cross sections σ_j and the partial decay widths Γ_j associated

---

[6] The spin-CP hypothesis is addressed in Ref. [10].

Table 10
Summary of the coupling benchmark models discussed in this Letter, where $\lambda_{ij} = \kappa_i/\kappa_j$, $\kappa_{ii} = \kappa_i\kappa_i/\kappa_H$, and the functional dependence assumptions are: $\kappa_V = \kappa_W = \kappa_Z$, $\kappa_F = \kappa_t = \kappa_b = \kappa_\tau$ (and similarly for the other fermions), $\kappa_g = \kappa_g(\kappa_b, \kappa_t)$, $\kappa_\gamma = \kappa_\gamma(\kappa_b, \kappa_t, \kappa_\tau, \kappa_W)$, and $\kappa_H = \kappa_H(\kappa_i)$. The tick marks indicate which assumptions are made in each case. The last column shows, as an example, the relative couplings involved in the $gg \to H \to \gamma\gamma$ process, see Eq. (7), and their functional dependence in the various benchmark models.

Model	Probed couplings	Parameters of interest	Functional assumptions					Example: $gg \to H \to \gamma\gamma$
			κ_V	κ_F	κ_g	κ_γ	κ_H	
1	Couplings to fermions and bosons	κ_V, κ_F	✓	✓	✓	✓	✓	$\kappa_F^2 \cdot \kappa_\gamma^2(\kappa_F, \kappa_V)/\kappa_H^2(\kappa_F, \kappa_V)$
2		$\lambda_{FV}, \kappa_{VV}$	✓	✓	✓	✓	–	$\kappa_{VV}^2 \cdot \lambda_{FV}^2 \cdot \kappa_\gamma^2(\lambda_{FV}, \lambda_{FV}, \lambda_{FV}, 1)$
3	Custodial symmetry	$\lambda_{WZ}, \lambda_{FZ}, \kappa_{ZZ}$	–	✓	✓	✓	–	$\kappa_{ZZ}^2 \cdot \lambda_{FZ}^2 \cdot \kappa_\gamma^2(\lambda_{FZ}, \lambda_{FZ}, \lambda_{FZ}, \lambda_{WZ})$
4		$\lambda_{WZ}, \lambda_{FZ}, \lambda_{\gamma Z}, \kappa_{ZZ}$	–	✓	✓	–	–	$\kappa_{ZZ}^2 \cdot \lambda_{FZ}^2 \cdot \lambda_{\gamma Z}^2$
5	Vertex loops	κ_g, κ_γ	= 1	= 1	–	–	✓	$\kappa_g^2 \cdot \kappa_\gamma^2/\kappa_H^2(\kappa_g, \kappa_\gamma)$

with the SM particle j scale with κ_j^2 compared to the SM prediction [119]. With this notation, and with κ_H^2 being the scale factor for the total Higgs boson width Γ_H, the cross section for the $gg \to H \to \gamma\gamma$ process, for example, can be expressed as:

$$\frac{\sigma \cdot B(gg \to H \to \gamma\gamma)}{\sigma_{SM}(gg \to H) \cdot B_{SM}(H \to \gamma\gamma)} = \frac{\kappa_g^2 \cdot \kappa_\gamma^2}{\kappa_H^2}. \quad (7)$$

In some of the fits, κ_H and the effective scale factors κ_γ and κ_g for the loop-induced $H \to \gamma\gamma$ and $gg \to H$ processes are expressed as a function of the more fundamental factors κ_W, κ_Z, κ_t, κ_b and κ_τ (only the dominant fermion contributions are indicated here for simplicity). The relevant relationships are:

$$\kappa_g^2(\kappa_b, \kappa_t) = \frac{\kappa_t^2 \cdot \sigma_{ggH}^{tt} + \kappa_b^2 \cdot \sigma_{ggH}^{bb} + \kappa_t\kappa_b \cdot \sigma_{ggH}^{tb}}{\sigma_{ggH}^{tt} + \sigma_{ggH}^{bb} + \sigma_{ggH}^{tb}},$$

$$\kappa_\gamma^2(\kappa_b, \kappa_t, \kappa_\tau, \kappa_W) = \frac{\sum_{i,j} \kappa_i \kappa_j \cdot \Gamma_{\gamma\gamma}^{ij}}{\sum_{i,j} \Gamma_{\gamma\gamma}^{ij}},$$

$$\kappa_H^2 = \sum_{\substack{jj=WW^*,ZZ^*,b\bar{b},\tau^-\tau^+, \\ \gamma\gamma,Z\gamma,t\bar{t},c\bar{c},s\bar{s},\mu^-\mu^+}} \frac{\kappa_j^2 \Gamma_{jj}^{SM}}{\Gamma_H^{SM}} \quad (8)$$

where σ_{ggH}^{ij}, $\Gamma_{\gamma\gamma}^{ij}$ and Γ_{ff}^{SM} are obtained from theory [14,119].

Results are extracted from fits to the data using the profile likelihood ratio $\Lambda(\boldsymbol{\kappa})$, where the κ_j couplings are treated either as parameters of interest or as nuisance parameters, depending on the measurement.

The assumptions made for the various measurements are summarised in Table 10 and discussed in the next sections together with the results.

7.4.1. Couplings to fermions and bosons

The first benchmark considered here (indicated as model 1 in Table 10) assumes one coupling scale factor for fermions, κ_F, and one for bosons, κ_V; in this scenario, the $H \to \gamma\gamma$ and $gg \to H$ loops and the total Higgs boson width depend only on κ_F and κ_V, with no contributions from physics beyond the Standard Model (BSM). The strongest constraint on κ_F comes indirectly from the $gg \to H$ production loop.

Fig. 10 shows the results of the fit to the data for the three channels and their combination. Since only the relative sign of κ_F and κ_V is physical, in the following $\kappa_V > 0$ is assumed. Some sensitivity to this relative sign is provided by the negative interference between the W boson loop and t-quark loop in the $H \to \gamma\gamma$ decay. The data prefer the minimum with positive relative sign, which is consistent with the SM prediction, but the local minimum with negative sign is also compatible with the observation (at the $\sim 2\sigma$ level). The two-dimensional compatibility of the SM
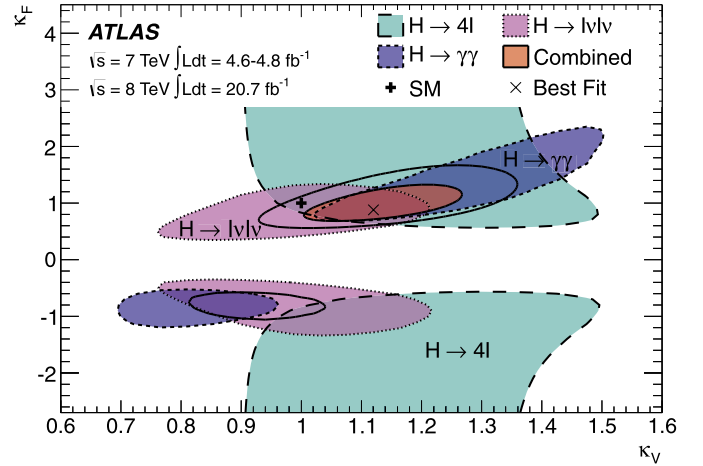
Fig. 10. Likelihood contours (68% CL) of the coupling scale factors κ_F and κ_V for fermions and bosons (benchmark model 1 in Table 10), as obtained from fits to the three individual channels and their combination (for the latter, the 95% CL contour is also shown). The best-fit result ($\times$) and the SM expectation ($+$) are also indicated.

prediction with the best-fit value is 12%. The 68% CL intervals of κ_F and κ_V, obtained by profiling over the other parameter, are:

$$\kappa_F \in [0.76, 1.18], \quad (9)$$

$$\kappa_V \in [1.05, 1.22] \quad (10)$$

with similar contributions from the statistical and systematic uncertainties.

In this benchmark model, the assumption of no contributions from new particles to the Higgs boson width provides strong constraints on the fermion coupling κ_F, as about 75% of the total SM width comes from decays to fermions or involving fermions. If this assumption is relaxed, only the ratio $\lambda_{FV} = \kappa_F/\kappa_V$ can be measured (benchmark model 2 in Table 10), which still provides useful information on the relationship between Yukawa and gauge couplings. Fits to the data give the following 68% CL intervals for λ_{FV} and $\kappa_{VV} = \kappa_V\kappa_V/\kappa_H$ (when profiling over the other parameter):

$$\lambda_{FV} \in [0.70, 1.01], \quad (11)$$

$$\kappa_{VV} \in [1.13, 1.45]. \quad (12)$$

The two-dimensional compatibility of the SM prediction with the best-fit value is 12%. These results also exclude vanishing couplings of the Higgs boson to fermions (indirectly, mainly through the $gg \to H$ production loop) by more than 5σ.

7.4.2. Ratio of couplings to the W and Z bosons

In the Standard Model, custodial symmetry imposes the constraint that the W and Z bosons have related couplings to the
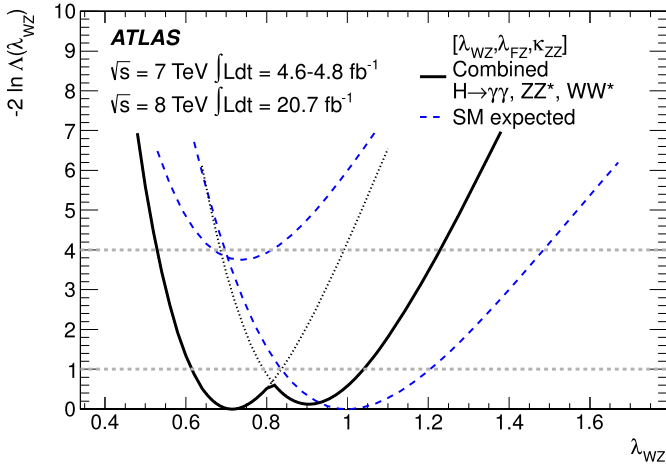
Fig. 11. Likelihood curve for the coupling scale factor λ_{WZ} (benchmark model 3 in Table 10). The thin dotted lines indicate the continuation of the likelihood curve when restricting λ_{FZ} to be either positive or negative. The dashed curves show the SM expectation with the right (left) minimum indicating λ_{FZ} positive (negative).

Fig. 12. Likelihood contours for the coupling scale factors κ_γ and κ_g probing BSM contributions to the $H \to \gamma\gamma$ and $gg \to H$ loops, assuming no BSM contributions to the total Higgs boson width (benchmark model 5 in Table 10). The best-fit result ($\times$) and the SM expectation ($+$) are also indicated.

Higgs boson, $g_{HVV} \sim m_V^2/v$ (where v is the vacuum expectation value of the Higgs field), and that $\rho = m_W^2/(m_Z^2 \cdot \cos^2 \theta_W)$ (where θ_W is the weak Weinberg angle) is equal to unity (as measured at LEP [120]). The former constraint is tested here by measuring the ratio $\lambda_{WZ} = \kappa_W/\kappa_Z$.

The simplest and most model-independent approach is to extract the ratio of branching ratios normalised to their SM expectation, $\lambda_{WZ}^2 = B(H \to WW^*)/B(H \to ZZ^*) \cdot B_{SM}(H \to ZZ^*)/B_{SM}(H \to WW^*)$, from the measured inclusive rates of the $H \to WW^*$ and $H \to ZZ^*$ channels. A fit to the data with the likelihood $\Lambda(\lambda_{WZ})$, where $\mu_{ggF+ttH} \times B(H \to ZZ^*)/B_{SM}(H \to ZZ^*)$ and $\mu_{VBF+VH}/\mu_{ggF+ttH}$ are profiled, gives $\lambda_{WZ} = 0.81^{+0.16}_{-0.15}$.

A more sensitive measurement can be obtained by also using information from WH and ZH production, from the VBF process (which in the SM is roughly 75% W-fusion and 25% Z-fusion mediated) and from the $H \to \gamma\gamma$ decay mode. A fit to the data using benchmark model 3 in Table 10 gives the likelihood curve shown in Fig. 11, with $\lambda_{WZ} \in [0.61, 1.04]$ at the 68% CL, dominated by the statistical uncertainty; the other parameters, λ_{FZ} and κ_{ZZ}, are profiled. The three-dimensional compatibility of the SM prediction with the best-fit value is 19%.

Potential contributions from BSM physics affecting the $H \to \gamma\gamma$ channel could produce apparent deviations of the ratio λ_{WZ} from unity even if custodial symmetry is not broken. It is therefore desirable to decouple the observed $H \to \gamma\gamma$ event rate from the measurement of λ_{WZ}. This is done with an extended fit for the ratio λ_{WZ}, where one extra degree of freedom ($\lambda_{\gamma Z} = \kappa_\gamma/\kappa_Z$) absorbs possible BSM effects in the $H \to \gamma\gamma$ channel (benchmark model 4 in Table 10). This measurement yields:

$$\lambda_{WZ} = 0.82 \pm 0.15 \tag{13}$$

and a four-dimensional compatibility of the SM prediction with the best-fit value of 20%.

7.4.3. Constraints on production and decay loops

Many BSM physics scenarios predict the existence of new heavy particles, which can contribute to loop-induced processes such as $gg \to H$ production and $H \to \gamma\gamma$ decay. In the approach used here (benchmark model 5 in Table 10), it is assumed that the new particles do not contribute to the Higgs boson width and that the couplings of the known particles to the Higgs boson have SM strength (*i.e.* $\kappa_i = 1$). Effective scale factors κ_g and κ_γ are introduced to parameterise the $gg \to H$ and $H \to \gamma\gamma$ loops. The results
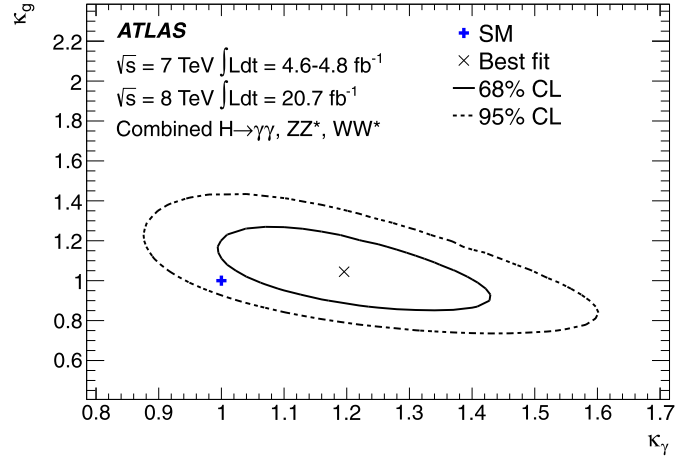
of their measurements from a fit to the data are shown in Fig. 12. The best-fit values when profiling over the other parameters are:

$$\kappa_g = 1.04 \pm 0.14, \tag{14}$$

$$\kappa_\gamma = 1.20 \pm 0.15. \tag{15}$$

The two-dimensional compatibility of the SM prediction with the best-fit value is 14%.

7.4.4. Summary

The results of the measurements of the coupling scale factors discussed in the previous sections, obtained under the assumptions detailed in Section 7.4 and Table 10, are summmarised in Fig. 13. The measurements in the various benchmark models are strongly correlated, as they are obtained from fits to the same experimental data. A simple χ^2-like compatibility test with the SM is therefore not meaningful.

The coupling of the new particle to gauge bosons κ_V is constrained by several channels, directly and indirectly, at the $\pm 10\%$ level. Couplings to fermions with a significance larger than 5σ are indirectly observed mainly through the gluon-fusion production process, assuming the loop is dominated by fermion exchange. The ratio of the relative couplings of the Higgs boson to the W and Z bosons, κ_W/κ_Z, is measured to be consistent with unity, as predicted by custodial symmetry. Under the hypothesis that all couplings of the Higgs boson to the known particles are fixed to their SM values, and assuming no BSM contributions to the Higgs boson width, no significant anomalous contributions to the $gg \to H$ and $H \to \gamma\gamma$ loops are observed.

8. Conclusions

Data recorded by the ATLAS experiment at the CERN Large Hadron Collider in 2011 and 2012, corresponding to an integrated luminosity of up to 25 fb^{-1}, at $\sqrt{s} = 7$ TeV and $\sqrt{s} = 8$ TeV, have been analysed to determine several properties of the recently discovered Higgs boson using the $H \to \gamma\gamma$, $H \to ZZ^* \to 4\ell$ and $H \to WW^* \to \ell\nu\ell\nu$ decay modes. The reported results include measurements of the mass and signal strength, evidence for production through vector-boson fusion, and constraints on couplings to bosons and fermions as well as on anomalous contributions to loop-induced processes. The precision exceeds previously published results in several cases. All measurements are consistent with expectations for the Standard Model Higgs boson.
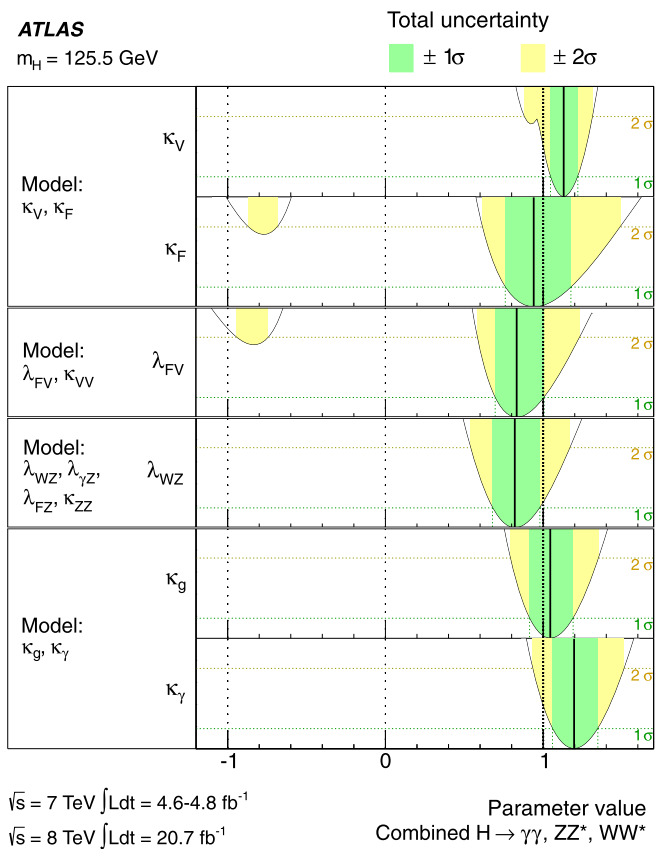
Fig. 13. Summary of the measurements of the coupling scale factors for a Higgs boson with mass $m_H = 125.5$ GeV. The best-fit values are represented by the solid vertical lines, with the $\pm 1\sigma$ and $\pm 2\sigma$ uncertainties given by the dark- and light-shaded band, respectively. For a more complete illustration, the distributions of the likelihood ratios from which the total uncertainties are extracted are overlaid. The measurements in the various benchmark models, separated by double horizontal lines, are strongly correlated.

Open access

References

[1] L. Evans, P. Bryant, LHC machine, JINST 3 (2008) S08001.
[2] ATLAS Collaboration, Observation of a new particle in the search for the Standard Model Higgs boson with the ATLAS detector at the LHC, Phys. Lett. B 716 (2012) 1, arXiv:1207.7214 [hep-ex].
[3] CMS Collaboration, Observation of a new boson at a mass of 125 GeV with the CMS experiment at the LHC, Phys. Lett. B 716 (2012) 30, arXiv:1207.7235 [hep-ex].
[4] F. Englert, R. Brout, Broken symmetry and the mass of gauge vector mesons, Phys. Rev. Lett. 13 (1964) 321.
[5] P.W. Higgs, Broken symmetries, massless particles and gauge fields, Phys. Lett. 12 (1964) 132.
[6] P.W. Higgs, Broken symmetries and the masses of gauge bosons, Phys. Rev. Lett. 13 (1964) 508.
[7] G.S. Guralnik, C.R. Hagen, T.W.B. Kibble, Global conservation laws and massless particles, Phys. Rev. Lett. 13 (1964) 585.
[8] P.W. Higgs, Spontaneous symmetry breakdown without massless bosons, Phys. Rev. 145 (1966) 1156.
[9] T.W.B. Kibble, Symmetry breaking in non-Abelian gauge theories, Phys. Rev. 155 (1967) 1554.
[10] ATLAS Collaboration, Evidence for the spin-zero nature of the Higgs boson using ATLAS data, Phys. Lett. B (2013), http://dx.doi.org/10.1016/j.physletb.2013.08.026, in press.
[11] ATLAS Collaboration, The ATLAS experiment at the CERN Large Hadron Collider, JINST 3 (2008) S08003.
[12] CMS Collaboration, Observation of a new boson with mass near 125 GeV in pp collisions at $\sqrt{s} = 7$ and 8 TeV, JHEP (2013), submitted to publication, arXiv:1303.4571 [hep-ex].
[13] ATLAS Collaboration, Improved luminosity determination in pp collisions at $\sqrt{s} = 7$ TeV using the ATLAS detector at the LHC, Eur. Phys. J. (2013), submitted to publication, arXiv:1302.4393 [hep-ex].
[14] LHC Higgs Cross Section Working Group, S. Dittmaier, C. Mariotti, G. Passarino, R. Tanaka (Eds.), Handbook of LHC Higgs Cross Sections: 1. Inclusive Observables, CERN, Geneva, 2011, CERN-2011-002, arXiv:1101.0593 [hep-ph].
[15] LHC Higgs Cross Section Working Group, S. Dittmaier, C. Mariotti, G. Passarino, R. Tanaka (Eds.), Handbook of LHC Higgs Cross Sections: 2. Differential Distributions, CERN, Geneva, 2012, CERN-2012-002, arXiv:1201.3084 [hep-ph].
[16] The Higgs Cross Section Working Group web page, https://twiki.cern.ch/twiki/bin/view/LHCPhysics/CrossSections, 2012.
[17] ATLAS Collaboration, Measurement of the $W \to l\nu$ and $Z/\gamma \to ll$ production cross sections in proton–proton collisions at $\sqrt{s} = 7$ TeV with the ATLAS detector, JHEP 1012 (2010) 060, arXiv:1010.2130 [hep-ex].
[18] ATLAS Collaboration, Electron performance measurements with the ATLAS detector using the 2010 LHC proton–proton collision data, Eur. Phys. J. C 72 (2012) 1909, arXiv:1110.3174 [hep-ex].
[19] ATLAS Collaboration, Improved electron reconstruction in ATLAS using the Gaussian Sum Filter-based model for bremsstrahlung, ATLAS-CONF-2012-047, 2012, http://cdsweb.cern.ch/record/1449796.
[20] ATLAS Collaboration, Muon reconstruction efficiency in reprocessed 2010 LHC proton–proton collision data recorded with the ATLAS detector, ATLAS-CONF-2011-063, 2011, http://cdsweb.cern.ch/record/1345743.
[21] ATLAS Collaboration, Measurement of the inclusive isolated prompt photon cross section in pp collisions at $\sqrt{s} = 7$ TeV with the ATLAS detector, Phys. Rev. D 83 (2011) 052005.
[22] ATLAS Collaboration, Jet energy measurement with the ATLAS detector in proton–proton collisions at $\sqrt{s} = 7$ TeV, Eur. Phys. J. C 73 (2013) 2304, arXiv:1112.6426 [hep-ex].
[23] ATLAS Collaboration, Jet energy scale and its systematic uncertainty in proton–proton collisions at $\sqrt{s} = 7$ TeV with ATLAS 2011 data, ATLAS-CONF-2013-004, 2013, https://cds.cern.ch/record/1509552.
[24] W. Lampl, S. Laplace, D. Lelas, P. Loch, H. Ma, S. Menke, S. Rajagopalan, D. Rousseau, S. Snyder, G. Unal, Calorimeter clustering algorithms: description and performance, ATL-LARG-PUB-002, http://cdsweb.cern.ch/record/1099735, 2008.

[25] M. Cacciari, G.P. Salam, G. Soyez, The anti-k_t jet clustering algorithm, JHEP 0804 (2008) 063.

[26] ATLAS Collaboration, Pile-up corrections for jets from proton–proton collisions at $\sqrt{s} = 7$ TeV ATLAS in 2011, ATLAS-CONF-2012-064, https://cds.cern.ch/record/1459529.

[27] ATLAS Collaboration, Measurement of the mistag rate with 5 fb^{-1} of data collected by the ATLAS detector, ATLAS-CONF-2012-040, 2012, https://cdsweb.cern.ch/record/1435194.

[28] ATLAS Collaboration, Measurement of the b-tag Efficiency in a sample of jets containing muons with 5 fb^{-1} of data from the ATLAS detector, ATLAS-CONF-2012-043, 2012, https://cdsweb.cern.ch/record/1435197.

[29] ATLAS Collaboration, Commissioning of the ATLAS high-performance b-tagging algorithms in the 7 TeV collision data, ATLAS-CONF-2011-102, 2011, http://cds.cern.ch/record/1369219.

[30] ATLAS Collaboration, Performance of missing transverse momentum reconstruction in proton–proton collisions at $\sqrt{s} = 7$ TeV with ATLAS, Eur. Phys. J. C 72 (2012) 1844, arXiv:1108.5602 [hep-ex].

[31] T. Sjostrand, S. Mrenna, P.Z. Skands, PYTHIA 6.4 physics and manual, JHEP 0605 (2006) 026.

[32] T. Sjostrand, S. Mrenna, P.Z. Skands, A brief introduction to PYTHIA 8.1, Comput. Phys. Commun. 178 (2008) 852.

[33] S. Alioli, P. Nason, C. Oleari, E. Re, NLO Higgs boson production via gluon fusion matched with shower in POWHEG, JHEP 0904 (2009) 002.

[34] P. Nason, C. Oleari, NLO Higgs boson production via vector-boson fusion matched with shower in POWHEG, JHEP 1002 (2010) 037.

[35] A. Bredenstein, A. Denner, S. Dittmaier, M.M. Weber, Precise predictions for the Higgs-boson decay $H \to WW/ZZ \to 4$ leptons, Phys. Rev. D 74 (2006) 013004, arXiv:hep-ph/0604011.

[36] A. Bredenstein, A. Denner, S. Dittmaier, M.M. Weber, Radiative corrections to the semileptonic and hadronic Higgs-boson decays $H \to WW/ZZ \to 4$ fermions, JHEP 0702 (2007) 080.

[37] M.L. Mangano, et al., ALPGEN, a generator for hard multiparton processes in hadronic collisions, JHEP 0307 (2003) 001.

[38] G. Corcella, I. Knowles, G. Marchesini, S. Moretti, K. Odagiri, et al., HERWIG 6: An event generator for hadron emission reactions with interfering gluons (including supersymmetric processes), JHEP 0101 (2001) 010.

[39] T. Gleisberg, et al., Event generation with SHERPA 1.1, JHEP 0902 (2009) 007.

[40] S. Frixione, B.R. Webber, Matching NLO QCD computations and parton shower simulations, JHEP 0206 (2002) 029.

[41] B.P. Kersevan, E. Richter-Was, The Monte Carlo event generator AcerMC version 2.0 with interfaces to PYTHIA 6.2 and HERWIG 6.5, arXiv:hep-ph/0405247.

[42] T. Binoth, M. Ciccolini, N. Kauer, M. Krämer, Gluon-induced W-boson pair production at the LHC, JHEP 0612 (2006) 046.

[43] N. Kauer, G. Passarino, Inadequacy of zero-width approximation for a light Higgs boson signal, JHEP 1208 (2012) 116, arXiv:1206.4803 [hep-ph].

[44] T. Melia, P. Nason, R. Rontsch, G. Zanderighi, W^+W^-, WZ and ZZ production in the POWHEG BOX, JHEP 1111 (2011) 078.

[45] T. Binoth, N. Kauer, P. Mertsch, Gluon-induced QCD corrections to $pp \to ZZ \to \ell\bar{\ell}\ell'\bar{\ell}'$, arXiv:0807.0024 [hep-ph].

[46] J. Alwall, et al., MadGraph/MadEvent v4: The new web generation, JHEP 0709 (2007) 028.

[47] J. Alwall, M. Herquet, F. Maltoni, O. Mattelaer, T. Stelzer, MadGraph 5: Going beyond, JHEP 1106 (2011) 128.

[48] R.C. Gray, C. Kilic, M. Park, S. Somalwar, S. Thomas, Backgrounds to Higgs boson searches from $W\gamma^* \to l\nu l(l)$ asymmetric internal conversion, arXiv:1110.1368 [hep-ph].

[49] H. Georgi, S. Glashow, M. Machacek, D.V. Nanopoulos, Higgs bosons from two gluon annihilation in proton proton collisions, Phys. Rev. Lett. 40 (1978) 692.

[50] A. Djouadi, M. Spira, P.M. Zerwas, Production of Higgs bosons in proton colliders: QCD corrections, Phys. Lett. B 264 (1991) 440.

[51] S. Dawson, Radiative corrections to Higgs boson production, Nucl. Phys. B 359 (1991) 283.

[52] M. Spira, A. Djouadi, D. Graudenz, P.M. Zerwas, Higgs boson production at the LHC, Nucl. Phys. B 453 (1995) 17.

[53] R. Harlander, W.B. Kilgore, Next-to-next-to-leading order Higgs production at hadron colliders, Phys. Rev. Lett. 88 (2002) 201801.

[54] C. Anastasiou, K. Melnikov, Higgs boson production at hadron colliders in NNLO QCD, Nucl. Phys. B 646 (2002) 220.

[55] V. Ravindran, J. Smith, W.L. van Neerven, NNLO corrections to the total cross section for Higgs boson production in hadron hadron collisions, Nucl. Phys. B 665 (2003) 325.

[56] U. Aglietti, R. Bonciani, G. Degrassi, A. Vicini, Two-loop light fermion contribution to Higgs production and decays, Phys. Lett. B 595 (2004) 432.

[57] S. Actis, G. Passarino, C. Sturm, S. Uccirati, NLO electroweak corrections to Higgs boson production at hadron colliders, Phys. Lett. B 670 (2008) 12.

[58] S. Catani, D. de Florian, M. Grazzini, P. Nason, Soft-gluon re-summation for Higgs boson production at hadron colliders, JHEP 0307 (2003) 028.

[59] D. de Florian, M. Grazzini, Higgs production at the LHC: updated cross sections at $\sqrt{s} = 8$ TeV, arXiv:1206.4133 [hep-ph].

[60] C. Anastasiou, S. Buehler, F. Herzog, A. Lazopoulos, Inclusive Higgs boson cross-section for the LHC at 8 TeV, JHEP 1204 (2012) 004.

[61] J. Baglio, A. Djouadi, Higgs production at the lHC, JHEP 1103 (2011) 055.

[62] D. de Florian, G. Ferrera, M. Grazzini, D. Tommasini, Transverse-momentum resummation: Higgs boson production at the Tevatron and the LHC, JHEP 1111 (2011) 064.

[63] E. Bagnaschi, G. Degrassi, P. Slavich, A. Vicini, Higgs production via gluon fusion in the POWHEG approach in the SM and in the MSSM, JHEP 1202 (2012) 88.

[64] R. Cahn, S. Dawson, Production of very massive Higgs bosons, Phys. Lett. B 136 (1984) 196;
R. Cahn, S. Dawson, Production of very massive Higgs bosons, Phys. Lett. B 138 (1984) 464, Erratum.

[65] M. Ciccolini, A. Denner, S. Dittmaier, Strong and electroweak corrections to the production of Higgs + 2jets via weak interactions at the LHC, Phys. Rev. Lett. 99 (2007) 161803.

[66] M. Ciccolini, A. Denner, S. Dittmaier, Electroweak and QCD corrections to Higgs production via vector-boson fusion at the LHC, Phys. Rev. D 77 (2008) 013002.

[67] K. Arnold, M. Bahr, G. Bozzi, F. Campanario, C. Englert, et al., VBFNLO: A parton level Monte Carlo for processes with electroweak bosons, Comput. Phys. Commun. 180 (2009) 1661.

[68] P. Bolzoni, F. Maltoni, S.-O. Moch, M. Zaro, Higgs production via vector-boson fusion at NNLO in QCD, Phys. Rev. Lett. 105 (2010) 011801.

[69] S. Glashow, D.V. Nanopoulos, A. Yildiz, Associated production of Higgs bosons and Z particles, Phys. Rev. D 18 (1978) 1724.

[70] T. Han, S. Willenbrock, QCD correction to the $pp \to WH$ and ZH total cross sections, Phys. Lett. B 273 (1991) 167.

[71] O. Brein, A. Djouadi, R. Harlander, NNLO QCD corrections to the Higgsstrahlung processes at hadron colliders, Phys. Lett. B 579 (2004) 149.

[72] M.L. Ciccolini, S. Dittmaier, M. Kramer, Electroweak radiative corrections to associated WH and ZH production at hadron colliders, Phys. Rev. D 68 (2003) 073003.

[73] Z. Kunszt, Associated production of heavy Higgs boson with top quarks, Nucl. Phys. B 247 (1984) 339.

[74] W. Beenakker, et al., Higgs radiation off top quarks at the Tevatron and the LHC, Phys. Rev. Lett. 87 (2001) 201805.

[75] W. Beenakker, et al., NLO QCD corrections to $t\bar{t}H$ production in hadron collisions, Nucl. Phys. B 653 (2003) 151.

[76] S. Dawson, L.H. Orr, L. Reina, D. Wackeroth, Next-to-leading order QCD corrections to $pp \to t\bar{t}h$ at the CERN large hadron collider, Phys. Rev. D 67 (2003) 071503.

[77] S. Dawson, C. Jackson, L.H. Orr, L. Reina, D. Wackeroth, Associated Higgs production with top quarks at the Large Hadron Collider: NLO QCD corrections, Phys. Rev. D 68 (2003) 034022.

[78] ATLAS Collaboration, New ATLAS event generator tunes to 2010 data, ATL-PHYS-PUB-2011-008, http://cdsweb.cern.ch/record/1345343, 2011.

[79] ATLAS Collaboration, ATLAS tunes of PYTHIA 6 and Pythia 8 for MC11, ATL-PHYS-PUB-2011-009, http://cdsweb.cern.ch/record/1363300, 2011.

[80] ATLAS Collaboration, Further ATLAS tunes of PYTHIA6 and Pythia 8, ATL-PHYS-PUB-2011-014, http://cdsweb.cern.ch/record/1400677, 2011.

[81] J.M. Butterworth, J.R. Forshaw, M.H. Seymour, Multiparton interactions in photoproduction at HERA, Z. Phys. C 72 (1996) 637.

[82] P. Golonka, Z. Was, PHOTOS Monte Carlo: A precision tool for QED corrections in Z and W decays, Eur. Phys. J. C 45 (2006) 97.

[83] N. Davidson, T. Przedzinski, Z. Was, PHOTOS interface in C++: technical and physics documentation, arXiv:1011.0937 [hep-ph].

[84] H.-L. Lai, et al., New parton distributions for collider physics, Phys. Rev. D 82 (2010) 074024.

[85] P.M. Nadolsky, et al., Implications of CTEQ global analysis for collider observables, Phys. Rev. D 78 (2008) 013004.

[86] A. Sherstnev, R.S. Thorne, Parton distributions for the LHC, Eur. Phys. J. C 55 (2009) 553, arXiv:0711.2473 [hep-ph].

[87] ATLAS Collaboration, The ATLAS simulation infrastructure, Eur. Phys. J. C 70 (2010) 823, arXiv:1005.4568 [physics.ins-det].

[88] S. Agostinelli, et al., Geant4, a simulation toolkit, Nucl. Instrum. Meth. A 506 (2003) 250.

[89] A. Djouadi, J. Kalinowski, M. Spira, HDECAY: A program for Higgs boson decays in the standard model and its supersymmetric extension, Comput. Phys. Commun. 108 (1998) 56.

[90] ATLAS Collaboration, Performance of the ATLAS trigger system in 2010, Eur. Phys. J. C 72 (2012) 1849, arXiv:1110.1530 [hep-ex].

[91] ATLAS Collaboration, Expected photon performance in the ATLAS experiment, ATL-PHYS-PUB-2011-007, http://cds.cern.ch/record/1345329, 2011.

[92] M. Cacciari, G.P. Salam, Pileup subtraction using jet areas, Phys. Lett. B 659 (2008) 119.

[93] ATLAS Collaboration, Search for the Standard Model Higgs boson in the two photon decay channel with the ATLAS detector at the LHC, Phys. Lett. B 705 (2011) 452.

[94] OPAL Collaboration, K. Ackerstaff, et al., Search for anomalous production of dilepton events with missing transverse momentum in e^+e^- collisions at $\sqrt{s} = 161$ GeV and 172 GeV, Eur. Phys. J. C 4 (1998) 47, arXiv:hep-ex/9710010.

[95] M. Vesterinen, T.R. Wyatt, A novel technique for studying the Z boson transverse momentum distribution at hadron colliders, Nucl. Instrum. Meth. A 602 (2009) 432.

[96] S.N. Bernstein, Démonstration du théorème de Weierstrass fondée sur le calcul des probabilités, Comm. Soc. Math. Kharkov 13 (1912) 1.

[97] M.J. Oreglia, A study of reactions $\psi' \to \gamma\gamma\psi$, PhD thesis, SLAC-R-0236, 1980, Appendix D.

[98] S. Gangal, F.J. Tackmann, NLO uncertainties in Higgs + 2 jets from gluon fusion, arXiv:1302.5437 [hep-ph].

[99] J.M. Campbell, R.K. Ellis, MCFM for the Tevatron and the LHC, Nucl. Phys. Proc. Suppl. 205–206 (2010) 10.

[100] ATLAS Collaboration, Updated results and measurements of properties of the new Higgs-like particle in the four-lepton decay channel with the ATLAS detector, ATLAS-CONF-2012-169, 2012, http://cds.cern.ch/record/1499628.

[101] ATLAS Collaboration, Reconstruction of collinear final-state radiation photons in Z decays to muons in $\sqrt{s} = 7$ TeV proton–proton collisions, ATLAS-CONF-2012-143, 2012, https://cds.cern.ch/record/1491697.

[102] ATLAS Collaboration, Measurements of the electron and muon inclusive cross-sections in proton–proton collisions at $\sqrt{s} = 7$ TeV with the ATLAS detector, Phys. Lett. B 707 (2012) 438, arXiv:1109.0525 [hep-ex].

[103] ATLAS Collaboration, Search for the Standard Model Higgs boson in the $H \to WW^{(*)} \to \ell\nu\ell\nu$ decay mode with 4.7 fb^{-1} of ATLAS data at $\sqrt{s} = 7$ TeV, Phys. Lett. B 716 (2012) 62, arXiv:1206.0756 [hep-ex].

[104] ATLAS Collaboration, Performance of missing transverse momentum reconstruction in ATLAS with 2011 proton–proton collisions at $\sqrt{s} = 7$ TeV, ATLAS-CONF-2012-101, 2012, http://cds.cern.ch/record/1463915.

[105] R.K. Ellis, et al., Higgs decay to $\tau^+\tau^-$: A possible signature of intermediate mass Higgs bosons at the SSC, Nucl. Phys. B 297 (1988) 221.

[106] J.M. Campbell, R.K. Ellis, An update on vector boson pair production at hadron colliders, Phys. Rev. D 60 (1999) 113006.

[107] ATLAS Collaboration, Measurements of the properties of the Higgs-like boson in the $WW^{(*)} \to \ell\nu\ell\nu$ decay channel with the ATLAS detector using 25 fb^{-1} of proton–proton collision data, ATLAS-CONF-2013-030, 2013, http://cds.cern.ch/record/1527126.

[108] S. Catani, M. Grazzini, An NNLO subtraction formalism in hadron collisions and its application to Higgs boson production at the LHC, Phys. Rev. Lett. 98 (2007) 222002, arXiv:hep-ph/0703012.

[109] M. Grazzini, NNLO predictions for the Higgs boson signal in the $H \to WW \to l\nu l\nu$ and $H \to ZZ \to 4l$ decay channels, JHEP 0802 (2008) 043, arXiv:0801.3232 [hep-ph].

[110] I. Stewart, F. Tackmann, Theory uncertainties for Higgs mass and other searches using jet bins, Phys. Rev. D 85 (2012) 034011.

[111] ATLAS Collaboration, Combined search for the Standard Model Higgs boson in pp collisions at $\sqrt{s} = 7$ TeV with the ATLAS detector, Phys. Rev. D 86 (2012) 032003, arXiv:1207.0319 [hep-ex].

[112] ATLAS and CMS Collaborations, Procedure for the LHC Higgs boson search combination in Summer 2011, ATL-PHYS-PUB-2011-011, CERN-CMS-NOTE-2011-005, http://cdsweb.cern.ch/record/1375842, 2011.

[113] L. Moneta, K. Belasco, K.S. Cranmer, S. Kreiss, A. Lazzaro, et al., The RooStats project, PoS ACAT2010 (2010) 057, arXiv:1009.1003 [physics.data-an].

[114] K. Cranmer, G. Lewis, L. Moneta, A. Shibata, W. Verkerke, HistFactory: A tool for creating statistical models for use with RooFit and RooStats, CERN-OPEN-2012-016, 2012, http://cdsweb.cern.ch/record/1456844.

[115] W. Verkerke, D. Kirkby, The RooFit toolkit for data modelling, Tech. Rep., arXiv:physics/0306116, SLAC, Stanford, CA, Jun 2003, arXiv:physics/0306116v1.

[116] G. Cowan, K. Cranmer, E. Gross, O. Vitells, Asymptotic formulae for likelihood-based tests of new physics, Eur. Phys. J. C 71 (2011) 1554.

[117] ATLAS Collaboration, Search for the Standard Model Higgs boson in $H \to \tau^+\tau^-$ decays in proton–proton collisions with the ATLAS detector, ATLAS-CONF-2012-160, 2012, http://cds.cern.ch/record/1493624.

[118] ATLAS Collaboration, Search for the Standard Model Higgs boson produced in association with a vector boson and decaying to bottom quarks with the ATLAS detector, ATLAS-CONF-2012-161, 2012, http://cds.cern.ch/record/1493625.

[119] LHC Higgs Cross Section Working Group, S. Heinemeyer, C. Mariotti, G. Passarino, R. Tanaka (Eds.), Handbook of LHC Higgs Cross Sections: 3. Higgs Properties, CERN, Geneva, 2013, CERN-2013-004, arXiv:1307.1347 [hep-ph].

[120] ALEPH, DELPHI, L3, OPAL and SLD Collaborations, LEP Electroweak Working Group, SLD electroweak heavy flavour groups, Precision electroweak measurements on the Z resonance, Phys. Rep. 427 (2006) 257, arXiv:hep-ex/0509008v3.

ATLAS Collaboration

G. Aad [48], T. Abajyan [21], B. Abbott [112], J. Abdallah [12], S. Abdel Khalek [116], O. Abdinov [11], R. Aben [106], B. Abi [113], M. Abolins [89], O.S. AbouZeid [159], H. Abramowicz [154], H. Abreu [137], Y. Abulaiti [147a,147b], B.S. Acharya [165a,165b,a], L. Adamczyk [38a], D.L. Adams [25], T.N. Addy [56], J. Adelman [177], S. Adomeit [99], T. Adye [130], S. Aefsky [23], T. Agatonovic-Jovin [13b], J.A. Aguilar-Saavedra [125b,b], M. Agustoni [17], S.P. Ahlen [22], A. Ahmad [149], M. Ahsan [41], G. Aielli [134a,134b], T.P.A. Åkesson [80], G. Akimoto [156], A.V. Akimov [95], M.A. Alam [76], J. Albert [170], S. Albrand [55], M.J. Alconada Verzini [70], M. Aleksa [30], I.N. Aleksandrov [64], F. Alessandria [90a], C. Alexa [26a], G. Alexander [154], G. Alexandre [49], T. Alexopoulos [10], M. Alhroob [165a,165c], M. Aliev [16], G. Alimonti [90a], L. Alio [84], J. Alison [31], B.M.M. Allbrooke [18], L.J. Allison [71], P.P. Allport [73], S.E. Allwood-Spiers [53], J. Almond [83], A. Aloisio [103a,103b], R. Alon [173], A. Alonso [36], F. Alonso [70], A. Altheimer [35], B. Alvarez Gonzalez [89], M.G. Alviggi [103a,103b], K. Amako [65], Y. Amaral Coutinho [24a], C. Amelung [23], V.V. Ammosov [129,*], S.P. Amor Dos Santos [125a], A. Amorim [125a,c], S. Amoroso [48], N. Amram [154], C. Anastopoulos [30], L.S. Ancu [17], N. Andari [30], T. Andeen [35], C.F. Anders [58b], G. Anders [58a], K.J. Anderson [31], A. Andreazza [90a,90b], V. Andrei [58a], X.S. Anduaga [70], S. Angelidakis [9], P. Anger [44], A. Angerami [35], F. Anghinolfi [30], A.V. Anisenkov [108], N. Anjos [125a], A. Annovi [47], A. Antonaki [9], M. Antonelli [47], A. Antonov [97], J. Antos [145b], F. Anulli [133a], M. Aoki [102], L. Aperio Bella [18], R. Apolle [119,d], G. Arabidze [89], I. Aracena [144], Y. Arai [65], A.T.H. Arce [45], S. Arfaoui [149], J-F. Arguin [94], S. Argyropoulos [42], E. Arik [19a,*], M. Arik [19a], A.J. Armbruster [88], O. Arnaez [82], V. Arnal [81], O. Arslan [21], A. Artamonov [96], G. Artoni [133a,133b], S. Asai [156], N. Asbah [94], S. Ask [28], B. Åsman [147a,147b], L. Asquith [6], K. Assamagan [25], R. Astalos [145a], A. Astbury [170], M. Atkinson [166], N.B. Atlay [142], B. Auerbach [6], E. Auge [116], K. Augsten [127], M. Aurousseau [146b], G. Avolio [30], D. Axen [169], G. Azuelos [94,e], Y. Azuma [156], M.A. Baak [30], C. Bacci [135a,135b], A.M. Bach [15], H. Bachacou [137],

K. Bachas [155], M. Backes [30], M. Backhaus [21], J. Backus Mayes [144], E. Badescu [26a],
P. Bagiacchi [133a,133b], P. Bagnaia [133a,133b], Y. Bai [33a], D.C. Bailey [159], T. Bain [35], J.T. Baines [130],
O.K. Baker [177], S. Baker [77], P. Balek [128], F. Balli [137], E. Banas [39], Sw. Banerjee [174], D. Banfi [30],
A. Bangert [151], V. Bansal [170], H.S. Bansil [18], L. Barak [173], S.P. Baranov [95],
A. Barbaro Galtieri [15], T. Barber [48], E.L. Barberio [87], D. Barberis [50a,50b], M. Barbero [84],
D.Y. Bardin [64], T. Barillari [100], M. Barisonzi [176], T. Barklow [144], N. Barlow [28], B.M. Barnett [130],
R.M. Barnett [15], A. Baroncelli [135a], G. Barone [49], A.J. Barr [119], F. Barreiro [81],
J. Barreiro Guimarães da Costa [57], R. Bartoldus [144], A.E. Barton [71], V. Bartsch [150],
A. Bassalat [116], A. Basye [166], R.L. Bates [53], L. Batkova [145a], J.R. Batley [28], M. Battistin [30],
F. Bauer [137], H.S. Bawa [144,*f*], S. Beale [99], T. Beau [79], P.H. Beauchemin [162], R. Beccherle [50a],
P. Bechtle [21], H.P. Beck [17], K. Becker [176], S. Becker [99], M. Beckingham [139], K.H. Becks [176],
A.J. Beddall [19c], A. Beddall [19c], S. Bedikian [177], V.A. Bednyakov [64], C.P. Bee [84],
L.J. Beemster [106], T.A. Beermann [176], M. Begel [25], C. Belanger-Champagne [86], P.J. Bell [49],
W.H. Bell [49], G. Bella [154], L. Bellagamba [20a], A. Bellerive [29], M. Bellomo [30], A. Belloni [57],
O.L. Beloborodova [108,*g*], K. Belotskiy [97], O. Beltramello [30], O. Benary [154],
D. Benchekroun [136a], K. Bendtz [147a,147b], N. Benekos [166], Y. Benhammou [154],
E. Benhar Noccioli [49], J.A. Benitez Garcia [160b], D.P. Benjamin [45], J.R. Bensinger [23],
K. Benslama [131], S. Bentvelsen [106], D. Berge [30], E. Bergeaas Kuutmann [16], N. Berger [5],
F. Berghaus [170], E. Berglund [106], J. Beringer [15], C. Bernard [22], P. Bernat [77], R. Bernhard [48],
C. Bernius [78], F.U. Bernlochner [170], T. Berry [76], C. Bertella [84], F. Bertolucci [123a,123b],
M.I. Besana [90a], G.J. Besjes [105], O. Bessidskaia [147a,147b], N. Besson [137], S. Bethke [100],
W. Bhimji [46], R.M. Bianchi [124], L. Bianchini [23], M. Bianco [30], O. Biebel [99], S.P. Bieniek [77],
K. Bierwagen [54], J. Biesiada [15], M. Biglietti [135a], J. Bilbao De Mendizabal [49], H. Bilokon [47],
M. Bindi [20a,20b], S. Binet [116], A. Bingul [19c], C. Bini [133a,133b], B. Bittner [100], C.W. Black [151],
J.E. Black [144], K.M. Black [22], D. Blackburn [139], R.E. Blair [6], J.-B. Blanchard [137], T. Blazek [145a],
I. Bloch [42], C. Blocker [23], J. Blocki [39], W. Blum [82,*], U. Blumenschein [54], G.J. Bobbink [106],
V.S. Bobrovnikov [108], S.S. Bocchetta [80], A. Bocci [45], C.R. Boddy [119], M. Boehler [48], J. Boek [176],
T.T. Boek [176], N. Boelaert [36], J.A. Bogaerts [30], A.G. Bogdanchikov [108], A. Bogouch [91,*],
C. Bohm [147a], J. Bohm [126], V. Boisvert [76], T. Bold [38a], V. Boldea [26a], N.M. Bolnet [137],
M. Bomben [79], M. Bona [75], M. Boonekamp [137], S. Bordoni [79], C. Borer [17], A. Borisov [129],
G. Borissov [71], M. Borri [83], S. Borroni [42], J. Bortfeldt [99], V. Bortolotto [135a,135b], K. Bos [106],
D. Boscherini [20a], M. Bosman [12], H. Boterenbrood [106], J. Bouchami [94], J. Boudreau [124],
E.V. Bouhova-Thacker [71], D. Boumediene [34], C. Bourdarios [116], N. Bousson [84],
S. Boutouil [136d], A. Boveia [31], J. Boyd [30], I.R. Boyko [64], I. Bozovic-Jelisavcic [13b], J. Bracinik [18],
P. Branchini [135a], A. Brandt [8], G. Brandt [15], O. Brandt [54], U. Bratzler [157], B. Brau [85],
J.E. Brau [115], H.M. Braun [176,*], S.F. Brazzale [165a,165c], B. Brelier [159], J. Bremer [30],
K. Brendlinger [121], R. Brenner [167], S. Bressler [173], T.M. Bristow [46], D. Britton [53],
F.M. Brochu [28], I. Brock [21], R. Brock [89], F. Broggi [90a], C. Bromberg [89], J. Bronner [100],
G. Brooijmans [35], T. Brooks [76], W.K. Brooks [32b], E. Brost [115], G. Brown [83], J. Brown [55],
P.A. Bruckman de Renstrom [39], D. Bruncko [145b], R. Bruneliere [48], S. Brunet [60], A. Bruni [20a],
G. Bruni [20a], M. Bruschi [20a], L. Bryngemark [80], T. Buanes [14], Q. Buat [55], F. Bucci [49],
J. Buchanan [119], P. Buchholz [142], R.M. Buckingham [119], A.G. Buckley [46], S.I. Buda [26a],
I.A. Budagov [64], B. Budick [109], F. Buehrer [48], L. Bugge [118], O. Bulekov [97], A.C. Bundock [73],
M. Bunse [43], H. Burckhart [30], S. Burdin [73], T. Burgess [14], S. Burke [130], E. Busato [34],
V. Büscher [82], P. Bussey [53], C.P. Buszello [167], B. Butler [57], J.M. Butler [22], C.M. Buttar [53],
J.M. Butterworth [77], W. Buttinger [28], A. Buzatu [53], M. Byszewski [10], S. Cabrera Urbán [168],
D. Caforio [20a,20b], O. Cakir [4a], P. Calafiura [15], G. Calderini [79], P. Calfayan [99], R. Calkins [107],
L.P. Caloba [24a], R. Caloi [133a,133b], D. Calvet [34], S. Calvet [34], R. Camacho Toro [49],
P. Camarri [134a,134b], D. Cameron [118], L.M. Caminada [15], R. Caminal Armadans [12],
S. Campana [30], M. Campanelli [77], V. Canale [103a,103b], F. Canelli [31], A. Canepa [160a],
J. Cantero [81], R. Cantrill [76], T. Cao [40], M.D.M. Capeans Garrido [30], I. Caprini [26a],
M. Caprini [26a], D. Capriotti [100], M. Capua [37a,37b], R. Caputo [82], R. Cardarelli [134a], T. Carli [30],

G. Carlino [103a], L. Carminati [90a,90b], S. Caron [105], E. Carquin [32b], G.D. Carrillo-Montoya [146c],
A.A. Carter [75], J.R. Carter [28], J. Carvalho [125a,h], D. Casadei [77], M.P. Casado [12], C. Caso [50a,50b,∗],
E. Castaneda-Miranda [146b], A. Castelli [106], V. Castillo Gimenez [168], N.F. Castro [125a],
G. Cataldi [72a], P. Catastini [57], A. Catinaccio [30], J.R. Catmore [30], A. Cattai [30],
G. Cattani [134a,134b], S. Caughron [89], V. Cavaliere [166], D. Cavalli [90a], M. Cavalli-Sforza [12],
V. Cavasinni [123a,123b], F. Ceradini [135a,135b], B. Cerio [45], A.S. Cerqueira [24b], A. Cerri [15],
L. Cerrito [75], F. Cerutti [15], A. Cervelli [17], S.A. Cetin [19b], A. Chafaq [136a], D. Chakraborty [107],
I. Chalupkova [128], K. Chan [3], P. Chang [166], B. Chapleau [86], J.D. Chapman [28], J.W. Chapman [88],
D.G. Charlton [18], V. Chavda [83], C.A. Chavez Barajas [30], S. Cheatham [86], S. Chekanov [6],
S.V. Chekulaev [160a], G.A. Chelkov [64], M.A. Chelstowska [88], C. Chen [63], H. Chen [25],
S. Chen [33c], X. Chen [174], Y. Chen [35], Y. Cheng [31], A. Cheplakov [64],
R. Cherkaoui El Moursli [136e], V. Chernyatin [25,∗], E. Cheu [7], L. Chevalier [137], V. Chiarella [47],
G. Chiefari [103a,103b], J.T. Childers [30], A. Chilingarov [71], G. Chiodini [72a], A.S. Chisholm [18],
R.T. Chislett [77], A. Chitan [26a], M.V. Chizhov [64], G. Choudalakis [31], S. Chouridou [9],
B.K.B. Chow [99], I.A. Christidi [77], A. Christov [48], D. Chromek-Burckhart [30], M.L. Chu [152],
J. Chudoba [126], G. Ciapetti [133a,133b], A.K. Ciftci [4a], R. Ciftci [4a], D. Cinca [62], V. Cindro [74],
A. Ciocio [15], M. Cirilli [88], P. Cirkovic [13b], Z.H. Citron [173], M. Citterio [90a], M. Ciubancan [26a],
A. Clark [49], P.J. Clark [46], R.N. Clarke [15], J.C. Clemens [84], B. Clement [55], C. Clement [147a,147b],
Y. Coadou [84], M. Cobal [165a,165c], A. Coccaro [139], J. Cochran [63], S. Coelli [90a], L. Coffey [23],
J.G. Cogan [144], J. Coggeshall [166], J. Colas [5], B. Cole [35], S. Cole [107], A.P. Colijn [106],
C. Collins-Tooth [53], J. Collot [55], T. Colombo [58c], G. Colon [85], G. Compostella [100],
P. Conde Muiño [125a], E. Coniavitis [167], M.C. Conidi [12], S.M. Consonni [90a,90b], V. Consorti [48],
S. Constantinescu [26a], C. Conta [120a,120b], G. Conti [57], F. Conventi [103a,i], M. Cooke [15],
B.D. Cooper [77], A.M. Cooper-Sarkar [119], N.J. Cooper-Smith [76], K. Copic [15], T. Cornelissen [176],
M. Corradi [20a], F. Corriveau [86,j], A. Corso-Radu [164], A. Cortes-Gonzalez [12], G. Cortiana [100],
G. Costa [90a], M.J. Costa [168], D. Costanzo [140], D. Côté [8], G. Cottin [32a], L. Courneyea [170],
G. Cowan [76], B.E. Cox [83], K. Cranmer [109], S. Crépé-Renaudin [55], F. Crescioli [79],
M. Cristinziani [21], G. Crosetti [37a,37b], C.-M. Cuciuc [26a], C. Cuenca Almenar [177],
T. Cuhadar Donszelmann [140], J. Cummings [177], M. Curatolo [47], C. Cuthbert [151], H. Czirr [142],
P. Czodrowski [44], Z. Czyczula [177], S. D'Auria [53], M. D'Onofrio [73], A. D'Orazio [133a,133b],
M.J. Da Cunha Sargedas De Sousa [125a], C. Da Via [83], W. Dabrowski [38a], A. Dafinca [119],
T. Dai [88], F. Dallaire [94], C. Dallapiccola [85], M. Dam [36], D.S. Damiani [138], A.C. Daniells [18],
V. Dao [105], G. Darbo [50a], G.L. Darlea [26c], S. Darmora [8], J.A. Dassoulas [42], W. Davey [21],
C. David [170], T. Davidek [128], E. Davies [119,d], M. Davies [94], O. Davignon [79], A.R. Davison [77],
Y. Davygora [58a], E. Dawe [143], I. Dawson [140], R.K. Daya-Ishmukhametova [23], K. De [8],
R. de Asmundis [103a], S. De Castro [20a,20b], S. De Cecco [79], J. de Graat [99], N. De Groot [105],
P. de Jong [106], C. De La Taille [116], H. De la Torre [81], F. De Lorenzi [63], L. De Nooij [106],
D. De Pedis [133a], A. De Salvo [133a], U. De Sanctis [165a,165c], A. De Santo [150],
J.B. De Vivie De Regie [116], G. De Zorzi [133a,133b], W.J. Dearnaley [71], R. Debbe [25],
C. Debenedetti [46], B. Dechenaux [55], D.V. Dedovich [64], J. Degenhardt [121], J. Del Peso [81],
T. Del Prete [123a,123b], T. Delemontex [55], M. Deliyergiyev [74], A. Dell'Acqua [30], L. Dell'Asta [22],
M. Della Pietra [103a,i], D. della Volpe [103a,103b], M. Delmastro [5], P.A. Delsart [55], C. Deluca [106],
S. Demers [177], M. Demichev [64], A. Demilly [79], B. Demirkoz [12,k], S.P. Denisov [129],
D. Derendarz [39], J.E. Derkaoui [136d], F. Derue [79], P. Dervan [73], K. Desch [21], P.O. Deviveiros [106],
A. Dewhurst [130], B. DeWilde [149], S. Dhaliwal [106], R. Dhullipudi [78,l], A. Di Ciaccio [134a,134b],
L. Di Ciaccio [5], C. Di Donato [103a,103b], A. Di Girolamo [30], B. Di Girolamo [30],
S. Di Luise [135a,135b], A. Di Mattia [153], B. Di Micco [135a,135b], R. Di Nardo [47], A. Di Simone [48],
R. Di Sipio [20a,20b], M.A. Diaz [32a], E.B. Diehl [88], J. Dietrich [42], T.A. Dietzsch [58a], S. Diglio [87],
K. Dindar Yagci [40], J. Dingfelder [21], F. Dinut [26a], C. Dionisi [133a,133b], P. Dita [26a], S. Dita [26a],
F. Dittus [30], F. Djama [84], T. Djobava [51b], M.A.B. do Vale [24c], A. Do Valle Wemans [125a,m],
T.K.O. Doan [5], D. Dobos [30], E. Dobson [77], J. Dodd [35], C. Doglioni [49], T. Doherty [53],
T. Dohmae [156], Y. Doi [65,∗], J. Dolejsi [128], Z. Dolezal [128], B.A. Dolgoshein [97,∗],

M. Donadelli [24d], J. Donini [34], J. Dopke [30], A. Doria [103a], A. Dos Anjos [174], A. Dotti [123a,123b],
M.T. Dova [70], A.T. Doyle [53], M. Dris [10], J. Dubbert [88], S. Dube [15], E. Dubreuil [34],
E. Duchovni [173], G. Duckeck [99], D. Duda [176], A. Dudarev [30], F. Dudziak [63], L. Duflot [116],
M-A. Dufour [86], L. Duguid [76], M. Dührssen [30], M. Dunford [58a], H. Duran Yildiz [4a],
M. Düren [52], M. Dwuznik [38a], J. Ebke [99], W. Edson [2], C.A. Edwards [76], N.C. Edwards [46],
W. Ehrenfeld [21], T. Eifert [144], G. Eigen [14], K. Einsweiler [15], E. Eisenhandler [75], T. Ekelof [167],
M. El Kacimi [136c], M. Ellert [167], S. Elles [5], F. Ellinghaus [82], K. Ellis [75], N. Ellis [30],
J. Elmsheuser [99], M. Elsing [30], D. Emeliyanov [130], Y. Enari [156], O.C. Endner [82],
R. Engelmann [149], A. Engl [99], J. Erdmann [177], A. Ereditato [17], D. Eriksson [147a], G. Ernis [176],
J. Ernst [2], M. Ernst [25], J. Ernwein [137], D. Errede [166], S. Errede [166], E. Ertel [82], M. Escalier [116],
H. Esch [43], C. Escobar [124], X. Espinal Curull [12], B. Esposito [47], F. Etienne [84], A.I. Etienvre [137],
E. Etzion [154], D. Evangelakou [54], H. Evans [60], L. Fabbri [20a,20b], C. Fabre [30], G. Facini [30],
R.M. Fakhrutdinov [129], S. Falciano [133a], Y. Fang [33a], M. Fanti [90a,90b], A. Farbin [8],
A. Farilla [135a], T. Farooque [159], S. Farrell [164], S.M. Farrington [171], P. Farthouat [30], F. Fassi [168],
P. Fassnacht [30], D. Fassouliotis [9], B. Fatholahzadeh [159], A. Favareto [90a,90b], L. Fayard [116],
P. Federic [145a], O.L. Fedin [122], W. Fedorko [169], M. Fehling-Kaschek [48], L. Feligioni [84],
C. Feng [33d], E.J. Feng [6], H. Feng [88], A.B. Fenyuk [129], J. Ferencei [145b], W. Fernando [6],
S. Ferrag [53], J. Ferrando [53], V. Ferrara [42], A. Ferrari [167], P. Ferrari [106], R. Ferrari [120a],
D.E. Ferreira de Lima [53], A. Ferrer [168], D. Ferrere [49], C. Ferretti [88], A. Ferretto Parodi [50a,50b],
M. Fiascaris [31], F. Fiedler [82], A. Filipčič [74], M. Filipuzzi [42], F. Filthaut [105],
M. Fincke-Keeler [170], K.D. Finelli [45], M.C.N. Fiolhais [125a,h], L. Fiorini [168], A. Firan [40],
J. Fischer [176], M.J. Fisher [110], E.A. Fitzgerald [23], M. Flechl [48], I. Fleck [142], P. Fleischmann [175],
S. Fleischmann [176], G.T. Fletcher [140], G. Fletcher [75], T. Flick [176], A. Floderus [80],
L.R. Flores Castillo [174], A.C. Florez Bustos [160b], M.J. Flowerdew [100], T. Fonseca Martin [17],
A. Formica [137], A. Forti [83], D. Fortin [160a], D. Fournier [116], H. Fox [71], P. Francavilla [12],
M. Franchini [20a,20b], S. Franchino [30], D. Francis [30], M. Franklin [57], S. Franz [61],
M. Fraternali [120a,120b], S. Fratina [121], S.T. French [28], C. Friedrich [42], F. Friedrich [44],
D. Froidevaux [30], J.A. Frost [28], C. Fukunaga [157], E. Fullana Torregrosa [128], B.G. Fulsom [144],
J. Fuster [168], C. Gabaldon [55], O. Gabizon [173], A. Gabrielli [20a,20b], A. Gabrielli [133a,133b],
S. Gadatsch [106], T. Gadfort [25], S. Gadomski [49], G. Gagliardi [50a,50b], P. Gagnon [60], C. Galea [99],
B. Galhardo [125a], E.J. Gallas [119], V. Gallo [17], B.J. Gallop [130], P. Gallus [127], G. Galster [36],
K.K. Gan [110], R.P. Gandrajula [62], Y.S. Gao [144,f], F.M. Garay Walls [46], F. Garberson [177],
C. García [168], J.E. García Navarro [168], M. Garcia-Sciveres [15], R.W. Gardner [31], N. Garelli [144],
V. Garonne [30], C. Gatti [47], G. Gaudio [120a], B. Gaur [142], L. Gauthier [94], P. Gauzzi [133a,133b],
I.L. Gavrilenko [95], C. Gay [169], G. Gaycken [21], E.N. Gazis [10], P. Ge [33d,n], Z. Gecse [169],
C.N.P. Gee [130], D.A.A. Geerts [106], Ch. Geich-Gimbel [21], K. Gellerstedt [147a,147b], C. Gemme [50a],
A. Gemmell [53], M.H. Genest [55], S. Gentile [133a,133b], M. George [54], S. George [76],
D. Gerbaudo [164], A. Gershon [154], H. Ghazlane [136b], N. Ghodbane [34], B. Giacobbe [20a],
S. Giagu [133a,133b], V. Giangiobbe [12], P. Giannetti [123a,123b], F. Gianotti [30], B. Gibbard [25],
S.M. Gibson [76], M. Gilchriese [15], T.P.S. Gillam [28], D. Gillberg [30], A.R. Gillman [130],
D.M. Gingrich [3,e], N. Giokaris [9], M.P. Giordani [165c], R. Giordano [103a,103b], F.M. Giorgi [16],
P. Giovannini [100], P.F. Giraud [137], D. Giugni [90a], C. Giuliani [48], M. Giunta [94], B.K. Gjelsten [118],
I. Gkialas [155,o], L.K. Gladilin [98], C. Glasman [81], J. Glatzer [21], A. Glazov [42], G.L. Glonti [64],
M. Goblirsch-Kolb [100], J.R. Goddard [75], J. Godfrey [143], J. Godlewski [30], M. Goebel [42],
C. Goeringer [82], S. Goldfarb [88], T. Golling [177], D. Golubkov [129], A. Gomes [125a,c],
L.S. Gomez Fajardo [42], R. Gonçalo [76], J. Goncalves Pinto Firmino Da Costa [42], L. Gonella [21],
S. González de la Hoz [168], G. Gonzalez Parra [12], M.L. Gonzalez Silva [27],
S. Gonzalez-Sevilla [49], J.J. Goodson [149], L. Goossens [30], P.A. Gorbounov [96], H.A. Gordon [25],
I. Gorelov [104], G. Gorfine [176], B. Gorini [30], E. Gorini [72a,72b], A. Gorišek [74], E. Gornicki [39],
A.T. Goshaw [6], C. Gössling [43], M.I. Gostkin [64], I. Gough Eschrich [164], M. Gouighri [136a],
D. Goujdami [136c], M.P. Goulette [49], A.G. Goussiou [139], C. Goy [5], S. Gozpinar [23],
H.M.X. Grabas [137], L. Graber [54], I. Grabowska-Bold [38a], P. Grafström [20a,20b], K-J. Grahn [42],

E. Gramstad [118], F. Grancagnolo [72a], S. Grancagnolo [16], V. Grassi [149], V. Gratchev [122],
H.M. Gray [30], J.A. Gray [149], E. Graziani [135a], O.G. Grebenyuk [122], Z.D. Greenwood [78,l],
K. Gregersen [36], I.M. Gregor [42], P. Grenier [144], J. Griffiths [8], N. Grigalashvili [64],
A.A. Grillo [138], K. Grimm [71], S. Grinstein [12,p], Ph. Gris [34], Y.V. Grishkevich [98], J.-F. Grivaz [116],
J.P. Grohs [44], A. Grohsjean [42], E. Gross [173], J. Grosse-Knetter [54], J. Groth-Jensen [173],
K. Grybel [142], F. Guescini [49], D. Guest [177], O. Gueta [154], C. Guicheney [34], E. Guido [50a,50b],
T. Guillemin [116], S. Guindon [2], U. Gul [53], J. Gunther [127], J. Guo [35], S. Gupta [119],
P. Gutierrez [112], N.G. Gutierrez Ortiz [53], N. Guttman [154], O. Gutzwiller [174], C. Guyot [137],
C. Gwenlan [119], C.B. Gwilliam [73], A. Haas [109], C. Haber [15], H.K. Hadavand [8], P. Haefner [21],
S. Hageboeck [21], Z. Hajduk [39], H. Hakobyan [178], D. Hall [119], G. Halladjian [62],
K. Hamacher [176], P. Hamal [114], K. Hamano [87], M. Hamer [54], A. Hamilton [146a,q],
S. Hamilton [162], L. Han [33b], K. Hanagaki [117], K. Hanawa [156], M. Hance [15], C. Handel [82],
P. Hanke [58a], J.R. Hansen [36], J.B. Hansen [36], J.D. Hansen [36], P.H. Hansen [36], P. Hansson [144],
K. Hara [161], A.S. Hard [174], T. Harenberg [176], S. Harkusha [91], D. Harper [88], R.D. Harrington [46],
O.M. Harris [139], J. Hartert [48], F. Hartjes [106], A. Harvey [56], S. Hasegawa [102], Y. Hasegawa [141],
S. Hassani [137], S. Haug [17], M. Hauschild [30], R. Hauser [89], M. Havranek [21], C.M. Hawkes [18],
R.J. Hawkings [30], A.D. Hawkins [80], T. Hayashi [161], D. Hayden [89], C.P. Hays [119],
H.S. Hayward [73], S.J. Haywood [130], S.J. Head [18], T. Heck [82], V. Hedberg [80], L. Heelan [8],
S. Heim [121], B. Heinemann [15], S. Heisterkamp [36], J. Hejbal [126], L. Helary [22], C. Heller [99],
M. Heller [30], S. Hellman [147a,147b], D. Hellmich [21], C. Helsens [30], J. Henderson [119],
R.C.W. Henderson [71], A. Henrichs [177], A.M. Henriques Correia [30], S. Henrot-Versille [116],
C. Hensel [54], G.H. Herbert [16], C.M. Hernandez [8], Y. Hernández Jiménez [168],
R. Herrberg-Schubert [16], G. Herten [48], R. Hertenberger [99], L. Hervas [30], G.G. Hesketh [77],
N.P. Hessey [106], R. Hickling [75], E. Higón-Rodriguez [168], J.C. Hill [28], K.H. Hiller [42], S. Hillert [21],
S.J. Hillier [18], I. Hinchliffe [15], E. Hines [121], M. Hirose [117], D. Hirschbuehl [176], J. Hobbs [149],
N. Hod [106], M.C. Hodgkinson [140], P. Hodgson [140], A. Hoecker [30], M.R. Hoeferkamp [104],
J. Hoffman [40], D. Hoffmann [84], J.I. Hofmann [58a], M. Hohlfeld [82], S.O. Holmgren [147a],
J.L. Holzbauer [89], T.M. Hong [121], L. Hooft van Huysduynen [109], J-Y. Hostachy [55], S. Hou [152],
A. Hoummada [136a], J. Howard [119], J. Howarth [83], M. Hrabovsky [114], I. Hristova [16],
J. Hrivnac [116], T. Hryn'ova [5], P.J. Hsu [82], S.-C. Hsu [139], D. Hu [35], X. Hu [25], Y. Huang [33a],
Z. Hubacek [30], F. Hubaut [84], F. Huegging [21], A. Huettmann [42], T.B. Huffman [119],
E.W. Hughes [35], G. Hughes [71], M. Huhtinen [30], T.A. Hülsing [82], M. Hurwitz [15],
N. Huseynov [64,r], J. Huston [89], J. Huth [57], G. Iacobucci [49], G. Iakovidis [10], I. Ibragimov [142],
L. Iconomidou-Fayard [116], J. Idarraga [116], P. Iengo [103a], O. Igonkina [106], Y. Ikegami [65],
K. Ikematsu [142], M. Ikeno [65], D. Iliadis [155], N. Ilic [159], Y. Inamaru [66], T. Ince [100], P. Ioannou [9],
M. Iodice [135a], K. Iordanidou [9], V. Ippolito [133a,133b], A. Irles Quiles [168], C. Isaksson [167],
M. Ishino [67], M. Ishitsuka [158], R. Ishmukhametov [110], C. Issever [119], S. Istin [19a],
A.V. Ivashin [129], W. Iwanski [39], H. Iwasaki [65], J.M. Izen [41], V. Izzo [103a], B. Jackson [121],
J.N. Jackson [73], M. Jackson [73], P. Jackson [1], M.R. Jaekel [30], V. Jain [2], K. Jakobs [48],
S. Jakobsen [36], T. Jakoubek [126], J. Jakubek [127], D.O. Jamin [152], D.K. Jana [112], E. Jansen [77],
H. Jansen [30], J. Janssen [21], M. Janus [171], R.C. Jared [174], G. Jarlskog [80], L. Jeanty [57],
G.-Y. Jeng [151], I. Jen-La Plante [31], D. Jennens [87], P. Jenni [48,s], J. Jentzsch [43], C. Jeske [171],
S. Jézéquel [5], M.K. Jha [20a], H. Ji [174], W. Ji [82], J. Jia [149], Y. Jiang [33b], M. Jimenez Belenguer [42],
S. Jin [33a], O. Jinnouchi [158], M.D. Joergensen [36], D. Joffe [40], K.E. Johansson [147a],
P. Johansson [140], S. Johnert [42], K.A. Johns [7], K. Jon-And [147a,147b], G. Jones [171],
R.W.L. Jones [71], T.J. Jones [73], P.M. Jorge [125a], K.D. Joshi [83], J. Jovicevic [148], X. Ju [174],
C.A. Jung [43], R.M. Jungst [30], P. Jussel [61], A. Juste Rozas [12,p], M. Kaci [168], A. Kaczmarska [39],
P. Kadlecik [36], M. Kado [116], H. Kagan [110], M. Kagan [144], E. Kajomovitz [153], S. Kalinin [176],
S. Kama [40], N. Kanaya [156], M. Kaneda [30], S. Kaneti [28], T. Kanno [158], V.A. Kantserov [97],
J. Kanzaki [65], B. Kaplan [109], A. Kapliy [31], D. Kar [53], K. Karakostas [10], N. Karastathis [10],
M. Karnevskiy [82], S.N. Karpov [64], V. Kartvelishvili [71], A.N. Karyukhin [129], L. Kashif [174],
G. Kasieczka [58b], R.D. Kass [110], A. Kastanas [14], Y. Kataoka [156], A. Katre [49], J. Katzy [42],

V. Kaushik [7], K. Kawagoe [69], T. Kawamoto [156], G. Kawamura [54], S. Kazama [156],
V.F. Kazanin [108], M.Y. Kazarinov [64], R. Keeler [170], P.T. Keener [121], R. Kehoe [40], M. Keil [54],
J.S. Keller [139], H. Keoshkerian [5], O. Kepka [126], B.P. Kerš/evan [74], S. Kersten [176], K. Kessoku [156],
J. Keung [159], F. Khalil-zada [11], H. Khandanyan [147a,147b], A. Khanov [113], D. Kharchenko [64],
A. Khodinov [97], A. Khomich [58a], T.J. Khoo [28], G. Khoriauli [21], A. Khoroshilov [176],
V. Khovanskiy [96], E. Khramov [64], J. Khubua [51b], H. Kim [147a,147b], S.H. Kim [161], N. Kimura [172],
O. Kind [16], B.T. King [73], M. King [66], R.S.B. King [119], S.B. King [169], J. Kirk [130], A.E. Kiryunin [100],
T. Kishimoto [66], D. Kisielewska [38a], T. Kitamura [66], T. Kittelmann [124], K. Kiuchi [161],
E. Kladiva [145b], M. Klein [73], U. Klein [73], K. Kleinknecht [82], M. Klemetti [86], P. Klimek [147a,147b],
A. Klimentov [25], R. Klingenberg [43], J.A. Klinger [83], E.B. Klinkby [36], T. Klioutchnikova [30],
P.F. Klok [105], E.-E. Kluge [58a], P. Kluit [106], S. Kluth [100], E. Kneringer [61], E.B.F.G. Knoops [84],
A. Knue [54], B.R. Ko [45], T. Kobayashi [156], M. Kobel [44], M. Kocian [144], P. Kodys [128], S. Koenig [82],
P. Koevesarki [21], T. Koffas [29], E. Koffeman [106], L.A. Kogan [119], S. Kohlmann [176], F. Kohn [54],
Z. Kohout [127], T. Kohriki [65], T. Koi [144], H. Kolanoski [16], I. Koletsou [90a], J. Koll [89],
A.A. Komar [95,*], Y. Komori [156], T. Kondo [65], K. Köneke [48], A.C. König [105], T. Kono [42,t],
R. Konoplich [109,u], N. Konstantinidis [77], R. Kopeliansky [153], S. Koperny [38a], L. Köpke [82],
A.K. Kopp [48], K. Korcyl [39], K. Kordas [155], A. Korn [46], A.A. Korol [108], I. Korolkov [12],
E.V. Korolkova [140], V.A. Korotkov [129], O. Kortner [100], S. Kortner [100], V.V. Kostyukhin [21],
S. Kotov [100], V.M. Kotov [64], A. Kotwal [45], C. Kourkoumelis [9], V. Kouskoura [155],
A. Koutsman [160a], R. Kowalewski [170], T.Z. Kowalski [38a], W. Kozanecki [137], A.S. Kozhin [129],
V. Kral [127], V.A. Kramarenko [98], G. Kramberger [74], A. Krasznahorkay [109], J.K. Kraus [21],
A. Kravchenko [25], S. Kreiss [109], J. Kretzschmar [73], K. Kreutzfeldt [52], N. Krieger [54],
P. Krieger [159], K. Kroeninger [54], H. Kroha [100], J. Kroll [121], J. Kroseberg [21], J. Krstic [13a],
U. Kruchonak [64], H. Krüger [21], T. Kruker [17], N. Krumnack [63], Z.V. Krumshteyn [64],
A. Kruse [174], M.K. Kruse [45], M. Kruskal [22], T. Kubota [87], S. Kuday [4a], S. Kuehn [48], A. Kugel [58c],
T. Kuhl [42], V. Kukhtin [64], Y. Kulchitsky [91], S. Kuleshov [32b], M. Kuna [79], J. Kunkle [121],
A. Kupco [126], H. Kurashige [66], M. Kurata [161], Y.A. Kurochkin [91], R. Kurumida [66], V. Kus [126],
E.S. Kuwertz [148], M. Kuze [158], J. Kvita [143], R. Kwee [16], A. La Rosa [49], L. La Rotonda [37a,37b],
L. Labarga [81], S. Lablak [136a], C. Lacasta [168], F. Lacava [133a,133b], J. Lacey [29], H. Lacker [16],
D. Lacour [79], V.R. Lacuesta [168], E. Ladygin [64], R. Lafaye [5], B. Laforge [79], T. Lagouri [177],
S. Lai [48], H. Laier [58a], E. Laisne [55], L. Lambourne [77], C.L. Lampen [7], W. Lampl [7], E. Lançon [137],
U. Landgraf [48], M.P.J. Landon [75], V.S. Lang [58a], C. Lange [42], A.J. Lankford [164], F. Lanni [25],
K. Lantzsch [30], A. Lanza [120a], S. Laplace [79], C. Lapoire [21], J.F. Laporte [137], T. Lari [90a],
A. Larner [119], M. Lassnig [30], P. Laurelli [47], V. Lavorini [37a,37b], W. Lavrijsen [15], P. Laycock [73],
B.T. Le [55], O. Le Dortz [79], E. Le Guirriec [84], E. Le Menedeu [12], T. LeCompte [6],
F. Ledroit-Guillon [55], C.A. Lee [152], H. Lee [106], J.S.H. Lee [117], S.C. Lee [152], L. Lee [177],
G. Lefebvre [79], M. Lefebvre [170], M. Legendre [137], F. Legger [99], C. Leggett [15], A. Lehan [73],
M. Lehmacher [21], G. Lehmann Miotto [30], A.G. Leister [177], M.A.L. Leite [24d], R. Leitner [128],
D. Lellouch [173], B. Lemmer [54], V. Lendermann [58a], K.J.C. Leney [146c], T. Lenz [106],
G. Lenzen [176], B. Lenzi [30], R. Leone [7], K. Leonhardt [44], S. Leontsinis [10], C. Leroy [94],
J-R. Lessard [170], C.G. Lester [28], C.M. Lester [121], J. Levêque [5], D. Levin [88], L.J. Levinson [173],
A. Lewis [119], G.H. Lewis [109], A.M. Leyko [21], M. Leyton [16], B. Li [33b,v], B. Li [84], H. Li [149],
H.L. Li [31], S. Li [45], X. Li [88], Z. Liang [119,w], H. Liao [34], B. Liberti [134a], P. Lichard [30], K. Lie [166],
J. Liebal [21], W. Liebig [14], C. Limbach [21], A. Limosani [87], M. Limper [62], S.C. Lin [152,x],
F. Linde [106], B.E. Lindquist [149], J.T. Linnemann [89], E. Lipeles [121], A. Lipniacka [14],
M. Lisovyi [42], T.M. Liss [166], D. Lissauer [25], A. Lister [169], A.M. Litke [138], B. Liu [152], D. Liu [152],
J.B. Liu [33b], K. Liu [33b,y], L. Liu [88], M. Liu [45], M. Liu [33b], Y. Liu [33b], M. Livan [120a,120b],
S.S.A. Livermore [119], A. Lleres [55], J. Llorente Merino [81], S.L. Lloyd [75], F. Lo Sterzo [133a,133b],
E. Lobodzinska [42], P. Loch [7], W.S. Lockman [138], T. Loddenkoetter [21], F.K. Loebinger [83],
A.E. Loevschall-Jensen [36], A. Loginov [177], C.W. Loh [169], T. Lohse [16], K. Lohwasser [48],
M. Lokajicek [126], V.P. Lombardo [5], R.E. Long [71], L. Lopes [125a], D. Lopez Mateos [57],
B. Lopez Paredes [140], J. Lorenz [99], N. Lorenzo Martinez [116], M. Losada [163], P. Loscutoff [15],

M.J. Losty [160a,∗], X. Lou [41], A. Lounis [116], J. Love [6], P.A. Love [71], A.J. Lowe [144,f], F. Lu [33a],
H.J. Lubatti [139], C. Luci [133a,133b], A. Lucotte [55], D. Ludwig [42], I. Ludwig [48], J. Ludwig [48],
F. Luehring [60], W. Lukas [61], L. Luminari [133a], E. Lund [118], J. Lundberg [147a,147b],
O. Lundberg [147a,147b], B. Lund-Jensen [148], M. Lungwitz [82], D. Lynn [25], R. Lysak [126],
E. Lytken [80], H. Ma [25], L.L. Ma [33d], G. Maccarrone [47], A. Macchiolo [100], B. Maček [74],
J. Machado Miguens [125a], D. Macina [30], R. Mackeprang [36], R. Madar [48], R.J. Madaras [15],
H.J. Maddocks [71], W.F. Mader [44], A. Madsen [167], M. Maeno [8], T. Maeno [25], L. Magnoni [164],
E. Magradze [54], K. Mahboubi [48], J. Mahlstedt [106], S. Mahmoud [73], G. Mahout [18],
C. Maiani [137], C. Maidantchik [24a], A. Maio [125a,c], S. Majewski [115], Y. Makida [65],
N. Makovec [116], P. Mal [137,z], B. Malaescu [79], Pa. Malecki [39], V.P. Maleev [122], F. Malek [55],
U. Mallik [62], D. Malon [6], C. Malone [144], S. Maltezos [10], V.M. Malyshev [108], S. Malyukov [30],
J. Mamuzic [13b], L. Mandelli [90a], I. Mandić [74], R. Mandrysch [62], J. Maneira [125a],
A. Manfredini [100], L. Manhaes de Andrade Filho [24b], J.A. Manjarres Ramos [137], A. Mann [99],
P.M. Manning [138], A. Manousakis-Katsikakis [9], B. Mansoulie [137], R. Mantifel [86], L. Mapelli [30],
L. March [168], J.F. Marchand [29], F. Marchese [134a,134b], G. Marchiori [79], M. Marcisovsky [126],
C.P. Marino [170], C.N. Marques [125a], F. Marroquim [24a], Z. Marshall [15], L.F. Marti [17],
S. Marti-Garcia [168], B. Martin [30], B. Martin [89], J.P. Martin [94], T.A. Martin [171], V.J. Martin [46],
B. Martin dit Latour [49], H. Martinez [137], M. Martinez [12,p], S. Martin-Haugh [150],
A.C. Martyniuk [170], M. Marx [139], F. Marzano [133a], A. Marzin [112], L. Masetti [82],
T. Mashimo [156], R. Mashinistov [95], J. Masik [83], A.L. Maslennikov [108], I. Massa [20a,20b],
N. Massol [5], P. Mastrandrea [149], A. Mastroberardino [37a,37b], T. Masubuchi [156],
H. Matsunaga [156], T. Matsushita [66], P. Mättig [176], S. Mättig [42], J. Mattmann [82],
C. Mattravers [119,d], J. Maurer [84], S.J. Maxfield [73], D.A. Maximov [108,g], R. Mazini [152],
L. Mazzaferro [134a,134b], M. Mazzanti [90a], S.P. Mc Kee [88], A. McCarn [166], R.L. McCarthy [149],
T.G. McCarthy [29], N.A. McCubbin [130], K.W. McFarlane [56,∗], J.A. Mcfayden [140],
G. Mchedlidze [51b], T. Mclaughlan [18], S.J. McMahon [130], R.A. McPherson [170,j], A. Meade [85],
J. Mechnich [106], M. Mechtel [176], M. Medinnis [42], S. Meehan [31], R. Meera-Lebbai [112],
S. Mehlhase [36], A. Mehta [73], K. Meier [58a], C. Meineck [99], B. Meirose [80], C. Melachrinos [31],
B.R. Mellado Garcia [146c], F. Meloni [90a,90b], L. Mendoza Navas [163], A. Mengarelli [20a,20b],
S. Menke [100], E. Meoni [162], K.M. Mercurio [57], S. Mergelmeyer [21], N. Meric [137], P. Mermod [49],
L. Merola [103a,103b], C. Meroni [90a], F.S. Merritt [31], H. Merritt [110], A. Messina [30,aa],
J. Metcalfe [25], A.S. Mete [164], C. Meyer [82], C. Meyer [31], J-P. Meyer [137], J. Meyer [30], J. Meyer [54],
S. Michal [30], R.P. Middleton [130], S. Migas [73], L. Mijović [137], G. Mikenberg [173],
M. Mikestikova [126], M. Mikuž [74], D.W. Miller [31], W.J. Mills [169], C. Mills [57], A. Milov [173],
D.A. Milstead [147a,147b], D. Milstein [173], A.A. Minaenko [129], M. Miñano Moya [168],
I.A. Minashvili [64], A.I. Mincer [109], B. Mindur [38a], M. Mineev [64], Y. Ming [174], L.M. Mir [12],
G. Mirabelli [133a], T. Mitani [172], J. Mitrevski [138], V.A. Mitsou [168], S. Mitsui [65],
P.S. Miyagawa [140], J.U. Mjörnmark [80], T. Moa [147a,147b], V. Moeller [28], S. Mohapatra [149],
W. Mohr [48], S. Molander [147a,147b], R. Moles-Valls [168], A. Molfetas [30], K. Mönig [42],
C. Monini [55], J. Monk [36], E. Monnier [84], J. Montejo Berlingen [12], F. Monticelli [70],
S. Monzani [20a,20b], R.W. Moore [3], C. Mora Herrera [49], A. Moraes [53], N. Morange [62],
J. Morel [54], D. Moreno [82], M. Moreno Llácer [168], P. Morettini [50a], M. Morgenstern [44],
M. Morii [57], S. Moritz [82], A.K. Morley [148], G. Mornacchi [30], J.D. Morris [75], L. Morvaj [102],
H.G. Moser [100], M. Mosidze [51b], J. Moss [110], R. Mount [144], E. Mountricha [10,ab],
S.V. Mouraviev [95,∗], E.J.W. Moyse [85], R.D. Mudd [18], F. Mueller [58a], J. Mueller [124],
K. Mueller [21], T. Mueller [28], T. Mueller [82], D. Muenstermann [49], Y. Munwes [154],
J.A. Murillo Quijada [18], W.J. Murray [130], I. Mussche [106], E. Musto [153], A.G. Myagkov [129,ac],
M. Myska [126], O. Nackenhorst [54], J. Nadal [12], K. Nagai [61], R. Nagai [158], Y. Nagai [84],
K. Nagano [65], A. Nagarkar [110], Y. Nagasaka [59], M. Nagel [100], A.M. Nairz [30], Y. Nakahama [30],
K. Nakamura [65], T. Nakamura [156], I. Nakano [111], H. Namasivayam [41], G. Nanava [21],
A. Napier [162], R. Narayan [58b], M. Nash [77,d], T. Nattermann [21], T. Naumann [42], G. Navarro [163],
H.A. Neal [88], P.Yu. Nechaeva [95], T.J. Neep [83], A. Negri [120a,120b], G. Negri [30], M. Negrini [20a],

S. Nektarijevic [49], A. Nelson [164], T.K. Nelson [144], S. Nemecek [126], P. Nemethy [109],
A.A. Nepomuceno [24a], M. Nessi [30,ad], M.S. Neubauer [166], M. Neumann [176], A. Neusiedl [82],
R.M. Neves [109], P. Nevski [25], F.M. Newcomer [121], P.R. Newman [18], D.H. Nguyen [6],
V. Nguyen Thi Hong [137], R.B. Nickerson [119], R. Nicolaidou [137], B. Nicquevert [30],
J. Nielsen [138], N. Nikiforou [35], A. Nikiforov [16], V. Nikolaenko [129,ac], I. Nikolic-Audit [79],
K. Nikolics [49], K. Nikolopoulos [18], P. Nilsson [8], Y. Ninomiya [156], A. Nisati [133a], R. Nisius [100],
T. Nobe [158], L. Nodulman [6], M. Nomachi [117], I. Nomidis [155], S. Norberg [112], M. Nordberg [30],
J. Novakova [128], M. Nozaki [65], L. Nozka [114], K. Ntekas [10], A.-E. Nuncio-Quiroz [21],
G. Nunes Hanninger [87], T. Nunnemann [99], E. Nurse [77], B.J. O'Brien [46], F. O'grady [7],
D.C. O'Neil [143], V. O'Shea [53], L.B. Oakes [99], F.G. Oakham [29,e], H. Oberlack [100], J. Ocariz [79],
A. Ochi [66], M.I. Ochoa [77], S. Oda [69], S. Odaka [65], J. Odier [84], H. Ogren [60], A. Oh [83], S.H. Oh [45],
C.C. Ohm [30], T. Ohshima [102], W. Okamura [117], H. Okawa [25], Y. Okumura [31], T. Okuyama [156],
A. Olariu [26a], A.G. Olchevski [64], S.A. Olivares Pino [46], M. Oliveira [125a,h],
D. Oliveira Damazio [25], E. Oliver Garcia [168], D. Olivito [121], A. Olszewski [39], J. Olszowska [39],
A. Onofre [125a,ae], P.U.E. Onyisi [31,af], C.J. Oram [160a], M.J. Oreglia [31], Y. Oren [154],
D. Orestano [135a,135b], N. Orlando [72a,72b], C. Oropeza Barrera [53], R.S. Orr [159],
B. Osculati [50a,50b], R. Ospanov [121], G. Otero y Garzon [27], H. Otono [69], J.P. Ottersbach [106],
M. Ouchrif [136d], E.A. Ouellette [170], F. Ould-Saada [118], A. Ouraou [137], K.P. Oussoren [106],
Q. Ouyang [33a], A. Ovcharova [15], M. Owen [83], S. Owen [140], V.E. Ozcan [19a], N. Ozturk [8],
K. Pachal [119], A. Pacheco Pages [12], C. Padilla Aranda [12], S. Pagan Griso [15], E. Paganis [140],
C. Pahl [100], F. Paige [25], P. Pais [85], K. Pajchel [118], G. Palacino [160b], C.P. Paleari [7], S. Palestini [30],
D. Pallin [34], A. Palma [125a], J.D. Palmer [18], Y.B. Pan [174], E. Panagiotopoulou [10],
J.G. Panduro Vazquez [76], P. Pani [106], N. Panikashvili [88], S. Panitkin [25], D. Pantea [26a],
A. Papadelis [147a], Th.D. Papadopoulou [10], K. Papageorgiou [155,o], A. Paramonov [6],
D. Paredes Hernandez [34], M.A. Parker [28], F. Parodi [50a,50b], J.A. Parsons [35], U. Parzefall [48],
S. Pashapour [54], E. Pasqualucci [133a], S. Passaggio [50a], A. Passeri [135a], F. Pastore [135a,135b,*],
Fr. Pastore [76], G. Pásztor [49,ag], S. Pataraia [176], N.D. Patel [151], J.R. Pater [83],
S. Patricelli [103a,103b], T. Pauly [30], J. Pearce [170], M. Pedersen [118], S. Pedraza Lopez [168],
M.I. Pedraza Morales [174], S.V. Peleganchuk [108], D. Pelikan [167], H. Peng [33b], B. Penning [31],
A. Penson [35], J. Penwell [60], D.V. Perepelitsa [35], T. Perez Cavalcanti [42], E. Perez Codina [160a],
M.T. Pérez García-Estañ [168], V. Perez Reale [35], L. Perini [90a,90b], H. Pernegger [30],
R. Perrino [72a], V.D. Peshekhonov [64], K. Peters [30], R.F.Y. Peters [54,ah], B.A. Petersen [30],
J. Petersen [30], T.C. Petersen [36], E. Petit [5], A. Petridis [147a,147b], C. Petridou [155], E. Petrolo [133a],
F. Petrucci [135a,135b], M. Petteni [143], R. Pezoa [32b], P.W. Phillips [130], G. Piacquadio [144],
E. Pianori [171], A. Picazio [49], E. Piccaro [75], M. Piccinini [20a,20b], S.M. Piec [42], R. Piegaia [27],
D.T. Pignotti [110], J.E. Pilcher [31], A.D. Pilkington [77], J. Pina [125a,c], M. Pinamonti [165a,165c,ai],
A. Pinder [119], J.L. Pinfold [3], A. Pingel [36], B. Pinto [125a], C. Pizio [90a,90b], M.-A. Pleier [25],
V. Pleskot [128], E. Plotnikova [64], P. Plucinski [147a,147b], S. Poddar [58a], F. Podlyski [34],
R. Poettgen [82], L. Poggioli [116], D. Pohl [21], M. Pohl [49], G. Polesello [120a], A. Policicchio [37a,37b],
R. Polifka [159], A. Polini [20a], C.S. Pollard [45], V. Polychronakos [25], D. Pomeroy [23],
K. Pommès [30], L. Pontecorvo [133a], B.G. Pope [89], G.A. Popeneciu [26b], D.S. Popovic [13a],
A. Poppleton [30], X. Portell Bueso [12], G.E. Pospelov [100], S. Pospisil [127], I.N. Potrap [64],
C.J. Potter [150], C.T. Potter [115], G. Poulard [30], J. Poveda [60], V. Pozdnyakov [64], R. Prabhu [77],
P. Pralavorio [84], A. Pranko [15], S. Prasad [30], R. Pravahan [25], S. Prell [63], D. Price [60], J. Price [73],
L.E. Price [6], D. Prieur [124], M. Primavera [72a], M. Proissl [46], K. Prokofiev [109], F. Prokoshin [32b],
E. Protopapadaki [137], S. Protopopescu [25], J. Proudfoot [6], X. Prudent [44], M. Przybycien [38a],
H. Przysiezniak [5], S. Psoroulas [21], E. Ptacek [115], E. Pueschel [85], D. Puldon [149],
M. Purohit [25,aj], P. Puzo [116], Y. Pylypchenko [62], J. Qian [88], A. Quadt [54], D.R. Quarrie [15],
W.B. Quayle [146c], D. Quilty [53], V. Radeka [25], V. Radescu [42], P. Radloff [115], F. Ragusa [90a,90b],
G. Rahal [179], S. Rajagopalan [25], M. Rammensee [48], M. Rammes [142], A.S. Randle-Conde [40],
C. Rangel-Smith [79], K. Rao [164], F. Rauscher [99], T.C. Rave [48], T. Ravenscroft [53], M. Raymond [30],
A.L. Read [118], D.M. Rebuzzi [120a,120b], A. Redelbach [175], G. Redlinger [25], R. Reece [121],

K. Reeves [41], A. Reinsch [115], I. Reisinger [43], M. Relich [164], C. Rembser [30], Z.L. Ren [152], A. Renaud [116], M. Rescigno [133a], S. Resconi [90a], B. Resende [137], P. Reznicek [99], R. Rezvani [94], R. Richter [100], E. Richter-Was [38b], M. Ridel [79], P. Rieck [16], M. Rijssenbeek [149], A. Rimoldi [120a,120b], L. Rinaldi [20a], R.R. Rios [40], E. Ritsch [61], I. Riu [12], G. Rivoltella [90a,90b], F. Rizatdinova [113], E. Rizvi [75], S.H. Robertson [86,j], A. Robichaud-Veronneau [119], D. Robinson [28], J.E.M. Robinson [83], A. Robson [53], J.G. Rocha de Lima [107], C. Roda [123a,123b], D. Roda Dos Santos [126], L. Rodrigues [30], A. Roe [54], S. Roe [30], O. Røhne [118], S. Rolli [162], A. Romaniouk [97], M. Romano [20a,20b], G. Romeo [27], E. Romero Adam [168], N. Rompotis [139], L. Roos [79], E. Ros [168], S. Rosati [133a], K. Rosbach [49], A. Rose [150], M. Rose [76], P.L. Rosendahl [14], O. Rosenthal [142], V. Rossetti [12], E. Rossi [133a,133b], L.P. Rossi [50a], R. Rosten [139], M. Rotaru [26a], I. Roth [173], J. Rothberg [139], D. Rousseau [116], C.R. Royon [137], A. Rozanov [84], Y. Rozen [153], X. Ruan [146c], F. Rubbo [12], I. Rubinskiy [42], N. Ruckstuhl [106], V.I. Rud [98], C. Rudolph [44], M.S. Rudolph [159], F. Rühr [7], A. Ruiz-Martinez [63], L. Rumyantsev [64], Z. Rurikova [48], N.A. Rusakovich [64], A. Ruschke [99], J.P. Rutherfoord [7], N. Ruthmann [48], P. Ruzicka [126], Y.F. Ryabov [122], M. Rybar [128], G. Rybkin [116], N.C. Ryder [119], A.F. Saavedra [151], A. Saddique [3], I. Sadeh [154], H.F-W. Sadrozinski [138], R. Sadykov [64], F. Safai Tehrani [133a], H. Sakamoto [156], G. Salamanna [75], A. Salamon [134a], M. Saleem [112], D. Salek [30], D. Salihagic [100], A. Salnikov [144], J. Salt [168], B.M. Salvachua Ferrando [6], D. Salvatore [37a,37b], F. Salvatore [150], A. Salvucci [105], A. Salzburger [30], D. Sampsonidis [155], A. Sanchez [103a,103b], J. Sánchez [168], V. Sanchez Martinez [168], H. Sandaker [14], H.G. Sander [82], M.P. Sanders [99], M. Sandhoff [176], T. Sandoval [28], C. Sandoval [163], R. Sandstroem [100], D.P.C. Sankey [130], A. Sansoni [47], C. Santoni [34], R. Santonico [134a,134b], H. Santos [125a], I. Santoyo Castillo [150], K. Sapp [124], A. Sapronov [64], J.G. Saraiva [125a], T. Sarangi [174], E. Sarkisyan-Grinbaum [8], B. Sarrazin [21], F. Sarri [123a,123b], G. Sartisohn [176], O. Sasaki [65], Y. Sasaki [156], N. Sasao [67], I. Satsounkevitch [91], G. Sauvage [5,*], E. Sauvan [5], J.B. Sauvan [116], P. Savard [159,e], V. Savinov [124], D.O. Savu [30], C. Sawyer [119], L. Sawyer [78,l], D.H. Saxon [53], J. Saxon [121], C. Sbarra [20a], A. Sbrizzi [3], T. Scanlon [30], D.A. Scannicchio [164], M. Scarcella [151], J. Schaarschmidt [116], P. Schacht [100], D. Schaefer [121], A. Schaelicke [46], S. Schaepe [21], S. Schaetzel [58b], U. Schäfer [82], A.C. Schaffer [116], D. Schaile [99], R.D. Schamberger [149], V. Scharf [58a], V.A. Schegelsky [122], D. Scheirich [88], M. Schernau [164], M.I. Scherzer [35], C. Schiavi [50a,50b], J. Schieck [99], C. Schillo [48], M. Schioppa [37a,37b], S. Schlenker [30], E. Schmidt [48], K. Schmieden [30], C. Schmitt [82], C. Schmitt [99], S. Schmitt [58b], B. Schneider [17], Y.J. Schnellbach [73], U. Schnoor [44], L. Schoeffel [137], A. Schoening [58b], A.L.S. Schorlemmer [54], M. Schott [82], D. Schouten [160a], J. Schovancova [126], M. Schram [86], C. Schroeder [82], N. Schroer [58c], N. Schuh [82], M.J. Schultens [21], H.-C. Schultz-Coulon [58a], H. Schulz [16], M. Schumacher [48], B.A. Schumm [138], Ph. Schune [137], A. Schwartzman [144], Ph. Schwegler [100], Ph. Schwemling [137], R. Schwienhorst [89], J. Schwindling [137], T. Schwindt [21], M. Schwoerer [5], F.G. Sciacca [17], E. Scifo [116], G. Sciolla [23], W.G. Scott [130], F. Scutti [21], J. Searcy [88], G. Sedov [42], E. Sedykh [122], S.C. Seidel [104], A. Seiden [138], F. Seifert [44], J.M. Seixas [24a], G. Sekhniaidze [103a], S.J. Sekula [40], K.E. Selbach [46], D.M. Seliverstov [122], G. Sellers [73], M. Seman [145b], N. Semprini-Cesari [20a,20b], C. Serfon [30], L. Serin [116], L. Serkin [54], T. Serre [84], R. Seuster [160a], H. Severini [112], F. Sforza [100], A. Sfyrla [30], E. Shabalina [54], M. Shamim [115], L.Y. Shan [33a], J.T. Shank [22], Q.T. Shao [87], M. Shapiro [15], P.B. Shatalov [96], K. Shaw [165a,165c], P. Sherwood [77], S. Shimizu [66], M. Shimojima [101], T. Shin [56], M. Shiyakova [64], A. Shmeleva [95], M.J. Shochet [31], D. Short [119], S. Shrestha [63], E. Shulga [97], M.A. Shupe [7], S. Shushkevich [42], P. Sicho [126], D. Sidorov [113], A. Sidoti [133a], F. Siegert [48], Dj. Sijacki [13a], O. Silbert [173], J. Silva [125a], Y. Silver [154], D. Silverstein [144], S.B. Silverstein [147a], V. Simak [127], O. Simard [5], Lj. Simic [13a], S. Simion [116], E. Simioni [82], B. Simmons [77], R. Simoniello [90a,90b], M. Simonyan [36], P. Sinervo [159], N.B. Sinev [115], V. Sipica [142], G. Siragusa [175], A. Sircar [78], A.N. Sisakyan [64,*], S.Yu. Sivoklokov [98], J. Sjölin [147a,147b], T.B. Sjursen [14], L.A. Skinnari [15], H.P. Skottowe [57], K.Yu. Skovpen [108], P. Skubic [112], M. Slater [18], T. Slavicek [127], K. Sliwa [162], V. Smakhtin [173], B.H. Smart [46], L. Smestad [118], S.Yu. Smirnov [97], Y. Smirnov [97], L.N. Smirnova [98,ak],

O. Smirnova [80], K.M. Smith [53], M. Smizanska [71], K. Smolek [127], A.A. Snesarev [95],
G. Snidero [75], J. Snow [112], S. Snyder [25], R. Sobie [170,j], J. Sodomka [127], A. Soffer [154],
D.A. Soh [152,w], C.A. Solans [30], M. Solar [127], J. Solc [127], E.Yu. Soldatov [97], U. Soldevila [168],
E. Solfaroli Camillocci [133a,133b], A.A. Solodkov [129], O.V. Solovyanov [129], V. Solovyev [122],
N. Soni [1], A. Sood [15], V. Sopko [127], B. Sopko [127], M. Sosebee [8], R. Soualah [165a,165c],
P. Soueid [94], A.M. Soukharev [108], D. South [42], S. Spagnolo [72a,72b], F. Spanò [76],
W.R. Spearman [57], R. Spighi [20a], G. Spigo [30], M. Spousta [128,al], T. Spreitzer [159], B. Spurlock [8],
R.D. St. Denis [53], J. Stahlman [121], R. Stamen [58a], E. Stanecka [39], R.W. Stanek [6],
C. Stanescu [135a], M. Stanescu-Bellu [42], M.M. Stanitzki [42], S. Stapnes [118], E.A. Starchenko [129],
J. Stark [55], P. Staroba [126], P. Starovoitov [42], R. Staszewski [39], A. Staude [99], P. Stavina [145a,∗],
G. Steele [53], P. Steinbach [44], P. Steinberg [25], I. Stekl [127], B. Stelzer [143], H.J. Stelzer [89],
O. Stelzer-Chilton [160a], H. Stenzel [52], S. Stern [100], G.A. Stewart [30], J.A. Stillings [21],
M.C. Stockton [86], M. Stoebe [86], K. Stoerig [48], G. Stoicea [26a], S. Stonjek [100], A.R. Stradling [8],
A. Straessner [44], J. Strandberg [148], S. Strandberg [147a,147b], A. Strandlie [118], E. Strauss [144],
M. Strauss [112], P. Strizenec [145b], R. Ströhmer [175], D.M. Strom [115], R. Stroynowski [40],
B. Stugu [14], I. Stumer [25,∗], J. Stupak [149], P. Sturm [176], N.A. Styles [42], D. Su [144],
HS. Subramania [3], R. Subramaniam [78], A. Succurro [12], Y. Sugaya [117], C. Suhr [107], M. Suk [127],
V.V. Sulin [95], S. Sultansoy [4c], T. Sumida [67], X. Sun [55], J.E. Sundermann [48], K. Suruliz [140],
G. Susinno [37a,37b], M.R. Sutton [150], Y. Suzuki [65], M. Svatos [126], S. Swedish [169],
M. Swiatlowski [144], I. Sykora [145a], T. Sykora [128], D. Ta [106], K. Tackmann [42], A. Taffard [164],
R. Tafirout [160a], N. Taiblum [154], Y. Takahashi [102], H. Takai [25], R. Takashima [68], H. Takeda [66],
T. Takeshita [141], Y. Takubo [65], M. Talby [84], A.A. Talyshev [108,g], J.Y.C. Tam [175],
M.C. Tamsett [78,am], K.G. Tan [87], J. Tanaka [156], R. Tanaka [116], S. Tanaka [132], S. Tanaka [65],
A.J. Tanasijczuk [143], K. Tani [66], N. Tannoury [84], S. Tapprogge [82], S. Tarem [153], F. Tarrade [29],
G.F. Tartarelli [90a], P. Tas [128], M. Tasevsky [126], T. Tashiro [67], E. Tassi [37a,37b],
A. Tavares Delgado [125a], Y. Tayalati [136d], C. Taylor [77], F.E. Taylor [93], G.N. Taylor [87],
W. Taylor [160b], M. Teinturier [116], F.A. Teischinger [30], M. Teixeira Dias Castanheira [75],
P. Teixeira-Dias [76], K.K. Temming [48], H. Ten Kate [30], P.K. Teng [152], S. Terada [65], K. Terashi [156],
J. Terron [81], M. Testa [47], R.J. Teuscher [159,j], J. Therhaag [21], T. Theveneaux-Pelzer [34],
S. Thoma [48], J.P. Thomas [18], E.N. Thompson [35], P.D. Thompson [18], P.D. Thompson [159],
A.S. Thompson [53], L.A. Thomsen [36], E. Thomson [121], M. Thomson [28], W.M. Thong [87],
R.P. Thun [88,∗], F. Tian [35], M.J. Tibbetts [15], T. Tic [126], V.O. Tikhomirov [95], Yu.A. Tikhonov [108,g],
S. Timoshenko [97], E. Tiouchichine [84], P. Tipton [177], S. Tisserant [84], T. Todorov [5],
S. Todorova-Nova [128], B. Toggerson [164], J. Tojo [69], S. Tokár [145a], K. Tokushuku [65],
K. Tollefson [89], L. Tomlinson [83], M. Tomoto [102], L. Tompkins [31], K. Toms [104], A. Tonoyan [14],
C. Topfel [17], N.D. Topilin [64], E. Torrence [115], H. Torres [79], E. Torró Pastor [168], J. Toth [84,ag],
F. Touchard [84], D.R. Tovey [140], H.L. Tran [116], T. Trefzger [175], L. Tremblet [30], A. Tricoli [30],
I.M. Trigger [160a], S. Trincaz-Duvoid [79], M.F. Tripiana [70], N. Triplett [25], W. Trischuk [159],
B. Trocmé [55], C. Troncon [90a], M. Trottier-McDonald [143], M. Trovatelli [135a,135b], P. True [89],
M. Trzebinski [39], A. Trzupek [39], C. Tsarouchas [30], J.C-L. Tseng [119], P.V. Tsiareshka [91],
D. Tsionou [137], G. Tsipolitis [10], S. Tsiskaridze [12], V. Tsiskaridze [48], E.G. Tskhadadze [51a],
I.I. Tsukerman [96], V. Tsulaia [15], J.-W. Tsung [21], S. Tsuno [65], D. Tsybychev [149], A. Tua [140],
A. Tudorache [26a], V. Tudorache [26a], J.M. Tuggle [31], A.N. Tuna [121], S. Turchikhin [98,ak],
D. Turecek [127], I. Turk Cakir [4d], R. Turra [90a,90b], P.M. Tuts [35], A. Tykhonov [74],
M. Tylmad [147a,147b], M. Tyndel [130], K. Uchida [21], I. Ueda [156], R. Ueno [29], M. Ughetto [84],
M. Ugland [14], M. Uhlenbrock [21], F. Ukegawa [161], G. Unal [30], A. Undrus [25], G. Unel [164],
F.C. Ungaro [48], Y. Unno [65], D. Urbaniec [35], P. Urquijo [21], G. Usai [8], A. Usanova [61],
L. Vacavant [84], V. Vacek [127], B. Vachon [86], S. Vahsen [15], N. Valencic [106],
S. Valentinetti [20a,20b], A. Valero [168], L. Valery [34], S. Valkar [128], E. Valladolid Gallego [168],
S. Vallecorsa [49], J.A. Valls Ferrer [168], R. Van Berg [121], P.C. Van Der Deijl [106],
R. van der Geer [106], H. van der Graaf [106], R. Van Der Leeuw [106], D. van der Ster [30],
N. van Eldik [30], P. van Gemmeren [6], J. Van Nieuwkoop [143], I. van Vulpen [106],

M. Vanadia [100], W. Vandelli [30], A. Vaniachine [6], P. Vankov [42], F. Vannucci [79], R. Vari [133a],
E.W. Varnes [7], T. Varol [85], D. Varouchas [15], A. Vartapetian [8], K.E. Varvell [151],
V.I. Vassilakopoulos [56], F. Vazeille [34], T. Vazquez Schroeder [54], J. Veatch [7], F. Veloso [125a],
S. Veneziano [133a], A. Ventura [72a,72b], D. Ventura [85], M. Venturi [48], N. Venturi [159],
V. Vercesi [120a], M. Verducci [139], W. Verkerke [106], J.C. Vermeulen [106], A. Vest [44],
M.C. Vetterli [143,e], I. Vichou [166], T. Vickey [146c,an], O.E. Vickey Boeriu [146c],
G.H.A. Viehhauser [119], S. Viel [169], R. Vigne [30], M. Villa [20a,20b], M. Villaplana Perez [168],
E. Vilucchi [47], M.G. Vincter [29], V.B. Vinogradov [64], J. Virzi [15], O. Vitells [173], M. Viti [42],
I. Vivarelli [48], F. Vives Vaque [3], S. Vlachos [10], D. Vladoiu [99], M. Vlasak [127], A. Vogel [21],
P. Vokac [127], G. Volpi [47], M. Volpi [87], G. Volpini [90a], H. von der Schmitt [100],
H. von Radziewski [48], E. von Toerne [21], V. Vorobel [128], M. Vos [168], R. Voss [30],
J.H. Vossebeld [73], N. Vranjes [137], M. Vranjes Milosavljevic [106], V. Vrba [126], M. Vreeswijk [106],
T. Vu Anh [48], R. Vuillermet [30], I. Vukotic [31], Z. Vykydal [127], W. Wagner [176], P. Wagner [21],
S. Wahrmund [44], J. Wakabayashi [102], S. Walch [88], J. Walder [71], R. Walker [99],
W. Walkowiak [142], R. Wall [177], P. Waller [73], B. Walsh [177], C. Wang [45], H. Wang [174],
H. Wang [40], J. Wang [152], J. Wang [33a], K. Wang [86], R. Wang [104], S.M. Wang [152], T. Wang [21],
X. Wang [177], A. Warburton [86], C.P. Ward [28], D.R. Wardrope [77], M. Warsinsky [48],
A. Washbrook [46], C. Wasicki [42], I. Watanabe [66], P.M. Watkins [18], A.T. Watson [18],
I.J. Watson [151], M.F. Watson [18], G. Watts [139], S. Watts [83], A.T. Waugh [151], B.M. Waugh [77],
S. Webb [83], M.S. Weber [17], J.S. Webster [31], A.R. Weidberg [119], P. Weigell [100],
J. Weingarten [54], C. Weiser [48], H. Weits [106], P.S. Wells [30], T. Wenaus [25], D. Wendland [16],
Z. Weng [152,w], T. Wengler [30], S. Wenig [30], N. Wermes [21], M. Werner [48], P. Werner [30],
M. Werth [164], M. Wessels [58a], J. Wetter [162], K. Whalen [29], A. White [8], M.J. White [87],
R. White [32b], S. White [123a,123b], D. Whiteson [164], D. Whittington [60], D. Wicke [176],
F.J. Wickens [130], W. Wiedenmann [174], M. Wielers [80,d], P. Wienemann [21], C. Wiglesworth [36],
L.A.M. Wiik-Fuchs [21], P.A. Wijeratne [77], A. Wildauer [100], M.A. Wildt [42,t], I. Wilhelm [128],
H.G. Wilkens [30], J.Z. Will [99], E. Williams [35], H.H. Williams [121], S. Williams [28], W. Willis [35,*],
S. Willocq [85], J.A. Wilson [18], A. Wilson [88], I. Wingerter-Seez [5], S. Winkelmann [48],
F. Winklmeier [30], M. Wittgen [144], T. Wittig [43], J. Wittkowski [99], S.J. Wollstadt [82],
M.W. Wolter [39], H. Wolters [125a,h], W.C. Wong [41], G. Wooden [88], B.K. Wosiek [39],
J. Wotschack [30], M.J. Woudstra [83], K.W. Wozniak [39], K. Wraight [53], M. Wright [53],
B. Wrona [73], S.L. Wu [174], X. Wu [49], Y. Wu [88], E. Wulf [35], T.R. Wyatt [83], B.M. Wynne [46],
S. Xella [36], M. Xiao [137], C. Xu [33b,ab], D. Xu [33a], L. Xu [33b,ao], B. Yabsley [151], S. Yacoob [146b,ap],
M. Yamada [65], H. Yamaguchi [156], Y. Yamaguchi [156], A. Yamamoto [65], K. Yamamoto [63],
S. Yamamoto [156], T. Yamamura [156], T. Yamanaka [156], K. Yamauchi [102], Y. Yamazaki [66],
Z. Yan [22], H. Yang [33e], H. Yang [174], U.K. Yang [83], Y. Yang [110], Z. Yang [147a,147b], S. Yanush [92],
L. Yao [33a], Y. Yasu [65], E. Yatsenko [42], K.H. Yau Wong [21], J. Ye [40], S. Ye [25], A.L. Yen [57],
E. Yildirim [42], M. Yilmaz [4b], R. Yoosoofmiya [124], K. Yorita [172], R. Yoshida [6], K. Yoshihara [156],
C. Young [144], C.J.S. Young [119], S. Youssef [22], D.R. Yu [15], J. Yu [8], J. Yu [113], L. Yuan [66],
A. Yurkewicz [107], B. Zabinski [39], R. Zaidan [62], A.M. Zaitsev [129,ac], S. Zambito [23],
L. Zanello [133a,133b], D. Zanzi [100], A. Zaytsev [25], C. Zeitnitz [176], M. Zeman [127], A. Zemla [39],
O. Zenin [129], T. Ženiš [145a], D. Zerwas [116], G. Zevi della Porta [57], D. Zhang [88], H. Zhang [89],
J. Zhang [6], L. Zhang [152], X. Zhang [33d], Z. Zhang [116], Z. Zhao [33b], A. Zhemchugov [64],
J. Zhong [119], B. Zhou [88], N. Zhou [164], C.G. Zhu [33d], H. Zhu [42], J. Zhu [88], Y. Zhu [33b],
X. Zhuang [33a], A. Zibell [99], D. Zieminska [60], N.I. Zimin [64], C. Zimmermann [82],
R. Zimmermann [21], S. Zimmermann [21], S. Zimmermann [48], Z. Zinonos [123a,123b],
M. Ziolkowski [142], R. Zitoun [5], L. Živković [35], G. Zobernig [174], A. Zoccoli [20a,20b],
M. zur Nedden [16], G. Zurzolo [103a,103b], V. Zutshi [107], L. Zwalinski [30]

[1] *School of Chemistry and Physics, University of Adelaide, Adelaide, Australia*
[2] *Physics Department, SUNY Albany, Albany, NY, United States*
[3] *Department of Physics, University of Alberta, Edmonton, AB, Canada*
[4] *(a) Department of Physics, Ankara University, Ankara; (b) Department of Physics, Gazi University, Ankara; (c) Division of Physics, TOBB University of Economics and Technology, Ankara; (d) Turkish Atomic Energy Authority, Ankara, Turkey*
[5] *LAPP, CNRS/IN2P3 and Université de Savoie, Annecy-le-Vieux, France*

[6] *High Energy Physics Division, Argonne National Laboratory, Argonne, IL, United States*

[7] *Department of Physics, University of Arizona, Tucson, AZ, United States*

[8] *Department of Physics, The University of Texas at Arlington, Arlington, TX, United States*

[9] *Physics Department, University of Athens, Athens, Greece*

[10] *Physics Department, National Technical University of Athens, Zografou, Greece*

[11] *Institute of Physics, Azerbaijan Academy of Sciences, Baku, Azerbaijan*

[12] *Institut de Física d'Altes Energies and Departament de Física de la Universitat Autònoma de Barcelona, Barcelona, Spain*

[13] [a] *Institute of Physics, University of Belgrade, Belgrade;* [b] *Vinca Institute of Nuclear Sciences, University of Belgrade, Belgrade, Serbia*

[14] *Department for Physics and Technology, University of Bergen, Bergen, Norway*

[15] *Physics Division, Lawrence Berkeley National Laboratory and University of California, Berkeley, CA, United States*

[16] *Department of Physics, Humboldt University, Berlin, Germany*

[17] *Albert Einstein Center for Fundamental Physics and Laboratory for High Energy Physics, University of Bern, Bern, Switzerland*

[18] *School of Physics and Astronomy, University of Birmingham, Birmingham, United Kingdom*

[19] [a] *Department of Physics, Bogazici University, Istanbul;* [b] *Department of Physics, Dogus University, Istanbul;* [c] *Department of Physics Engineering, Gaziantep University, Gaziantep, Turkey*

[20] [a] *INFN Sezione di Bologna;* [b] *Dipartimento di Fisica e Astronomia, Università di Bologna, Bologna, Italy*

[21] *Physikalisches Institut, University of Bonn, Bonn, Germany*

[22] *Department of Physics, Boston University, Boston, MA, United States*

[23] *Department of Physics, Brandeis University, Waltham, MA, United States*

[24] [a] *Universidade Federal do Rio De Janeiro COPPE/EE/IF, Rio de Janeiro;* [b] *Federal University of Juiz de Fora (UFJF), Juiz de Fora;* [c] *Federal University of Sao Joao del Rei (UFSJ), Sao Joao del Rei;* [d] *Instituto de Fisica, Universidade de Sao Paulo, Sao Paulo, Brazil*

[25] *Physics Department, Brookhaven National Laboratory, Upton, NY, United States*

[26] [a] *National Institute of Physics and Nuclear Engineering, Bucharest;* [b] *National Institute for Research and Development of Isotopic and Molecular Technologies, Physics Department, Cluj Napoca;* [c] *University Politehnica Bucharest, Bucharest;* [d] *West University in Timisoara, Timisoara, Romania*

[27] *Departamento de Física, Universidad de Buenos Aires, Buenos Aires, Argentina*

[28] *Cavendish Laboratory, University of Cambridge, Cambridge, United Kingdom*

[29] *Department of Physics, Carleton University, Ottawa, ON, Canada*

[30] *CERN, Geneva, Switzerland*

[31] *Enrico Fermi Institute, University of Chicago, Chicago, IL, United States*

[32] [a] *Departamento de Física, Pontificia Universidad Católica de Chile, Santiago;* [b] *Departamento de Física, Universidad Técnica Federico Santa María, Valparaíso, Chile*

[33] [a] *Institute of High Energy Physics, Chinese Academy of Sciences, Beijing;* [b] *Department of Modern Physics, University of Science and Technology of China, Anhui;* [c] *Department of Physics, Nanjing University, Jiangsu;* [d] *School of Physics, Shandong University, Shandong;* [e] *Physics Department, Shanghai Jiao Tong University, Shanghai, China*

[34] *Laboratoire de Physique Corpusculaire, Clermont Université and Université Blaise Pascal and CNRS/IN2P3, Clermont-Ferrand, France*

[35] *Nevis Laboratory, Columbia University, Irvington, NY, United States*

[36] *Niels Bohr Institute, University of Copenhagen, Kobenhavn, Denmark*

[37] [a] *INFN Gruppo Collegato di Cosenza;* [b] *Dipartimento di Fisica, Università della Calabria, Rende, Italy*

[38] [a] *AGH University of Science and Technology, Faculty of Physics and Applied Computer Science, Krakow;* [b] *Marian Smoluchowski Institute of Physics, Jagiellonian University, Krakow, Poland*

[39] *The Henryk Niewodniczanski Institute of Nuclear Physics, Polish Academy of Sciences, Krakow, Poland*

[40] *Physics Department, Southern Methodist University, Dallas, TX, United States*

[41] *Physics Department, University of Texas at Dallas, Richardson, TX, United States*

[42] *DESY, Hamburg and Zeuthen, Germany*

[43] *Institut für Experimentelle Physik IV, Technische Universität Dortmund, Dortmund, Germany*

[44] *Institut für Kern- und Teilchenphysik, Technische Universität Dresden, Dresden, Germany*

[45] *Department of Physics, Duke University, Durham, NC, United States*

[46] *SUPA – School of Physics and Astronomy, University of Edinburgh, Edinburgh, United Kingdom*

[47] *INFN Laboratori Nazionali di Frascati, Frascati, Italy*

[48] *Fakultät für Mathematik und Physik, Albert-Ludwigs-Universität, Freiburg, Germany*

[49] *Section de Physique, Université de Genève, Geneva, Switzerland*

[50] [a] *INFN Sezione di Genova;* [b] *Dipartimento di Fisica, Università di Genova, Genova, Italy*

[51] [a] *E. Andronikashvili Institute of Physics, Iv. Javakhishvili Tbilisi State University, Tbilisi;* [b] *High Energy Physics Institute, Tbilisi State University, Tbilisi, Georgia*

[52] *II Physikalisches Institut, Justus-Liebig-Universität Giessen, Giessen, Germany*

[53] *SUPA – School of Physics and Astronomy, University of Glasgow, Glasgow, United Kingdom*

[54] *II Physikalisches Institut, Georg-August-Universität, Göttingen, Germany*

[55] *Laboratoire de Physique Subatomique et de Cosmologie, Université Joseph Fourier and CNRS/IN2P3 and Institut National Polytechnique de Grenoble, Grenoble, France*

[56] *Department of Physics, Hampton University, Hampton, VA, United States*

[57] *Laboratory for Particle Physics and Cosmology, Harvard University, Cambridge, MA, United States*

[58] [a] *Kirchhoff-Institut für Physik, Ruprecht-Karls-Universität Heidelberg, Heidelberg;* [b] *Physikalisches Institut, Ruprecht-Karls-Universität Heidelberg, Heidelberg;* [c] *ZITI Institut für technische Informatik, Ruprecht-Karls-Universität Heidelberg, Mannheim, Germany*

[59] *Faculty of Applied Information Science, Hiroshima Institute of Technology, Hiroshima, Japan*

[60] *Department of Physics, Indiana University, Bloomington, IN, United States*

[61] *Institut für Astro- und Teilchenphysik, Leopold-Franzens-Universität, Innsbruck, Austria*

[62] *University of Iowa, Iowa City, IA, United States*

[63] *Department of Physics and Astronomy, Iowa State University, Ames, IA, United States*

[64] *Joint Institute for Nuclear Research, JINR Dubna, Dubna, Russia*

[65] *KEK, High Energy Accelerator Research Organization, Tsukuba, Japan*

[66] *Graduate School of Science, Kobe University, Kobe, Japan*

[67] *Faculty of Science, Kyoto University, Kyoto, Japan*

[68] *Kyoto University of Education, Kyoto, Japan*

[69] *Department of Physics, Kyushu University, Fukuoka, Japan*

[70] *Instituto de Física La Plata, Universidad Nacional de La Plata and CONICET, La Plata, Argentina*

[71] *Physics Department, Lancaster University, Lancaster, United Kingdom*

[72] [a] *INFN Sezione di Lecce;* [b] *Dipartimento di Matematica e Fisica, Università del Salento, Lecce, Italy*

[73] *Oliver Lodge Laboratory, University of Liverpool, Liverpool, United Kingdom*

[74] *Department of Physics, Jožef Stefan Institute and University of Ljubljana, Ljubljana, Slovenia*

[75] School of Physics and Astronomy, Queen Mary University of London, London, United Kingdom
[76] Department of Physics, Royal Holloway University of London, Surrey, United Kingdom
[77] Department of Physics and Astronomy, University College London, London, United Kingdom
[78] Louisiana Tech University, Ruston, LA, United States
[79] Laboratoire de Physique Nucléaire et de Hautes Energies, UPMC and Université Paris-Diderot and CNRS/IN2P3, Paris, France
[80] Fysiska institutionen, Lunds universitet, Lund, Sweden
[81] Departamento de Fisica Teorica C-15, Universidad Autonoma de Madrid, Madrid, Spain
[82] Institut für Physik, Universität Mainz, Mainz, Germany
[83] School of Physics and Astronomy, University of Manchester, Manchester, United Kingdom
[84] CPPM, Aix-Marseille Université and CNRS/IN2P3, Marseille, France
[85] Department of Physics, University of Massachusetts, Amherst, MA, United States
[86] Department of Physics, McGill University, Montreal, QC, Canada
[87] School of Physics, University of Melbourne, Victoria, Australia
[88] Department of Physics, The University of Michigan, Ann Arbor, MI, United States
[89] Department of Physics and Astronomy, Michigan State University, East Lansing, MI, United States
[90] (a) INFN Sezione di Milano; (b) Dipartimento di Fisica, Università di Milano, Milano, Italy
[91] B.I. Stepanov Institute of Physics, National Academy of Sciences of Belarus, Minsk, Belarus
[92] National Scientific and Educational Centre for Particle and High Energy Physics, Minsk, Belarus
[93] Department of Physics, Massachusetts Institute of Technology, Cambridge, MA, United States
[94] Group of Particle Physics, University of Montreal, Montreal, QC, Canada
[95] P.N. Lebedev Institute of Physics, Academy of Sciences, Moscow, Russia
[96] Institute for Theoretical and Experimental Physics (ITEP), Moscow, Russia
[97] Moscow Engineering and Physics Institute (MEPhI), Moscow, Russia
[98] D.V. Skobeltsyn Institute of Nuclear Physics, M.V. Lomonosov Moscow State University, Moscow, Russia
[99] Fakultät für Physik, Ludwig-Maximilians-Universität München, München, Germany
[100] Max-Planck-Institut für Physik (Werner-Heisenberg-Institut), München, Germany
[101] Nagasaki Institute of Applied Science, Nagasaki, Japan
[102] Graduate School of Science and Kobayashi–Maskawa Institute, Nagoya University, Nagoya, Japan
[103] (a) INFN Sezione di Napoli; (b) Dipartimento di Scienze Fisiche, Università di Napoli, Napoli, Italy
[104] Department of Physics and Astronomy, University of New Mexico, Albuquerque, NM, United States
[105] Institute for Mathematics, Astrophysics and Particle Physics, Radboud University Nijmegen/Nikhef, Nijmegen, Netherlands
[106] Nikhef National Institute for Subatomic Physics and University of Amsterdam, Amsterdam, Netherlands
[107] Department of Physics, Northern Illinois University, DeKalb, IL, United States
[108] Budker Institute of Nuclear Physics, SB RAS, Novosibirsk, Russia
[109] Department of Physics, New York University, New York, NY, United States
[110] Ohio State University, Columbus, OH, United States
[111] Faculty of Science, Okayama University, Okayama, Japan
[112] Homer L. Dodge Department of Physics and Astronomy, University of Oklahoma, Norman, OK, United States
[113] Department of Physics, Oklahoma State University, Stillwater, OK, United States
[114] Palacký University, RCPTM, Olomouc, Czech Republic
[115] Center for High Energy Physics, University of Oregon, Eugene, OR, United States
[116] LAL, Université Paris-Sud and CNRS/IN2P3, Orsay, France
[117] Graduate School of Science, Osaka University, Osaka, Japan
[118] Department of Physics, University of Oslo, Oslo, Norway
[119] Department of Physics, Oxford University, Oxford, United Kingdom
[120] (a) INFN Sezione di Pavia; (b) Dipartimento di Fisica, Università di Pavia, Pavia, Italy
[121] Department of Physics, University of Pennsylvania, Philadelphia, PA, United States
[122] Petersburg Nuclear Physics Institute, Gatchina, Russia
[123] (a) INFN Sezione di Pisa; (b) Dipartimento di Fisica E. Fermi, Università di Pisa, Pisa, Italy
[124] Department of Physics and Astronomy, University of Pittsburgh, Pittsburgh, PA, United States
[125] (a) Laboratorio de Instrumentacao e Fisica Experimental de Particulas – LIP, Lisboa, Portugal; (b) Departamento de Fisica Teorica y del Cosmos and CAFPE, Universidad de Granada, Granada, Spain
[126] Institute of Physics, Academy of Sciences of the Czech Republic, Praha, Czech Republic
[127] Czech Technical University in Prague, Praha, Czech Republic
[128] Faculty of Mathematics and Physics, Charles University in Prague, Praha, Czech Republic
[129] State Research Center Institute for High Energy Physics, Protvino, Russia
[130] Particle Physics Department, Rutherford Appleton Laboratory, Didcot, United Kingdom
[131] Physics Department, University of Regina, Regina, SK, Canada
[132] Ritsumeikan University, Kusatsu, Shiga, Japan
[133] (a) INFN Sezione di Roma I; (b) Dipartimento di Fisica, Università La Sapienza, Roma, Italy
[134] (a) INFN Sezione di Roma Tor Vergata; (b) Dipartimento di Fisica, Università di Roma Tor Vergata, Roma, Italy
[135] (a) INFN Sezione di Roma Tre; (b) Dipartimento di Matematica e Fisica, Università Roma Tre, Roma, Italy
[136] (a) Faculté des Sciences Ain Chock, Réseau Universitaire de Physique des Hautes Energies – Université Hassan II, Casablanca; (b) Centre National de l'Energie des Sciences Techniques Nucleaires, Rabat; (c) Faculté des Sciences Semlalia, Université Cadi Ayyad, LPHEA, Marrakech; (d) Faculté des Sciences, Université Mohamed Premier and LPTPM, Oujda; (e) Faculté des sciences, Université Mohammed V-Agdal, Rabat, Morocco
[137] DSM/IRFU (Institut de Recherches sur les Lois Fondamentales de l'Univers), CEA Saclay (Commissariat à l'Energie Atomique et aux Energies Alternatives), Gif-sur-Yvette, France
[138] Santa Cruz Institute for Particle Physics, University of California Santa Cruz, Santa Cruz, CA, United States
[139] Department of Physics, University of Washington, Seattle, WA, United States
[140] Department of Physics and Astronomy, University of Sheffield, Sheffield, United Kingdom
[141] Department of Physics, Shinshu University, Nagano, Japan
[142] Fachbereich Physik, Universität Siegen, Siegen, Germany
[143] Department of Physics, Simon Fraser University, Burnaby, BC, Canada
[144] SLAC National Accelerator Laboratory, Stanford, CA, United States
[145] (a) Faculty of Mathematics, Physics & Informatics, Comenius University, Bratislava; (b) Department of Subnuclear Physics, Institute of Experimental Physics of the Slovak Academy of Sciences, Kosice, Slovak Republic
[146] (a) Department of Physics, University of Cape Town, Cape Town; (b) Department of Physics, University of Johannesburg, Johannesburg; (c) School of Physics, University of the Witwatersrand, Johannesburg, South Africa
[147] (a) Department of Physics, Stockholm University; (b) The Oskar Klein Centre, Stockholm, Sweden

[148] *Physics Department, Royal Institute of Technology, Stockholm, Sweden*
[149] *Departments of Physics & Astronomy and Chemistry, Stony Brook University, Stony Brook, NY, United States*
[150] *Department of Physics and Astronomy, University of Sussex, Brighton, United Kingdom*
[151] *School of Physics, University of Sydney, Sydney, Australia*
[152] *Institute of Physics, Academia Sinica, Taipei, Taiwan*
[153] *Department of Physics, Technion: Israel Institute of Technology, Haifa, Israel*
[154] *Raymond and Beverly Sackler School of Physics and Astronomy, Tel Aviv University, Tel Aviv, Israel*
[155] *Department of Physics, Aristotle University of Thessaloniki, Thessaloniki, Greece*
[156] *International Center for Elementary Particle Physics and Department of Physics, The University of Tokyo, Tokyo, Japan*
[157] *Graduate School of Science and Technology, Tokyo Metropolitan University, Tokyo, Japan*
[158] *Department of Physics, Tokyo Institute of Technology, Tokyo, Japan*
[159] *Department of Physics, University of Toronto, Toronto, ON, Canada*
[160] [a] *TRIUMF, Vancouver, BC;* [b] *Department of Physics and Astronomy, York University, Toronto, ON, Canada*
[161] *Faculty of Pure and Applied Sciences, University of Tsukuba, Tsukuba, Japan*
[162] *Department of Physics and Astronomy, Tufts University, Medford, MA, United States*
[163] *Centro de Investigaciones, Universidad Antonio Narino, Bogota, Colombia*
[164] *Department of Physics and Astronomy, University of California Irvine, Irvine, CA, United States*
[165] [a] *INFN Gruppo Collegato di Udine;* [b] *ICTP, Trieste;* [c] *Dipartimento di Chimica, Fisica e Ambiente, Università di Udine, Udine, Italy*
[166] *Department of Physics, University of Illinois, Urbana, IL, United States*
[167] *Department of Physics and Astronomy, University of Uppsala, Uppsala, Sweden*
[168] *Instituto de Física Corpuscular (IFIC) and Departamento de Física Atómica, Molecular y Nuclear and Departamento de Ingeniería Electrónica and Instituto de Microelectrónica de Barcelona (IMB-CNM), University of Valencia and CSIC, Valencia, Spain*
[169] *Department of Physics, University of British Columbia, Vancouver, BC, Canada*
[170] *Department of Physics and Astronomy, University of Victoria, Victoria, BC, Canada*
[171] *Department of Physics, University of Warwick, Coventry, United Kingdom*
[172] *Waseda University, Tokyo, Japan*
[173] *Department of Particle Physics, The Weizmann Institute of Science, Rehovot, Israel*
[174] *Department of Physics, University of Wisconsin, Madison, WI, United States*
[175] *Fakultät für Physik und Astronomie, Julius-Maximilians-Universität, Würzburg, Germany*
[176] *Fachbereich C Physik, Bergische Universität Wuppertal, Wuppertal, Germany*
[177] *Department of Physics, Yale University, New Haven, CT, United States*
[178] *Yerevan Physics Institute, Yerevan, Armenia*
[179] *Centre de Calcul de l'Institut National de Physique Nucléaire et de Physique des Particules (IN2P3), Villeurbanne, France*

[a] Also at Department of Physics, King's College London, London, United Kingdom.
[b] Also at Laboratorio de Instrumentacao e Fisica Experimental de Particulas – LIP, Lisboa, Portugal.
[c] Also at Faculdade de Ciencias and CFNUL, Universidade de Lisboa, Lisboa, Portugal.
[d] Also at Particle Physics Department, Rutherford Appleton Laboratory, Didcot, United Kingdom.
[e] Also at TRIUMF, Vancouver, BC, Canada.
[f] Also at Department of Physics, California State University, Fresno, CA, United States.
[g] Also at Novosibirsk State University, Novosibirsk, Russia.
[h] Also at Department of Physics, University of Coimbra, Coimbra, Portugal.
[i] Also at Università di Napoli Parthenope, Napoli, Italy.
[j] Also at Institute of Particle Physics (IPP), Canada.
[k] Also at Department of Physics, Middle East Technical University, Ankara, Turkey.
[l] Also at Louisiana Tech University, Ruston, LA, United States.
[m] Also at Departamento de Fisica and CEFITEC of Faculdade de Ciencias e Tecnologia, Universidade Nova de Lisboa, Caparica, Portugal.
[n] Also at Department of Physics and Astronomy, Michigan State University, East Lansing, MI, United States.
[o] Also at Department of Financial and Management Engineering, University of the Aegean, Chios, Greece.
[p] Also at Institucio Catalana de Recerca i Estudis Avancats, ICREA, Barcelona, Spain.
[q] Also at Department of Physics, University of Cape Town, Cape Town, South Africa.
[r] Also at Institute of Physics, Azerbaijan Academy of Sciences, Baku, Azerbaijan.
[s] Also at CERN, Geneva, Switzerland.
[t] Also at Institut für Experimentalphysik, Universität Hamburg, Hamburg, Germany.
[u] Also at Manhattan College, New York, NY, United States.
[v] Also at Institute of Physics, Academia Sinica, Taipei, Taiwan.
[w] Also at School of Physics and Engineering, Sun Yat-sen University, Guanzhou, China.
[x] Also at Academia Sinica Grid Computing, Institute of Physics, Academia Sinica, Taipei, Taiwan.
[y] Also at Laboratoire de Physique Nucléaire et de Hautes Energies, UPMC and Université Paris-Diderot and CNRS/IN2P3, Paris, France.
[z] Also at School of Physical Sciences, National Institute of Science Education and Research, Bhubaneswar, India.
[aa] Also at Dipartimento di Fisica, Università La Sapienza, Roma, Italy.
[ab] Also at DSM/IRFU (Institut de Recherches sur les Lois Fondamentales de l'Univers), CEA Saclay (Commissariat à l'Energie Atomique et aux Energies Alternatives), Gif-sur-Yvette, France.
[ac] Also at Moscow Institute of Physics and Technology State University, Dolgoprudny, Russia.
[ad] Also at Section de Physique, Université de Genève, Geneva, Switzerland.
[ae] Also at Departamento de Fisica, Universidade de Minho, Braga, Portugal.
[af] Also at Department of Physics, The University of Texas at Austin, Austin, TX, United States.
[ag] Also at Institute for Particle and Nuclear Physics, Wigner Research Centre for Physics, Budapest, Hungary.
[ah] Also at DESY, Hamburg and Zeuthen, Germany.
[ai] Also at International School for Advanced Studies (SISSA), Trieste, Italy.
[aj] Also at Department of Physics and Astronomy, University of South Carolina, Columbia, SC, United States.
[ak] Also at Faculty of Physics, M.V. Lomonosov Moscow State University, Moscow, Russia.
[al] Also at Nevis Laboratory, Columbia University, Irvington, NY, United States.
[am] Also at Physics Department, Brookhaven National Laboratory, Upton, NY, United States.

[an] Also at Department of Physics, Oxford University, Oxford, United Kingdom.
[ao] Also at Department of Physics, The University of Michigan, Ann Arbor, MI, United States.
[ap] Also at Discipline of Physics, University of KwaZulu-Natal, Durban, South Africa.
 * Deceased.